TÉCNICO LISBOA

Interference Cancellation Receivers in a Device-to-Device Network

Raquel de Almeida Martins

Thesis to obtain the Master of Science Degree in

Electrical and Computer Engineering

Supervisor(s): Prof. António José Castelo Branco Rodrigues

Prof. Maria Paula dos Santos Queluz Rodrigues

Examination Committee

Chairperson: Prof. José Eduardo Charters Ribeiro da Cunha Sanguino

Supervisor: Prof. António José Castelo Branco Rodrigues

Member of Committee: Prof. Francisco António Bucho Cercas

November 2018

Declaration

I declare that this document is an original work of my own authorship and that it fulfills all the requirements of the Code of Conduct and Good Practices of the Universidade de Lisboa.

To my parents and brother

Acknowledgments

First of all, I would like to thank my supervisor Prof. António Rodrigues and my co-supervisor Prof. Paula Rodrigues for all the guidance, support and infinite availability given during the development of this thesis.

I would like to thank Instituto de Telecomunicações for providing me with the required means for the completion of this dissertation.

I would also like to thank Intel, for giving me the opportunity of working in this project, and my team, especially Dr. Nuno Pratas for all the advices on life, for the patience and for challenging me every day.

I would also like to express my gratitude to my colleague and friend Filipa for coming to this incredible adventure with me, for always having my back no matter what and to put up with me even when I am in an impossible mood.

Last but not the least, I must thank my Family and Friends for everything. For all the love and extraordinary support through life.

Abstract

Nowadays, the number of users and connected devices linked to a network is very large. For that reason, new technologies that do not need network support, such as Device-to-Device communication (D2D), have been explored. Due to the lack of support from the cellular network infrastructures, communications between devices occur randomly, uncoordinated and un-scheduled, resulting in the appearance of a great amount of interference. Hence, the purpose of this thesis is to study and create new procedures that allow the resolution of this problem in order to enhance the communications in a D2D network without cellular network support.

To achieve this aim, a link level simulator and a system level simulator are designed with the purpose of evaluate, in terms of complexity and performance, several processes that take advantage of the Successive Interference Cancellation (SIC) technique. Particularly, the D2D network performance is assessed when there is no use of any kind of SIC, when intra-SIC is applied and when intra-SIC and inter-SIC are both used in a typical Slotted ALOHA scheme.

With the simulations and studies presented in this thesis, it was proven that the use of SIC, although it increases the complexity of the system in consideration, it also boosts its performance. When there is no use of any type of SIC, the performance obtained is very low. However, with the increase of complexity, applying intra-SIC, the performance increases up to 50% and the increase reaches 70% when the two types of SIC, intra-SIC and inter-SIC, are applied.

Keywords: Device-to-Device communication, Successive Interference Cancellation, intra-SIC, inter-SIC.

Resumo

Atualmente, o número de utilizadores e dispositivos ligados à rede móvel é muito elevado. Por esse motivo, novas tecnologias que não necessitam do suporte da rede, tal como a comunicação Dispositivo-para-Dispositivo (D2D), têm vindo a ser exploradas. Por não tirarem partido das infraestruturas da rede, as comunicações entre dispositivos ocorrem aleatoriamente, não são coordenadas nem agendadas, resultando em graves problemas de interferência. Atendendo à problemática apresentada, o objetivo desta tese é o estudo e criação de novos procedimentos que permitem resolver esta questão, aprimorando as comunicações de uma rede D2D sem suporte de rede móvel.

Para atingir esse fim, foram concebidos um simulador ao nível da ligação e um simulador ao nível do sistema cujo objetivo é avaliar, em termos de complexidade e desempenho, diversos processos que utilizam a técnica de Cancelamento Sucessivo de Interferência (em inglês, *Successive Interference Cancellation* - *SIC*). Em particular, avaliam-se redes D2D em que *SIC* não é usado, em que se utiliza o processo *intra-SIC* e em que se utilizam *intra-SIC* e *inter-SIC*, num esquema de *Slotted ALOHA*.

Através das simulações e estudos apresentados nesta tese, provou-se que o uso de *SIC*, apesar de aumentar a complexidade do sistema em consideração, também impulsiona o desempenho do mesmo. Quando *SIC* não é utilizado, o sistema apresenta baixo desempenho. No entanto, aumentando ligeiramente a complexidade, aplicando *intra-SIC*, o seu desempenho aumenta até 50% e o aumento chega a atingir 70% com o uso simultâneo de *intra-SIC* e *inter-SIC*.

Palavras-Chave: Comunicação Dispositivo-para-Dispositivo, Cancelamento Sucessivo de Interferência, *intra-SIC*, *inter-SIC*.

Contents

Acknowledgments vii
Abstract ix
Resumo xi
List of Tables xv
List of Figures xvii
List of Acronyms xxi
List of Symbols xxv
1. Introduction 1
1.1. Motivation 1
1.2. State of the Art 4
1.3. Objectives 5
1.4. Thesis Outline 6
1.5. Contributions and Outputs 6
2. Fundamental Concepts 9
2.1. Theoretical foundations of interference in multi-user networks 9
2.2. Physical layer 12
2.2.1. Frame Structure: Narrowband-IoT 12
2.2.2. Reference Signals and Channel Estimation 14
2.2.3. Types of SIC in respect to the PHY layer 15
2.3. Media Access Control layer 16
2.3.1. Random Access Protocols 17
2.3.2. Types of SIC in respect to the MAC layer 21
3. Proposed Solution 23
3.1. Brief Introduction 23
3.2. Key Concepts 24
3.3. Transmitter Side 26
3.4. Receiver Side 33
3.4.1. Pilot Activity Detection 34
3.4.2. Intra-SIC process 38
3.4.3. Inter-SIC process 45
4. Implementation 49
4.1. System Level Simulator 49
4.2. Link Level Simulator 52
4.2.1. No SIC 54
4.2.2. Intra-SIC 55
4.2.3. Intra and Inter-SIC 56

5. Results Analysis 57
5.1. Performance 57
5.1.1. Preliminary Results 57
5.1.2. Pilot Activity Detection 59
5.1.3. Receiver Architectures 62
5.2. Complexity 71
6. Conclusion 75
6.1. Summary 75
6.2. Future Work 76
Bibliography 79
Appendix A 83

List of Tables

Table 1.1: Improvements of 5G compared to 4G (based on [4]) 2
Table 1.2: Requirements of the network in analysis. 3
Table 3.1: Example of a set of orthogonal pilot sequences. 32
Table 3.2: Correspondent bits to QPSK symbols. 41
Table 3.3: Example of LLRs for two bits. 44
Table 5.1: System parameters for preliminary simulations. 57
Table 5.2: System parameters for simulation of different pilot activity detection architectures. 60
Table 5.3: Summary of characteristics and results obtained from different pilot activity detection architectures. 61
Table 5.4: System parameters used in SLS. 62
Table 5.5: System parameters used in LLS. 62
Table 5.6: Parameters for simulation of inter-SIC/intra-SIC architecture for channel estimations MMSE-MRC and MMSE-IRC 67
Table 5.7: Parameters for simulation of inter-SIC/intra-SIC architecture for channel estimations MMSE-MRC with MMSE-IRC in the inter-SIC process and MMSE-IRC with MMSE-MRC in the inter-SIC process. 69
Table 6.1: Size of the VF based on level of interference experienced. 76

List of Figures

Figure 1.1: Connected devices (in billions) over the years (based on [3]). 1
Figure 1.2: D2D Network setting for this case study. 3
Figure 2.1: Specific scheme for posterior analysis. 9
Figure 2.2: Capacity region of a MACh (based on [17]). 11
Figure 2.3: Layers of the OSI model (based on [19]). 12
Figure 2.4: Resource grid used in NB-IoT (based on [21]). 13
Figure 2.5: Function of the Cyclic Prefix (based on [20]). 14
Figure 2.6: Difference between Symbol-level (fill line) and Codeword-level (dash line) interference cancellation (based on [23]). 16
Figure 2.7: Setting for explanation of Framed Slotted ALOHA (based on [24]). 17
Figure 2.8: Setting variating in time for explanation of Coded Random Access (based on [24]). 19
Figure 2.9: Setting variating in time to explain how B-CSA works (based on [25]). 20
Figure 2.10: Real process that includes intra and inter-slot cancellation. 22
Figure 3.1: Example of random access. 23
Figure 3.2: Average number of discovery sessions completed per minute for three different receiver architectures. 24
Figure 3.3: Discovery Protocol. 24
Figure 3.4: Frame Structure composed with the three phases. 25
Figure 3.5: Resources saved for the discovery process. 25
Figure 3.6: Subcarriers reserved for MSGs1 and MSGs2. 25
Figure 3.7: Virtual Frame construction. 26
Figure 3.8: Possible patterns that a DI can choose from in a virtual frame of 5 slots and 2 available replicas. 27
Figure 3.9: Transmitter chain. 27
Figure 3.10: Turbo encoder block diagram. 28
Figure 3.11: Rate-Matching block diagram. 29
Figure 3.12: QPSK constellation used. 30
Figure 3.13: Payload of MSGs1 and MSGs2. 30
Figure 3.14: Comparison between the use of multiple orthogonal pilot sequences and a single one for different types of channel estimation in two different SIRs: -15 dB (left) and 15 dB (right). 31
Figure 3.15: Number of pilot sequences associated with the supported load within a channel resource for a collision threshold. 31
Figure 3.16: Receiver chain 33
Figure 3.17: Proposed adaptive architecture for the receiver side. 33
Figure 3.18: Receiver architecture for different results of pilot activity detection: (a) for when only one pilot sequence is detected; (b) for when multiple pilot sequences are detected. 34
Figure 3.19: Matched filter baseline block diagram. 35
Figure 3.20: Parallel matched filter with adaptive threshold via common neural network. 36

Figure 3.21: Feedforward neural network architecture. 37
Figure 3.22: Parallel matched filter with adaptive threshold via individual neural network. 37
Figure 3.23: Intra-SIC block diagram. 38
Figure 3.24: SIC loop process. 38
Figure 3.25: Mechanism of MMSE-MRC with pilot symbols. 39
Figure 3.26: Mechanism of MMSE-IRC with pilot symbols. 40
Figure 3.27: Turbo decoder/encoder block diagram. 42
Figure 3.28: Localization of the obtained symbol in the QPSK constellation. 45
Figure 3.29: Inter-SIC block diagram. 45
Figure 3.30: Mechanism of MMSE-MRC with pilot and data symbols. 46
Figure 3.31: Mechanism of MMSE-IRC with pilot and data symbols. 46
Figure 4.1: State machine of a DI in the SLS system. 50
Figure 4.2: State machine of a DR in the SLS system. 52
Figure 4.3: Transmitter chain in the LLS system. 53
Figure 4.4: Receiver architecture without SIC in the LLS system. 55
Figure 4.5: Receiver architecture with intra-SIC in the LLS system. 55
Figure 4.6: Receiver architecture with intra and inter-SIC in the LLS system. 56
Figure 5.1: Comparison between two types of channel estimation in presence of interference: MMSE-MRC (left) and MMSE-IRC (right). 58
Figure 5.2: Comparison between no use of SIC and use of SIC for two types of channel estimation in different amounts of interference: SIR=-20 dB (left) and SIR=20 dB (right). 59
Figure 5.3: Percentage of true positives for different pilot activity detection architectures. 61
Figure 5.4: Comparison between the two types of channel estimation for a system with no SIC in both MSGs. 63
Figure 5.5: Average number of discovery sessions completed per minute for a system with intra-SIC only in MSG1 and applying MMSE-MRC. 64
Figure 5.6: Average number of discovery sessions completed per minute for a system with intra-SIC only in MSG2 and applying MMSE-MRC. 64
Figure 5.7: Average number of discovery sessions completed per minute for a system with intra-SIC in both MSGs and applying MMSE-MRC. 65
Figure 5.8: Comparison between the three systems where intra-SIC can be applied. 65
Figure 5.9: Average number of discovery sessions completed per minute for a system with intra-SIC only in MSG1 and applying MMSE-IRC. 66
Figure 5.10: Comparison between the two types of channel estimation for a system where intra-SIC is applied only in MSG1. 66
Figure 5.11: Average number of discovery sessions completed per minute for a system with intra-SIC and inter-SIC only in MSG1 and applying MMSE-MRC. 67
Figure 5.12: Average number of discovery sessions completed per minute for a system with intra-SIC and inter-SIC only in MSG1 and applying MMSE-IRC. 68

Figure 5.13: Comparison between the two types of channel estimation for a system where intra-SIC and inter-SIC are applied only in MSG1. 68
Figure 5.14: Average number of discovery sessions completed per minute for a system with intra-SIC and inter-SIC only in MSG1 and applying MMSE-MRC except in the process of inter-SIC where MMSE-IRC is applied. 69
Figure 5.15: Average number of discovery sessions completed per minute for a system with intra-SIC and inter-SIC only in MSG1 and applying MMSE-IRC except in the process of inter-SIC where MMSE-MRC is applied. 70
Figure 5.16: Comparison between the different architectures when intra-SIC and inter-SIC are applied only in MSG1. 71
Figure 5.17: Comparison between all systems for the two types of channel estimation in consideration. 71
Figure 5.18: Comparison of complexity between all systems for the two types of channel estimation in consideration (in MIPS – Millions of Instructions Per Second). 73
Figure A.1: Example of a communication between a DI and a DR. 83

List of Acronyms

2G	2nd Generation
3GPP	3rd Generation Partnership Project
4G	4th Generation
5G	5th Generation
B-CSA	Broadcast Coded Slotted ALOHA
BCJR	Bahl, Cocke, Jelinek and Raviv
BLER	Block Error Rate
BS	Base Station
CDMA	Code Division Multiple Access
CP	Cyclic Prefix
CRC	Cyclic Redundancy Check
D2D	Device-to-Device
DFT	Discrete Fourier Transform
DI	Discover Initiator
DM-RS	Demodulation Reference Signals
DR	Discover Replier
EDGE	Enhanced Data Rates for GSM Evolution
eMBB	Enhanced Mobile Broadband
EPA	Extended Pedestrian A model
FDMA	Frequency Division Multiple Access
GPRS	General Packet Radio System
GSM	Global System for Mobile Communications
IDFT	Inverse Discrete Fourier Transform

IoT	Internet of Things
ISM	Industrial, Scientific and Medical
JD	Joint Decoding
LAA	Licensed Assisted Access
LLR	Logarithm Likelihood Ratio
LLS	Link Level Simulator
LoS	Line of Sight
LS	Least Square
LTE	Long Term Evolution
MAC	Media Access Control
MACh[1]	Multiple Access Channel
MCS	Modulation and Coding Scheme
MIMO	Multiple-Input Multiple-Output
MMSE	Minimum Mean Square Error
MMSE-IRC	Minimum Mean Square Error – Interference Rejection Combining
MMSE-MRC	Minimum Mean Square Error – Maximum Ratio Combining
mMTC	Massive Machine Type Communications
MS	Mobile Station
MSG	Message
MUX	Multiplexer
NB-IoT	Narrowband-Internet of Things
NLoS	Non Line of Sight

[1] Usually Multiple Access Channel is represented by MAC. However, in this document is represented by MACh because MAC is already associated with Media Access Control.

NPUSCH	Narrowband Physical Uplink Shared Channel
OFDMA	Orthogonal Frequency Division Multiple Access
OSI	Open Systems Interconnection
PHY	Physical
PIC	Parallel Interference Cancellation
ProSe	Proximity Services
QPSK	Quadrature Phase Shift Keying
RE	Resource Element
RS	Reference Signals
RV	Redundancy Version
Rx	Reception
SC-FDMA	Single Carrier-Frequency Division Multiple Access
SIC	Successive Interference Cancellation
SINR	Signal-to-Interference-plus-Noise Ratio
SIR	Signal-to-Interference Ratio
SLS	System Level Simulator
SNR	Signal-to-Noise Ratio
TDMA	Time Division Multiple Access
TR	Technical Report
TS	Technical Specification
Tx	Transmission
UE	User Equipment
uRLLC	Ultra-Reliable and Low Latency Communications
VF	Virtual Frame

List of Symbols

$\widehat{\ }$	Estimation
Δf	Subcarrier spacing
λ	Arrival rate
π	Pi
$\phi_{k,l}$	Phase rotation
τ	Threshold
$a_{k^{(-)},l}$	Modulated value of SC-FDMA symbol l
A_i	Attenuation due to i
b_i	Bit i
B	Total bandwidth
c	Free space wave propagation speed
C_{ij}	Channel capacity from user i to j
d	Systematic bit sequence
dt	Distance
e	Euler's number
$E[\ ]$	Expected value
f_c	System frequency
f_{Dmax}	Maximum Doppler shift
$f_{map}([a,b])$	Mapping of bits a and b to QPSK symbols
g	Channel load
$G_{antennas}$	Antennas gain
H	Conjugate transpose operation

h_{ij}	Complex gains of the channels from device i to j
h_{BS}	Antenna height at the base station
h_{MS}	Antenna height at the mobile station
h'_{BS}	Effective antenna height at the base station
h'_{MS}	Effective antenna height at the mobile station
$\widehat{h_{MMSEı}}$	Minimum Mean Square Error channel estimation of signal i
$\widehat{h_{MMSEı,p}}$	Minimum Mean Square Error channel estimation of signal i in pilot positions
$\widehat{h_{MMSEı,d}}$	Minimum Mean Square Error channel estimation of signal i in data positions
$\widehat{h_{LSı}}$	Least Square channel estimation of signal i
$\widehat{h_{LSı,p}}$	Least Square channel estimation of signal i in pilot positions
I	Identity matrix
J_0	Zeroth-order Bessel function
k	Index in frequency domain
K_i	Complexity of block i
l	Index in time domain
L	Size of virtual frame
LLR_c	Channel logarithm likelihood ratio
LLR_{Ai}	A priori logarithm likelihood ratio for decoder i
LLR_{APi}	A posteriori logarithm likelihood ratio from decoder i
LLR_{Ei}	Extrinsic logarithm likelihood ratio from decoder i
n	Complex Gaussian noise
n_p	Number of pilots
n_q	Number of pilots plus data

N	Constant power level of noise
N_{sc}	Number of subcarriers
N_{symb}	Number of SC-FDMA symbols
$N_{interferes}$	Number of interferers
O_i	Total complexity of architecture i
p	Packet loss rate
p_1	Parity bit sequence 1
p_2	Parity bit sequence 2
$p_{seq,i}$	Pilot sequence i
P_i	Constant power level used by device i
$P_{payload}$	Power of payload
P_{tx}	Transmitted power
P	Total number of pilot sequences
Pr	Probability
PL_i	Path loss in i conditions
r	Number of replicas
R_{ij}	Data rate from user i to j
$R_{n,n'}$	Covariance matrix between n and n'
R_{ri}	Noise covariance matrix of signal i
$s_{k,l}(t)$	Time-continuous signal for subcarrier index k and in SC-FDMA symbol l
$SINR_{ij}$	Signal-to-interference-plus-noise ratio of user i at j
SNR_{ij}	Signal-to-noise ratio of user i at j
t	Time

T	Throughput
T_{sym}	SC-FDMA symbol period
T_s	Basic time unit
x	Symbol
x_i	Transmitted signal by device i
$x_{i,p}$	Transmitted signal by device i in pilot positions
(x_i, y_i)	Cartesian coordinates of position of device i
y	Received signal
y_p	Received signal in pilot positions
y_d	Received signal in data positions
$y_{d,MMSE}$	Signal detected after equalization

1. Introduction

This chapter describes the motivation of this dissertation, its objective, its structure and finally a description of the outputs obtained during the development of this work.

1.1. Motivation

In the past years, due to larger improvements at engineering level and continuous development of technologies, smarter devices have reached the world. Their complexity exceeded the current mobile network capabilities requiring the development of a new network standard.

Next, a few examples of new technologies and their network requirements that justify why the current generation of broadband cellular network (4th generation) do not have the abilities to fulfil the necessary requirements anymore will be exposed. One of the reasons is the countless smartphones currently being used and the wide range of mobile applications, requiring high-speed multimedia data throughput. This leads to a great interest in more techniques to support high data rates and lower latencies. Also, the appearance of the “Internet of Things” (IoT) concept has revolutionized the way people connect equipment with their everyday life, leading to an exponential growth of devices. It is estimated that in 2025, there will be 75.44 billion of connected devices worldwide, as depicted in Figure 1.1, which is nine times more than the expected world population at that time [1]. This growth leads to a massive growth in traffic volume and requires a network that can deal with the massive connectivity between equipments. Finally, another scientific area that is being heavily discussed is artificial intelligence. As the name suggests, this topic consists in the construction of machines capable of doing tasks that usually require human intelligence [2], as driving a car. In addition to all the social aspects that this technology entails, there is also some requirements at the technical level: for example, in the case of the self-driving car, there is a need to have a network with low latency and high reliability, since the car operates based on sensors and without human supervision.

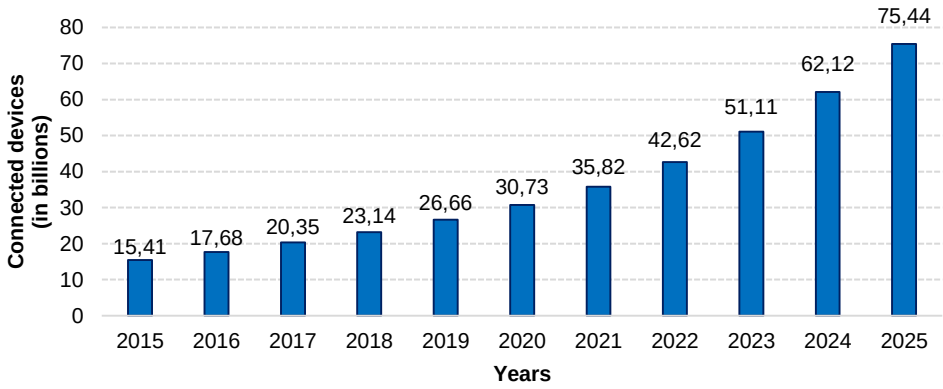

Figure 1.1: Connected devices (in billions) over the years (based on [3]).

These and other technologies require the birth of a new network standard to deal with their requirements. The 5th generation (5G) standard was released in order to meet all user demands. The 5G services are

focused on the combination of three categories: Massive Machine Type Communications (mMTC), Ultra-Reliable and Low Latency Communications (uRLLC) and Enhanced Mobile Broadband (eMBB). mMTC focus on situations where massive connectivity is needed, uRLLC focus on services where the minimization of delay and quick response is very important and eMBB focus on services where high data rate is crucial. In Table 1.1 the expected improvements of 5G in relation to 4G are presented.

Table 1.1: Improvements of 5G compared to 4G (based on [4]).

	4G	5G
Latency [ms]	10	<1
Data Traffic [Exabytes/Month]	7.2	50
Peak Data Rates [Gb/s]	1	20
Available Spectrum [GHz]	3	30
Connection Density [Connections/km^2]	100 Thousand	1 Million

One of the promising technologies, currently being study, to insert in 5G cellular networks is Device-to-Device (D2D) communications.

In conventional cellular systems, all communications must go through the base station (BS), even if both users are within a small distance. The BS is responsible for resource allocation, synchronization and almost every aspect that enables the communication between multiple devices. However, in accordance with the 3GPP (3rd Generation Partnership Project) standard, in specific cases where user's equipment are in proximity, as commercial/social services, or even in case of cellular network infrastructure failure, with D2D technology there is no need to pass the information through the cellular network infrastructure. In the 3GPP, this is called D2D Proximity Services (ProSe). Studies and simulations have shown that this type of communication (D2D) has some potential benefits such as improving spectral efficiency, throughput, power efficiency, delay, outage probability and frame loss ratio [5].

At this point, a different type of network can be established. When there is a certain amount of devices in a specific area, communicating between each other using only D2D communication, a D2D network is created. There are diversified manners to classify D2D networks. One way is based on the degree of involvement of the BS in assisting the change of information between D2D devices [6]. Another one is based on the band used by the D2D devices (unlicensed or licensed spectrum) [5]. Also, the communications can be in coverage or out-of-coverage. A D2D device is considered to be out-of-coverage when the average signal-to-interference-plus-noise ratio (SINR) received from the cellular network infrastructures is less than -6 dB [7].

This project is focused on a D2D network working in unlicensed spectrum (low ISM - Industrial, Scientific and Medical - band) and out-of-cellular coverage which implies that it does not have any support from cellular infrastructures. Notice that although the D2D Proximity Services standardization in 3GPP do

indeed promote higher rates, in the setting proposed the use case is different since the study is done for long range communications (up to 2km with 163 dB of coupling loss) which can lead to lower rates. Hence, the D2D network in study involves the use of a system that can fulfil the requirements presented in Table 1.2.

Table 1.2: Requirements of the network in analysis.

	Requirements
Type of Communication	Device-to-Device
Band	Unlicensed
Coverage by Cellular Network	Out-of-coverage
Involvement of Cellular Infrastructures	No
Communication Range	Up to 2 km with 163 dB of coupling loss

The target applications for this setting includes places with poor or no cellular network coverage, such isolated places like mountains, open sea, etc. and even public safety services in case of radio infrastructure failure. The D2D network setting is presented in Figure 1.2.

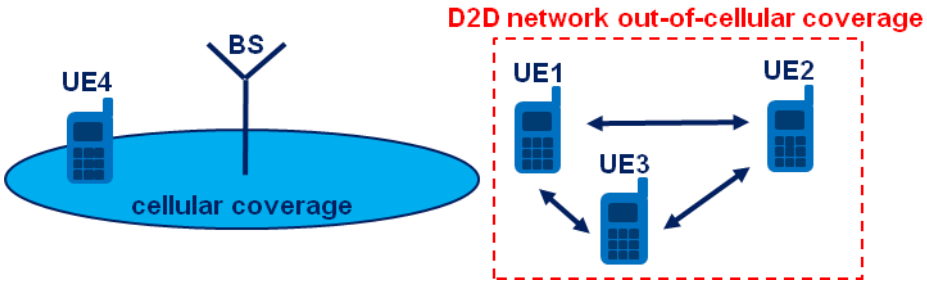

Figure 1.2: D2D Network setting for this case study.

Before a D2D link can be established, the following three processes need to be completed:

- Synchronization: all devices in a certain area have to be synchronized. This means that they have to share the same clock and find the same timeslot/frequency so they can communicate between each other without infrastructure support.

- Discovery: one device has to be able to find other nearby devices.

- Communication: that includes the actual exchange of information between devices and techniques used to prevent loss of information during the passage from the transmitter to the receiver.

In this dissertation, the emphasis is put on the discovery process and there are several challenges to be overcome during this process due to the lack of coordination in the proposed setting.

For example, devices participating in a discovery procedure are susceptible to:

- Interference: caused by ongoing discovery procedures and other communications between D2D devices. Also, it can be created by other devices transmitting in unlicensed bands.

- Rendezvous mismatch: happens when there is no specific resource for transmission and reception of discovery messages. Because of that, devices do not know in which time and frequency resource they should transmit, so the other devices can hear the message and reply.

- Proximity uncertainty: a device only knows with certainty that another device is in proximity when the associated discovery procedure is done successfully.

The main focus of this thesis is in the interference caused by the lack of coordination inherent to non-cellular networks.

1.2. State of the Art

The proposed D2D network involves the creation of a new system since the ones currently being used do not fulfil the requirements. Some of those systems and the reason why they do not fulfil the requirements are presented:

- Wi-Fi and Bluetooth: Although these connectivity standards allow direct communications, they are designed for wireless communications in short distances, so their maximum range is lower than required [8].

- GSM (Global System for Mobile Communications)/EDGE (Enhanced Data rates for GSM Evolution): These technologies described the first digital cellular networks. GSM was the key of the 2nd Generation (2G) and it is focused in voice. Later, a new technology GPRS (General Packet Radio System) allowed the introduction of data packets transmissions. Finally, an upgrade of GPRS – EDGE – was defined to provide higher data rates [9]. These technologies do not support unlicensed bands and their protocols only allow device-network communications and not device-device communications. D2D communications appeared later, in LTE (Long Term Evolution) release 12 of 3GPP.

- D2D ProSe: As mentioned before, D2D appeared in LTE release 12 and the main purpose of these services was in public safety use cases, commercial scenarios and for network offloading. So, although it allows direct communications, it was not designed to be used in unlicensed bands. Also, its maximum range is lower than the required. For example, LTE-Direct is one D2D technology working in the LTE licensed band allowing a maximum distance between devices of 500 meters [10].

- NB-IoT (Narrowband-Internet of Things): This technology emerged to turn IoT possible. It creates the environment required for a network with massive connectivity, supporting low power

consumption and a wide coverage range for IoT devices. However, it is not optimized to work in unlicensed bands and it does not support device-to-device communications. Also, its downlink and uplink rates do not allow voice services [11].

- LAA (Licensed Assisted Access)/MuLTEfire: These LTE based technologies work in unlicensed band with the goal of lightning the data traffic in the LTE licensed band. The standardization of these systems is still ongoing and has no yet covered D2D functionality. Yet some initial architectural studies have been made [12].

In terms of how to deal with interference, many researchers and mobile companies are concentrated in interference between cellular networks and D2D devices because their current focus is in the introduction of D2D in 5G cellular networks. Hence, a significant amount of research papers present in the literature describe interference cancellation techniques that take advantage of network support done by the infrastructures or the fact that D2D and cellular devices share the same licensed spectrum [13] [14].

However, in the system model considered in this thesis, the D2D devices do not have any support from the network infrastructures and work in unlicensed spectrum, the focus is then on methods to cope with the interference between these D2D devices. One solution proposed in the literature to deal with this kind of interference is to introduce interference cancellation at the receiver; this can be implemented into the receiver architecture of the D2D devices in the form of successive interference cancellation (SIC) or parallel interference cancellation (PIC). These techniques allow the detection of the multiple signals (signal of interest and interferers) present in a received signal. In SIC, the signals presented in a received signal are estimated and cancelled one by one from the total signal, starting with the strongest one and going in a descending order of power. In PIC the interfering signals from a received signal are estimated all at the same time, in a parallel manner and then cancelled from the total signal [15]. Another strategy that can be inserted in D2D devices to cancel or mitigate interference is power control. Namely, when a device receives a signal from another device and it has to reply to it, it first tries to estimate the channel through which the signal went through and with its inversion calculates the minimum power that has to be transmitted to reach a certain signal-to-noise ratio (SNR) at the destination, thus reducing the interference towards other devices [16].These techniques are the fundamental blocks of the interference mitigation solutions presented in this thesis.

1.3. Objectives

This thesis was done in collaboration with the company Intel Mobile Communications in Aalborg, Denmark, and it addresses interference cancellation techniques to deal with the problem of interference within D2D communications without cellular network support.

The purpose of this thesis is to create an original solution that can take advantage of the two sides of a D2D communication – transmitter and receiver – and of a known existing technique – SIC – creating a

new procedure that has benefits when comparing to existing techniques and can be used to mitigate interference in the specific setting in consideration.

First, to achieve this goal, the proposed solution is well-designed having into account the physical (PHY) and Media Access Control (MAC) layers. Then, in order to evaluate it, a system is developed with the implementation of a Link Level Simulator (LLS) and a System Level Simulator (SLS) with the support of the software Matlab 2017a. Finally, an evaluation of the proposed solution, in terms of performance and complexity is performed.

1.4. Thesis Outline

The remaining of this report is organized as following:

- In chapter 2, fundamental concepts to understand how the proposed solution is inserted in the technologies that already exist, are presented. Here it is explained the SIC process, and how to connect it with the physical (PHY) and Media Access Control (MAC) layers.

- In chapter 3, the solution proposed to mitigate the problem in consideration is described. First, basic notions used to establish the proposed solution are defined. Then, the developed solution and different employed techniques are presented.

- In chapter 4, the system implementation that allowed the evaluation of the proposed solution is described.

- In chapter 5, results are presented and analysed and different techniques are studied and discussed in terms of performance and complexity.

- In chapter 6, conclusions and future work are drawn.

1.5. Contributions and Outputs

This dissertation addresses a new way to tackle the interference problem in a D2D network without cellular infrastructure support. With this work, three invention disclosure reports have been made, which have now been filed jointly into one jumbo Intel patent. This being said, it is possible to divide the work in three major contributions for the research of improved interference cancellation techniques.

The first technical contribution of this dissertation arose from the resolution of an initial problem detected when the proposed solution was still an idea. It was the fact that since in this type of network the devices establish communication links between each other through a random access scheme, the number of contending devices is unknown to the receiver. Hence, there is a possibility that the receiver is not applying the appropriate decoding process (e.g. number of SIC rounds). To solve this problem, the use of multiple orthogonal pilot sequences by the transmitter devices was considered jointly with a remarkable new receiver block – pilot activity detection block – that allows the receiver to detect the

active pilot sequences in a signal and therefore to have an extra information about the received signal. The invention disclosure report made to describe this inside the Intel company is: “Interference Aware Receiver Architecture with Adaptive Complexity for Random Access Based Networks”, R. Martins, D. Brocco, R. Kotaba, N. Pratas, E. Jakobsen, B. Badic and C. Drewes, June 6, 2018.

A second technical contribution and the most important is the actual solution proposed in this dissertation. Mainly, this solution consists in the execution of different types of SIC (intra and inter-SIC) by a receiver device. However, sometimes modifications only in the receiver architecture are not enough to take the most of the techniques. Therefore, one of the most relevant parts in this work is the fact that both sides of the communication link are taken into account. In the transmitter side, in addition to the use of multiple orthogonal pilot sequences as mentioned before, the device also randomly chooses a transmission pattern, from a pre-defined set, to send its packets. This is possible due to the creation of a new concept of frame – virtual frame. While in the receiver side, with the assistance of a pilot activity detection block, the receiver device performs different types of SIC in order to mitigate the interference received. The solution was presented in an internal Intel report: “Random Access Scheme with Inter and Intra Slot Interference Cancellation Capabilities for Uncoordinated Device-to-Device Network”, R. Martins, D. Brocco, R. Kotaba, N. Pratas, E. Jakobsen, B. Badic and C. Drewes, June 29, 2018.

Finally, a third technical contribution came from the detailed study and implementation of the pilot activity detection block mentioned before. Since this is a new and invented block, it cannot be found in the literature. Hence, during the development of this dissertation, three different architectures for this block were also built and tested. The description and simulation results obtained for each architecture were presented in an internal Intel report: “Pilot Activity Detection for Random Access in an Uncoordinated Network”, R. Martins, D. Brocco, R. Kotaba, N. Pratas, E. Jakobsen, B. Badic and C. Drewes, July 13, 2018.

The detailed description of all techniques that allowed the writing of the three invention disclosure reports and consequently the creation of the Intel patent is presented in chapter 3 of this dissertation.

2. Fundamental Concepts

In this chapter, fundamental concepts required to understand and develop the thesis are described.

2.1. Theoretical foundations of interference in multi-user networks

In D2D communications, multiple users can send their information to a common receiver; multiple access techniques allow the division of the channel between the users - TDMA (Time Division Multiple Access), FDMA (Frequency Division Multiple Access) and CDMA (Code Division Multiple Access) are examples of channel access schemes [17]. However, these schemes need coordination, for example from a BS. In the specific setting, defined in the previous chapter, since it is an uncoordinated network, the focus is on a multiple access scheme named slotted ALOHA. In this scheme, the time is divided in equal-duration slots, that allow the transmission of packets, and each user can start the packet transmission only at the beginning of a timeslot. Furthermore, the access is half-duplex, this means that one device can be a receiver and a transmitter, but not on the same timeslot. This will be explored in more detail in the next sections.

In a standard network, when multiple users transmit to the same device, this would result in a collision and in most cases only the strongest signal would be decoded by the receiver. Successive Interference Cancellation (SIC) is a method that allows a receiver to decode multiple received signals, thus coping with the collided received signals. First, as said in the previous chapter, SIC decodes the strongest signal and subtracts it from the received signal. This procedure is iteratively repeated with the rest of the signals. This process will be described in more detail in the next sections.

In the following it is shown a specific case of Multiple Access Channel (MACh), how the SIC method theoretically works and how to relate it with the capacity of a MACh.

Gaussian Multiple Access Channel

Consider the scheme of Figure 2.1.

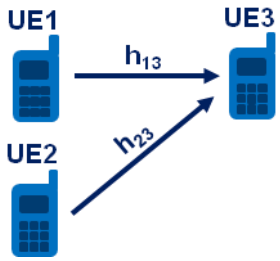

Figure 2.1: Specific scheme for posterior analysis.

The Gaussian MACh for the specific case represented where there are two senders (user 1 and user 2) and one receiver (user 3) is described as follows:

$$y = h_{13} \cdot x_1 + h_{23} \cdot x_2 + n \tag{2.1}$$

where x_1 and x_2 are, respectively, the zero-mean Gaussian complex signal transmitted by the devices 1 and 2, such that the respective variances are $E[|x_1|^2] = P_1$ and $E[|x_2|^2] = P_2$, where $P_1$and P_2 represent the constant power levels used by the devices 1 and 2, respectively; n is a complex Gaussian variable that contains the noise such that the respective variance is $E[|n|^2] = N$, where N is its power level; h_{13} and h_{23} are the complex gains of the channels from device 1 to 3 and from device 2 to 3 respectively; and finally, y is the received signal in device 3 [18]. Note that for ease of explanation it is assumed that the channel between the devices, h_{13} and h_{23}, are constant and for simplification equal to 1.

As previously stated, when using SIC, the process starts with the decoding of the strongest signal (as an example it is assumed that the strongest signal is x_2). To decode x_2, x_1 is treated as interference. Hence, if the signal-to-interference-plus-noise ratio of user 2 at user 3 ($SINR_{23}$) is higher than a certain threshold:

$$SINR_{23} = \frac{P_2}{P_1 + N} > \tau \tag{2.2}$$

the signal from user 2 can be decoded and according to [17] and assuming that B is the total bandwidth, the transmitted rate from user 2 to user 3 has to be below the following channel capacity:

$$C_{23} = B \cdot log_2(1 + \frac{P_2}{P_1 + N}). \tag{2.3}$$

If x_2 is decoded correctly, it is then subtracted from the received signal and this becomes:

$$\hat{y} = y - \widehat{h_{23}} \cdot x_2 \sim h_{13} \cdot x_1 + n \tag{2.4}$$

where $\hat{y}$ is the received signal without the contribution of the user 2 and $\widehat{h_{23}}$ is the user 2 channel estimation. After, from what is left, $\hat{y}$, if the signal-to-noise ratio of user 1 at user 3 (SNR_{13}) is higher than a certain threshold,

$$SNR_{13} = \frac{P_1}{N} > \tau \tag{2.5}$$

x_1 can be decoded and the highest transmitted rate possible for it becomes:

$$C_{13} = B \cdot log_2(1 + \frac{P_1}{N}). \tag{2.6}$$

So, for this case, SIC is theoretically feasible if x_1 and x_2 are transmitted with rates lower than C_{13} and C_{23} respectively. Figure 2.2 shows the rates that can be achieved by all the users simultaneously with arbitrarily small bit error probability; this kind of diagram is known as the capacity region of a multiple access channel.

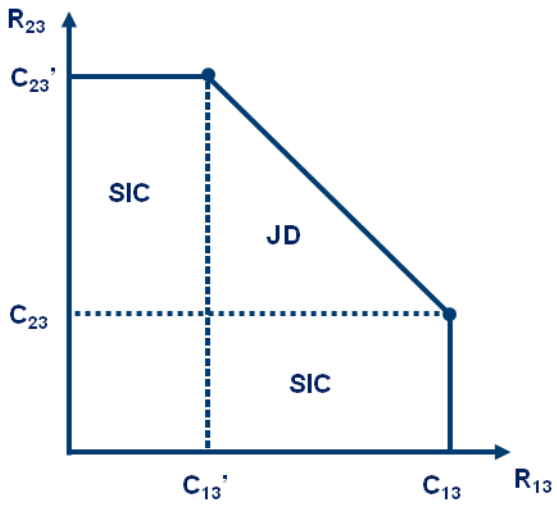

Figure 2.2: Capacity region of a MACh (based on [17]).

The previous given example, describes the case of the corner point (C_{13}, C_{23}) of the figure. If x_1 had been chosen as the strongest signal, it would be considered the region related to the corner point (C_{13}', C_{23}'), and for SIC to be theoretically feasible, the rates would have to be below the following:

$$C_{13}' = B \cdot log_2(1 + \frac{P_1}{P_2 + N}) \tag{2.7}$$

$$C_{23}' = B \cdot log_2(1 + \frac{P_2}{N}). \tag{2.8}$$

In the points $(C_{13}, 0)$ and $(0, C_{23}')$ one of the senders is transmitting its information at maximum rate while the other is not sending any information.

Regarding the other regions, the one represented with JD (Joint Decoding) is the most complex region of operation because in there the receiver jointly decodes both signals, exploiting coding strategies using, for example, a hybrid of SIC and rate-splitting or time-splitting coding. In the one below the pair of rates (C_{13}', C_{23}), both signals are decoded assuming the other transmission as noise, meaning that signal 1 is decoded assuming signal 2 as noise and vice versa.

With this simple example it is shown that SIC and JD can provide an increase in the channel capacity, being the borders of the capacity region of a MACh the following:

$$R_{13} \leq B \cdot log_2\left(1 + \frac{P_1}{N}\right) \tag{2.9}$$

$$R_{23} \leq B \cdot log_2\left(1 + \frac{P_2}{N}\right) \tag{2.10}$$

$$R_{13} + R_{23} \leq B \cdot log_2\left(1 + \frac{P_1 + P_2}{N}\right). \quad (2.11)$$

Notice that depending on channel realizations, the Gaussian MACh capacity region can expand, contract and even skews. The spatial dimensions, can also change, depending on the number of signals [18].

In the next section, fundamental concepts of great importance, related with the PHY layer, for the development of the proposed system will be described.

2.2. Physical layer

To get a model that characterizes the communication protocols between different communication systems, the Open Systems Interconnection model (OSI model) was created. This model divides the communication process into seven layers as depicted in Figure 2.3.

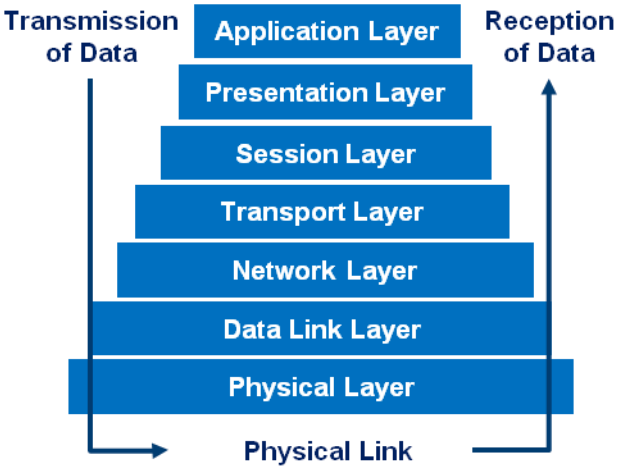

Figure 2.3: Layers of the OSI model (based on [19]).

The PHY layer is the lowest layer in the OSI model and is responsible for the network hardware and the data transmission in a communication link. Its responsibilities include all the aspects related with data processing before entering the channel, data transmission and reception [20]. This layer has a great importance in this project, since one of the goals of this project is to perform a form of cross-layer optimization between the Physical and Data Link Layer, in order to increase the performance in the proposed network setting.

2.2.1. Frame Structure: Narrowband-IoT

For the progress of this project, and especially for the development of the LLS, it was considered the frame structure presented in chapter 10 of the 3GPP TS 36.211 [21] and usually used in Narrowband-IoT Uplink. Here, the modulated symbols are mapped in resource elements (RE) and they can be defined by the index pair (k, l), being k and l the indices in the frequency and time domain, respectively,

in the resource grid. This resource grid is composed by a certain number of slots that together form a resource unit. Each slot is defined by a certain number of subcarriers and Single Carrier-Frequency Division Multiple Access symbols, as shown in Figure 2.4.

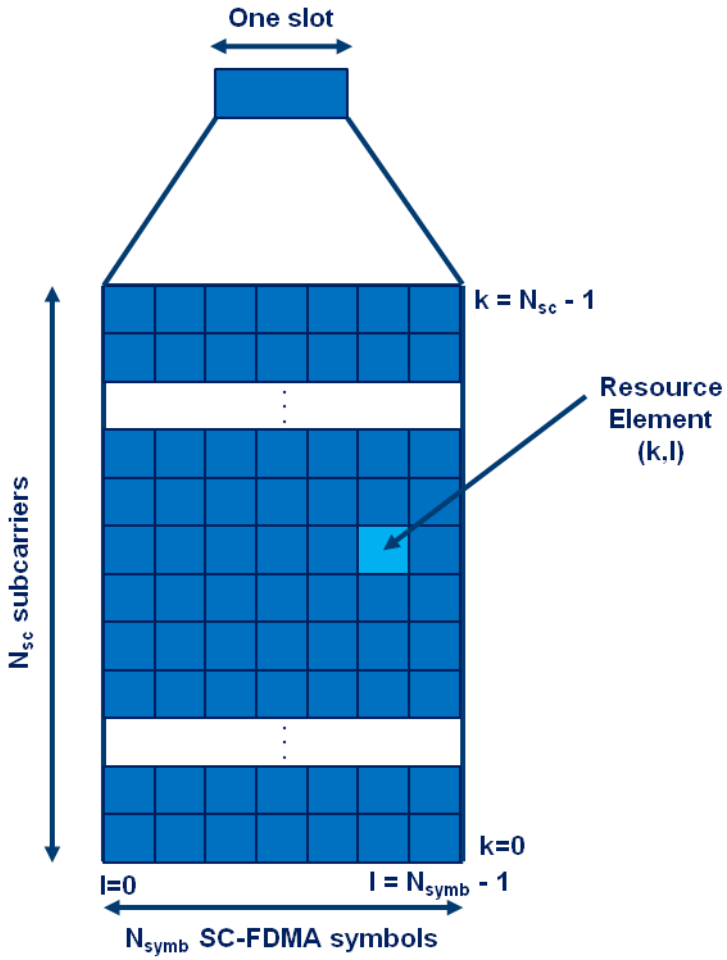

Figure 2.4: Resource grid used in NB-IoT (based on [21]).

The biggest difference between the technique of Single Carrier-Frequency Division Multiple Access (SC-FDMA) and the known Orthogonal Frequency Division Multiple Access (OFDMA) is that in the last one each subcarrier only carries information about one specific symbol while, due to the inclusion of a Discrete Fourier Transform (DFT) and an Inverse DFT (IDFT) in the transceiver chain of the SC-FDMA, SC-FDMA allows each subcarrier to contain information of all symbols. Because all subcarriers have the same symbol, in a certain period of time, the inter-symbol interference will be reduced and the information can be recovered from the subcarriers experiencing better channel conditions [22].

Also, when passing to time domain, there is a need to apply a guard interval named Cyclic Prefix (CP) to the SC-FDMA symbols. The purpose of CP is to avoid inter-symbol interference and inter-carrier interference. When the receiver is receiving a certain SC-FDMA symbol, it receives multiple SC-FDMA symbols due to multipath. The CP is put in the beginning of the symbols, preventing the delayed symbols from interfering the next symbols, as shown in Figure 2.5; as CP is composed by the last part of the SC-FDMA symbols, it provides a continuous spectrum.

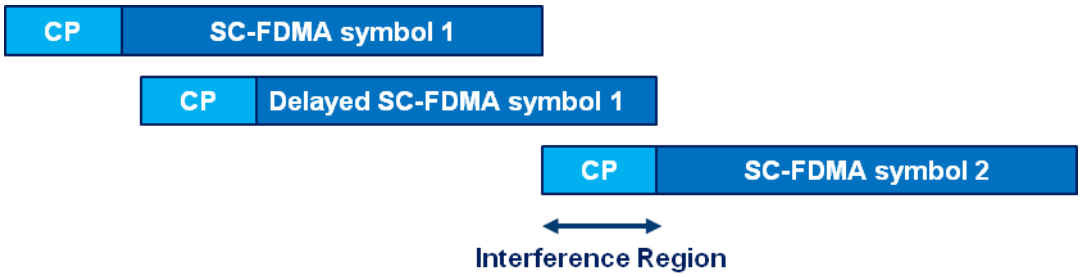

Figure 2.5: Function of the Cyclic Prefix (based on [20]).

In the development of the LLS, taking in consideration the standard for the NB-IoT Uplink, it was considered a frame structure of type 1, using NPUSCH format 1 with subcarrier spacing of 3.75 kHz or 15 kHz, and 16 slots per resource unit with 7 SC-FDMA symbols and 48 or 12 subcarriers per slot, with only one of the subcarriers occupied with modulated symbols.

Furthermore, in order to enable the receiver to estimate the channel, reference signals (RS) or pilots, which are specific data placed in specific positions in the resource grid of the transmitted data and are known by the receiver, are used.

2.2.2. Reference Signals and Channel Estimation

Channel properties change as a function of place and time, so with the knowledge of the received pilots and the transmitted pilots, the receiver can estimate the channel at given positions. In the specific case of D2D, Demodulation Reference Signals (DM-RS) are used and all of them are in all of the subcarriers of one specific SC-FDMA symbol. For example, it is standardized [21] that for NPUSCH format 1 and frequency spacing of 15 kHz, all reference signals are in the SC-FDMA symbol number 3.

Now that it is known how the reference signals are used and the channel estimation at given positions, channel estimators, to obtain the channel estimation for all the transmitted data, can be used. The channel estimators used in this project are Minimum Mean Square Error (MMSE) based. This is already a complex type of channel estimation because it requires matrix inversion and the calculation of covariance matrixes,

$$\widehat{H_{MMSEi}} = R_{h,h_p} \cdot \left(R_{h_p,h_p} + R_{ri} \cdot I\right)^{-1} \cdot \widehat{H_{LSi,p}} \tag{2.12}$$

$$\widehat{H_{LSi,p}} = x_{i,p}^{-1} \cdot y_p \tag{2.13}$$

$$R_{n,n'} = J_0\left[2 \cdot \pi \cdot f_{Dmax} \cdot (n - n') \cdot T_{sym}\right] \tag{2.14}$$

being $\widehat{H_{MMSEi}}$ the MMSE channel estimation of signal i , $\widehat{H_{LSi,p}}$ the least square (LS) channel estimation, with pilot symbols, of signal i, R_{h,h_p} the covariance matrix between pilots and data, R_{h_p,h_p} the pilot's auto-covariance matrix, J_0 the zeroth-order Bessel function, f_{Dmax} the maximum Doppler shift, T_{sym} an SC-FDMA symbol period, $(n - n')$ the difference between index n and n', R_{ri} the noise covariance

matrix of signal i , I the identity matrix and $x_{i,p}$ and y_p the transmitted pilot symbols from signal i and received pilot symbols respectively. With this baseline it is possible to differentiate two types of channel estimation:

- MMSE-Maximum Ratio Combining (MRC), that treats the interference of other signals that may interfere as noise, and whose noise covariance matrix for a signal of interest is

$$R_{r0} = R_N = \frac{1}{n_p}\sum_{p=1}^{n_p}\left(\left(y_p - \widehat{H_{MMSE0,p}}\cdot x_{0,p}\right)\left(y_p - \widehat{H_{MMSE0,p}}\cdot x_{0,p}\right)^H\right) \quad (2.15)$$

  being n_p the number of pilots used, y_p the received pilots, $x_{0,p}$ the transmitted pilots in the signal of interest, $\widehat{H_{MMSE0,p}}$ the channel estimation of the signal of interest in pilot positions and the H the conjugate transpose operation.

- MMSE-Interference Rejection Combining (IRC), that considers the effect of other interfering signals in the noise covariance matrix as following

$$R_{r0} = \frac{1}{n_p}\sum_{p=1}^{n_p}(\widehat{H_{MMSE1,p}}\cdot \widehat{H_{MMSE1,p}}^H) + R_N \quad (2.16)$$

$$R_N = \frac{1}{n_p}\sum_{p=1}^{n_p}\left(\left(y_p - \widehat{H_{MMSE0,p}}\cdot x_{0,p} - \widehat{H_{MMSE1,p}}\cdot x_{1,p}\right)\left(y_p - \widehat{H_{MMSE0,p}}\cdot x_{0,p} - \widehat{H_{MMSE1,p}}\cdot x_{1,p}\right)^H\right) \quad (2.17)$$

  being n_p the number of pilots used, y_p the received pilots, $x_{0,p}$ the transmitted pilots in the signal of interest, $\widehat{H_{MMSE0,p}}$ the channel estimation of the signal of interest in pilot positions, $x_{1,p}$ the transmitted pilots of an interfering signal, $\widehat{H_{MMSE1,p}}$ the channel estimation of an interfering signal in pilot positions and the H is the conjugate transpose operation.

Note that although MMSE-IRC requires more complexity, since it needs to know the pilots used by the interfering signals and to estimate its channels, it has better performance due to the fact that takes its consideration in its process.

2.2.3.Types of SIC in respect to the PHY layer

Even though there are several types of interference cancellation receivers, the most common and the one of interest in this project is the Successive Interference Cancellation (SIC). The SIC receiver is basically, as said before, a continuous cancellation of signals in the receiver. In a case where there is more than one device transmitting, in each iteration, the energy of the user signals is estimated and the signal with the largest energy is the one to be subtracted from the received signal. Thus, in every iteration the signals are withdrawn one by one from the received signal in a descending order of estimated energy. When withdrawing each signal, the receiver can choose if it only wants to decode/obtain a signal of interest or all signals. The main disadvantage of this kind of interference

cancellation is that if the number of users increase, the processing time will increase as well [15]. Additionally, there is also two types of SIC receivers, exposed in Figure 2.6: at Symbol-level and at Codeword-level.

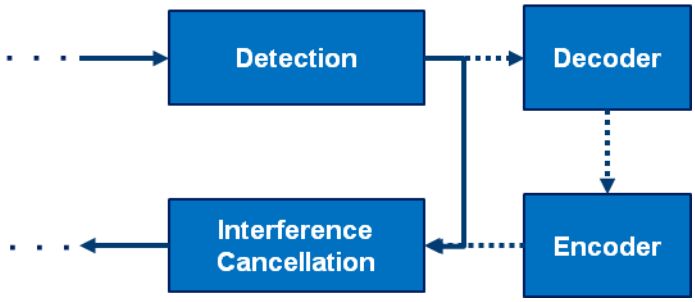

Figure 2.6: Difference between Symbol-level (fill line) and Codeword-level (dash line) interference cancellation (based on [23]).

At Symbol-level, the signals are demodulated and the subtraction is done without a priori decoding while at Codeword-level, the signals are demodulated, decoded and re-encoded before being subtracted. Although the Codeword-level approach is more complex, it achieves a better performance than the Symbol-level one due to the fact that the decoder allows correction of errors. Note that to allow the subtraction of the signals, the receiver has to know some parameters such as the MIMO (Multiple-Input Multiple-Output) configuration (for example, number of antennas and mapping of the symbols to each antenna), the modulation and coding scheme (MCS) and the information of the signals channel. In addition to that, when using Codeword-level SIC, the receiver has to be aware of any technique of encryption that could have been used in the transmission of the signal, so it can decode and re-encode the signal.

2.3. Media Access Control layer

This chapter is focused on the aspects of the Media Access Control layer that enable interference cancellation in the proposed solution.

This layer is, actually, a sub-layer of the Data Link layer from the OSI model and is responsible for the construction of frames before the transmission and for the frame recovery and error detection in the receiver. In a random access setting, the MAC layer is also responsible for when the device should transmit and controls the retransmission procedure, for example, in the setting in consideration, a device A has to retransmit its message until it receives a message from device B, saying that the communication was done successfully.

In a cellular network, when data is exchanged between network nodes, the access is scheduled, possible through a BS. The exception is when the user is connecting to the network for the first time, where a random access occurs. In the setting in consideration, because there is no centralized control, all the devices are always contending when transmitting data. In both cases, random access protocols exist to recover transmitted user data packets, in the receiver.

2.3.1.Random Access Protocols

First, let us see which is the random access protocol used in a cellular network nowadays, and from there, reach the one that meets the necessary requirements for the D2D setting in study.

Framed Slotted ALOHA

Currently, in a cellular network, the random access protocol being used is the framed slotted ALOHA. This protocol divides the time into equal-duration slots and these ones are organized in frames. Each user can transmit each packet of information in only one random slot of a frame. The slots with multiple user transmissions are called collision slots, the ones with no transmissions are called idle slots, and the ones with one transmission are named singletons. If a slot has only a single transmission, the information can be obtained by the receiver, otherwise, the slot is considered as wasted [24]. Notice that here it is considered a simplifying assumption that the collisions are destructive. Yet, in practice a receiver (even one without interference cancellation) can decode a transmission even if other transmissions are interfering, if its SINR is above a certain threshold. This will be further discussed later.

This being said, it is possible to understand in the setting depicted in Figure 2.7 that for example, in slot 1 and 3 in the first frame there are collision slots because there are two users trying to send information at the same time, slot 2 and 4 in the first frame are idle slots because they are not transmitting any information and with slot 2 and 3 of the second frame the receiver can obtain the information from user 4 and 1 respectively.

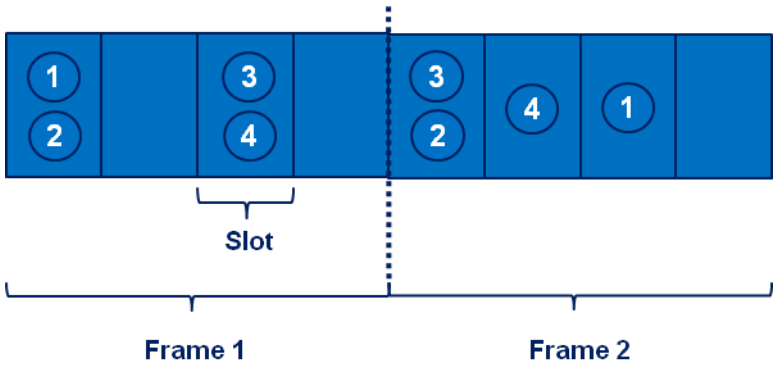

Figure 2.7: Setting for explanation of Framed Slotted ALOHA (based on [24]).

Here it is possible to impose the throughput concept which is the probability of successful receiving a user packet per slot. Because in this concept only the singleton slots are taken into account, the throughput is rather low for this kind of random access. This can be shown, considering Poisson arrivals with arrival rate λ as following:

$$Pr(X = x) = \frac{\lambda^x \cdot e^{-\lambda}}{x!}. \tag{2.18}$$

The probability that in a given slot there is only one arrival is:

$$Pr(X = 1) = \frac{\lambda^1 \cdot e^{-\lambda}}{1!} = \lambda \cdot e^{-\lambda}. \quad (2.19)$$

This means that in the best case the throughput is:

$$T = \frac{1}{e} = 0.37\ packets/slot. \quad (2.20)$$

In a more realistic setting, the throughput will be higher than that, because as mentioned before, there is a non-zero probability that the SINR will be higher than the decoding threshold, thus transmissions can be decoded even in collision slots.

To allow a throughput growth, new techniques that permit the resolution of collisions have been developed. These advances connect random access protocols with SIC and are generally termed as Coded Random Access.

Coded Random Access

The procedure of this kind of technique is the following: each user transmits replicas of the same packet in multiple slots of a frame. When the receiver finds a singleton slot, it recovers its information and with SIC removes all of the replicas of this packet from the rest of the slots, transforming some collision slots in singleton slots allowing the receiver to recover these packets as well. The recovery and removal of replicas is done in an iterative way and each packet has pointers that indicate the position of the others replicas [24].

In Figure 2.8 (t=0), it is possible to see that in this unique frame, it exists two singleton slots (slot 2 and 4) and two collision slots (1 and 3). Starting with the decoding process in the first singleton, the receiver obtains packet 4 (t=1) and with SIC deletes its replica from slot 3 (t=2). Therefore, slot 3 passes from collision to singleton slot and the information from user 3 can now be obtain from slot 3 (t=3), which before the application of SIC, it could not. Then, it decodes packet 1 from singleton slot 4 (t=4) and, using SIC the replica of this packet is deleted from slot 1 (t=5), allowing the decoding of packet 2 that now is inserted in a singleton slot (t=6). Again, here it is considered that the singletons are always decoded and that the collision slots without the application of SIC are destructed, which is not what happens in reality and as said before, it will be further explained.

Knowing the definition of throughput, it is possible to calculate it for this last example as following:

$$T_{without\ SIC} = \frac{2}{4} = 0.5\ packets/slot \quad (2.21)$$

$$T_{with\ SIC} = \frac{4}{4} = 1\ packets/slot. \quad (2.22)$$

Thus, it is showed that using coding theory with random access, the throughput increases.

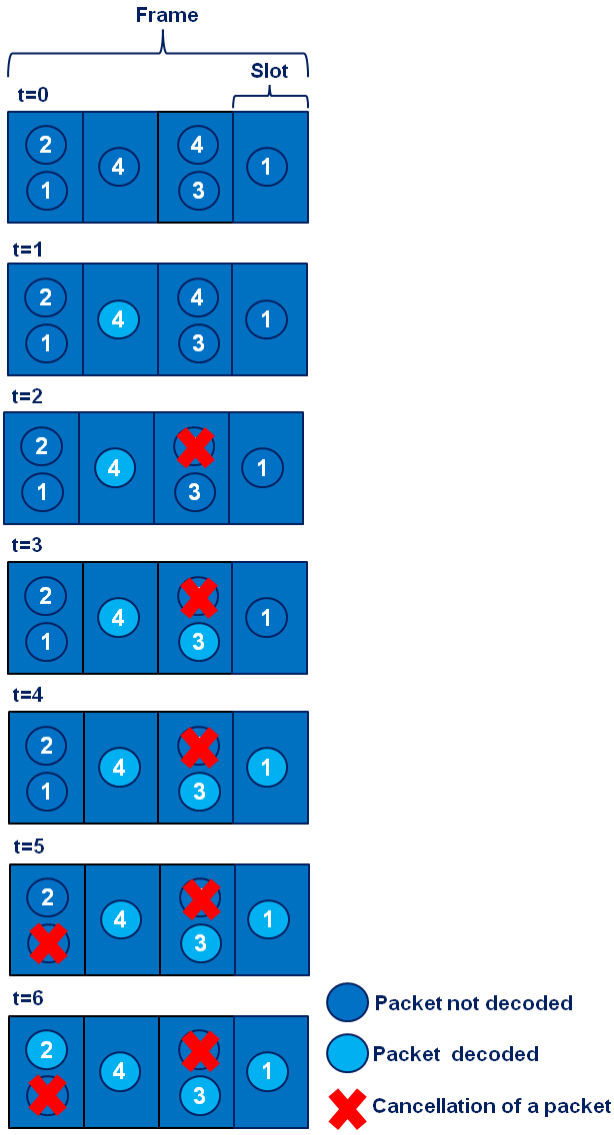

Figure 2.8: Setting variating in time for explanation of Coded Random Access (based on [24]).

However, in the last approaches that were discussed, unicast transmission was considered, this is, when several users transmit to a common receiver, for example a BS. In the case of D2D out-of-coverage, the setting presents different user's equipment working as transmitters and receivers. In this case, broadcast which is a scenario where users exchange information between each other, is studied. So, next, a new random access protocol is explained, called all-to-all broadcast coded slotted ALOHA (B-CSA), which mixes broadcast with coded random access.

Broadcast Coded Slotted ALOHA

In B-CSA, as in coded random access, the structure for transmission/reception is done through frames that are divided in slots of equal duration. Because, is this case, one user can be a receiver and a transmitter, and the slots that it uses for transmission, cannot be used for reception, the access is, as mentioned before, half-duplex . This means that if it spends its slots transmitting many replicas of its packet, it will not have slots to receive packets from other users. Hence, there is a kind of trade-off here

and B-CSA performance depends on it. Whenever it is not transmitting, the user buffers the received signal. For example, as depicted in Figure 2.9, user 1 sends a replica of a packet through slots 1, 2 and 3. Due to that, it can only receive packets from other users in slots 4, 5, 6 and 7. Notice that, like in coded random access, each packet has pointers to its copies so later, SIC can be applied.

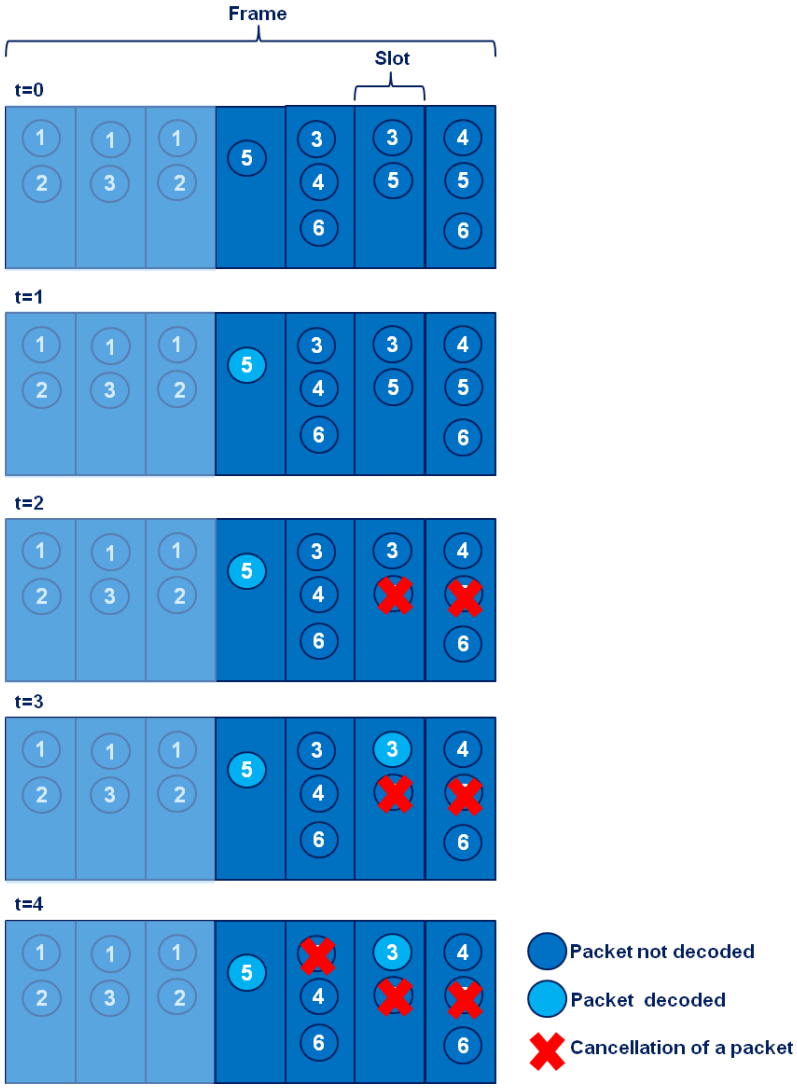

Figure 2.9: Setting variating in time to explain how B-CSA works (based on [25]).

Let us see how this works, by focusing on the performance of user 1 (t=0). As before, the slots with only one transmission are called singletons and the ones with more than one transmission are collision slots. Here, once more, it is considered that only singletons can be decoded. Hence, user 1 starts by decoding the singletons. In Figure 2.9, it is possible to see that slot 4 is a singleton, so user 1 decodes the packet from user 5 (t=1). After this, it subtracts the packet replicas from slot 6 and 7, through SIC, and the first one turns into a singleton slot (t=2). Therefore, user 1 can now decode the packet from user 3 (t=3), in slot 6, and cancel its replicas from the other slots (t=4). At this time, there are no more singletons to decode. However, user 4 and 6 still have two replicas each in slot 5 and 7 that cannot be decoded. This set of users are called stopping set, and are harmful structures that do not allow a complete decoding,

increasing the packet loss rate which will be explained next [25] [26].

To analyse the performance of this protocol, two parameters can be defined:

- Channel load: shows how "busy" the medium is,

$$g = \frac{n^{\underline{o}}\ users + 1}{n^{\underline{o}}\ slots}. \tag{2.23}$$

- Packet loss rate: shows the probability of a user to be unresolved by the receiver,

$$p = \frac{average\ n^{\underline{o}}\ users\ that\ are\ not\ successfully\ resolved\ by\ user\ A}{n^{\underline{o}} users}. \tag{2.24}$$

In an infinite frame length, all users are successively resolved if the channel load is lower than a certain threshold. However, in a case where the number of slots of a frame is limited and stopping sets can be created, an error floor appears in the performance of the packet loss rate. This means that after a certain point, even if the channel load is decreased, the packet loss rate does not decrease much. So, ideally to improve this protocol, the packet loss rate point where the error floor starts should be minimized [25] [26].

2.3.2. Types of SIC in respect to the MAC layer

Although, it was previously considered that singletons are always decoded and in collision slots the receiver cannot recover any data, in real life this is not what really happens, as stated before. Regarding singleton slots, they can only be decoded if the signal-to-noise ratio is above a certain threshold and concerning collision slots, as commented before there is non-zero probability that the signal-to-interference-and-noise ratio will be higher than the decoding threshold, so a receiver can decode a strong signal even when it is also receiving interference signals. This is called capture effect.

So in practice, the real process can be composed by two types of SIC: intra-SIC (realization of SIC within a slot) and inter-SIC (realization of SIC with data from a priori processing). Let us analyse this process with the example in Figure 2.10. Here, it is shown three users (1, 2 and 3) transmitting replicas of its packets in multiple slots of a frame. The receiver will process each slot of the frame starting by analysing slot 1. Exploiting the capture effect and the physical layer decoding techniques, it tries to decode the strongest signal in this collision slot, even with the presence of other interferers in it. Here it is considered that the signal from user 1 is the strongest. If this signal is decoded correctly, it is subtracted from the received signal in this slot and it tries to decode the second strongest signal in this slot (for example, signal from user 2) and so one. At this stage the receiver tries to decode a maximum number of signals in this slot and the ones that are decoded correctly are subtracted from the received signal in that slot and kept its information in a memory buffer. This subtraction process is called intra-SIC. Imaging that the signal from user 1 was decoded correctly but the signals from user 2 and 3 were not. At this point, the decoded user packet from user 1 is stored in a memory buffer. Later, when the receiver is processing slot 4, it can use the information kept in the memory buffer to cancel/subtract

(inter-SIC) the replica of the packet from user 1 and try to decode the packet from user 2 again without the presence of the packet from user 1.

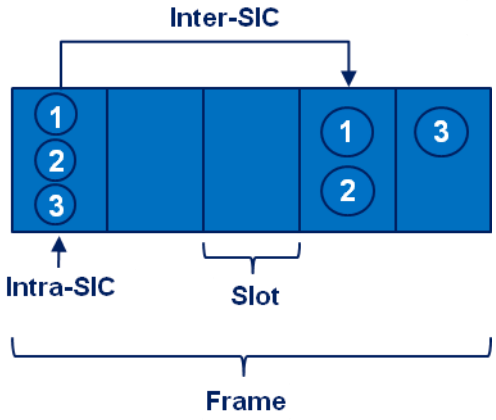

Figure 2.10: Real process that includes intra and inter-slot cancellation.

Hence, the final received signal at each slot, after the process is the following:

$$\hat{y} = y - \sum_{m=1}^{M} h_m \cdot x_m - \sum_{n=1}^{N} h_n \cdot x_n \tag{2.25}$$

where y is the received signal in a slot, $\hat{y}$ is the received signal after slot processing, x's are the transmitted signals, h's are the respective channels, M is the total number of decoded signals in a slot and N is the total number of decoded signals from other slots. Therefore $-\sum_{m=1}^{M} h_m \cdot x_m$ represents the intra-SIC and $-\sum_{n=1}^{N} h_n \cdot x_n$ the inter-SIC.

With this explanation, it is verified that now the receiver is capable of decoding multiple colliding packets with the junction between techniques that exploit the capture effect and the coded random access. Notice that although the explanation was referred to unicast, this applies to broadcast as well.

3. Proposed Solution

In this chapter, the solution proposed in this dissertation that take advantage of the two types of SIC mentioned before is described in detail.

3.1. Brief Introduction

As explained before, the setting studied in this project is focused in a D2D network without infrastructure network support and out-of-cellular coverage. Because of the limited network infrastructure support, the devices establish communication links between each other in a random access manner, using Slotted ALOHA. Hence, when there is a high number of devices attempting access to the wireless channel, the amount of interference experienced at the receiver will also increase making it difficult for the receiver to decode the received packets. Figure 3.1 depicts an example of random access, where devices 1 and 2 transmit for device 3. The reception of the signal of interest coming from device 1 is affected by the interference coming from the device 2 transmission, which will affect in a negative way the decoding process of the signal of interest.

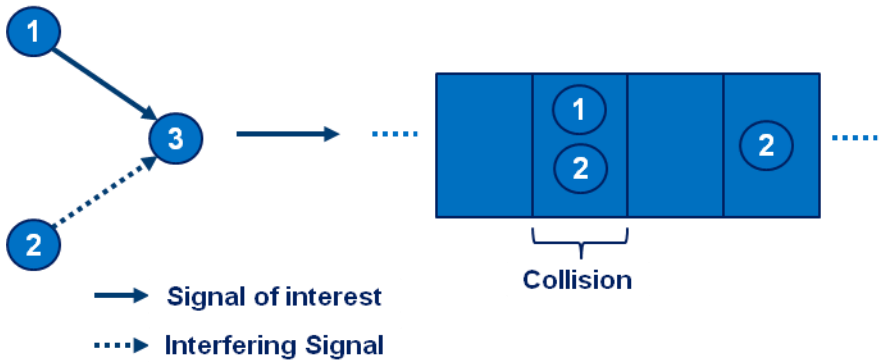

Figure 3.1: Example of random access.

In traditional networks, whenever the receiver cannot decode the intended packets, retransmission will occur, which will decrease the system level performance since it is transmitting more packets in a network that is already overloaded.

Hence, the purpose of this project is to mitigate the interference problem with a technique that includes both sides of the communication link:

- at the transmitter side, it is used a set of transmission patterns that are used in a random manner by the transmitter to send its packets and a set of multiple orthogonal pilot sequences from where a user randomly chooses one to insert in its message payload structure;
- at the receiver side, it is proposed an adaptive architecture that allows the use of two different types of Successive Interference Cancellation (SIC), inter and intra, taking into account the PHY and MAC layer of a system.

The concepts that this proposed solution entails gave rise to the second invention disclosure presented in section 1.5.

In Figure 3.2, it is shown that this random access scheme formulated with two types of SIC has significant improvements when compared to traditional solutions where SIC is not used or even if SIC is only used inside a slot (intra-SIC). An extended presentation of the obtained results will be presented in chapter 5.

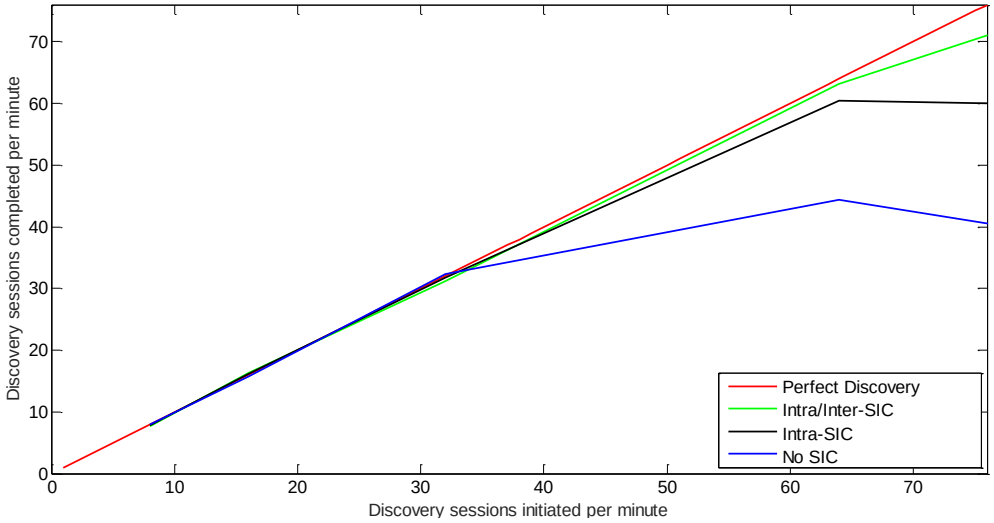

Figure 3.2: Average number of discovery sessions completed per minute for three different receiver architectures.

Before providing the full description of the proposed solution and its required changes at both transmitter and receiver side, it is important to clarify first the key concepts such as the protocol and frame structure applied in the proposed technique.

3.2. Key Concepts

As said before, this project is focused on the discovery process. In the discovery process, as shown in Figure 3.3, a discover initiator (DI) device sends a message 1 (MSG1) to a discover replier (DR) device, so it can be discovered by it. If a DR receives its message, it sends a message 2 (MSG2) back to DI. If the DI successfully receives MSG2, a discovery session just occurred. In case the DI does not receive MSG2 when expected, it sends a retransmission of MSG1.To reduce complexity in the devices, it is assumed that the Modulation and Coding Scheme (MCS) of MSG1 and MSG2 are fixed and, as said before, the multiplexing scheme is SC-FDMA.

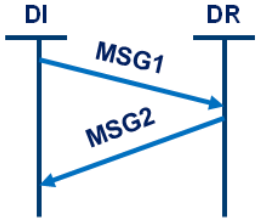

Figure 3.3: Discovery Protocol.

As introduced, a D2D link is divided into three phases: Synchronization, Discovery and Communication. Hence, each frame has different resources available for each phase. Independently of the frame duration, the resources available for the discovery process have a fixed duration of 32 ms, as depicted in Figure 3.4. Hence, for a device to know in which resources MSG1 and MSG2 are transmitted, there is a specific position in each frame that is saved for them, as shown in Figure 3.5. This solves the problem of rendezvous mismatch.

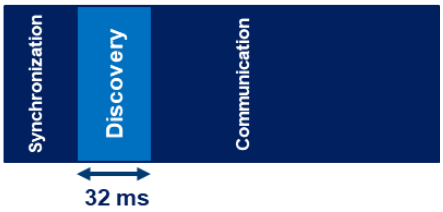

Figure 3.4: Frame Structure composed with the three phases.

Figure 3.5: Resources saved for the discovery process.

Also, MSG1 and MSG2 are transmitted with singletons in the discovery resource. Out of 48 available subcarriers, only 21 are usable (1 of the subcarriers is reserved for the MSG1 payloads and 20 are reserved for MSG2 payloads) to reduce interference due to leakage between subcarriers. Notice that the choice of this configuration was due to the fact that, as it will be explained later, the transmission of all MSGs1 is done with a fixed maximum power of 30 dBm while for the transmission of MSGs2, its transmission power calculation is done with the use of power control. Also, it is assumed that the subcarriers reserved for MSG1 and MSG2 are orthogonal to each other, hence the receiver can distinguish between MSG1 and MSG2 based on the subcarrier where the payload was received. The configuration used for the subcarriers is depicted in Figure 3.6, where MSGs1 occupy the subcarrier 1, while MSGs2 occupy even subcarriers, starting in subcarrier 10 and finishing at subcarrier 48.

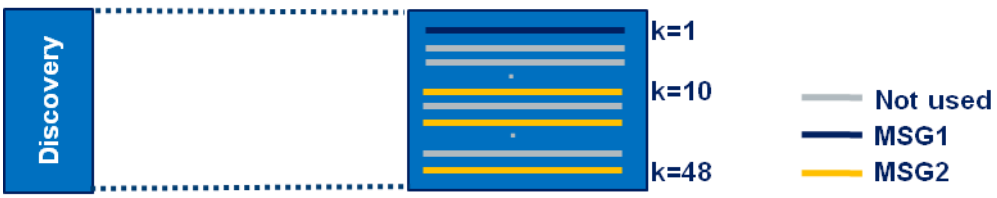

Figure 3.6: Subcarriers reserved for MSGs1 and MSGs2.

In order to have a flexible architecture at the receiver side and to take advantage of the use of inter-SIC, the concept of virtual frame is introduced. A virtual frame (VF) is a group of L consecutive discovery

slots in which it is possible to exchange information between slots belonging to the same VF. As will be seen later, the number of discovery slots in a VF is one of the key design parameters of this method, which allows to satisfy latency and memory requirements. The way the VF is constructed is presented in Figure 3.7.

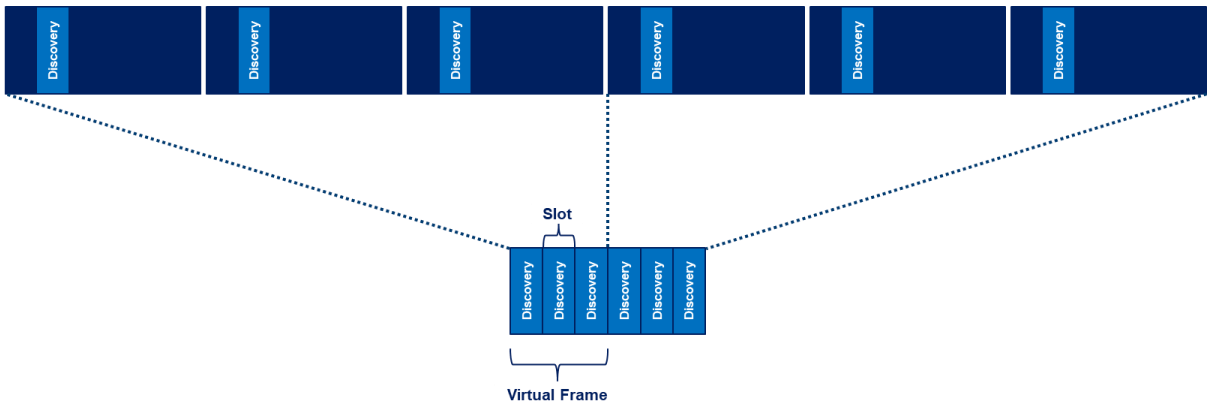

Figure 3.7: Virtual Frame construction.

Now that it was given some contextualization, let us see how the transmitter side was developed.

3.3. Transmitter Side

At the transmitter side, the simultaneous transmission of MSG1 generates interference for the DRs that are waiting for their reception. Hence, our goal is to avoid this overlap between MSGs1. Taking as parameters the number of replicas per packet per virtual frame and the size of the virtual frame, a set of possible patterns from where the DI can choose from, to send its message, is created. The purpose of this choice is to balance the number of interferers across the slots of the virtual frame. One logical way to optimize the size of the virtual frame is based on interference level. When the network does not present a significant amount of interference (devices trying to transmit) the virtual frame can be kept small, in order to keep memory and processing time low. Otherwise, the size of the virtual frame increases so it can deal with the substantial amount of interference. Note that, as said before, the devices are half-duplex, meaning that if MSG1 is transmitted in one slot by a DI, it expects the response to its message (MSG2) in the next slot. Hence, between MSG1 transmissions it has to exist at least one free slot.

So, in an example where it is considered a virtual frame of 5 discovery slots, and it is transmitted, in a virtual frame, 2 replicas of a MSG1, it is possible to observe that the total number of possible patterns that a DI can choose from to send its payload replicas is

$$\binom{L-r+1}{r} = \binom{5-2+1}{2} = 6 \tag{3.1}$$

as shown in Figure 3.8, with L being the size of the virtual frame and r the number of replicas in consideration.

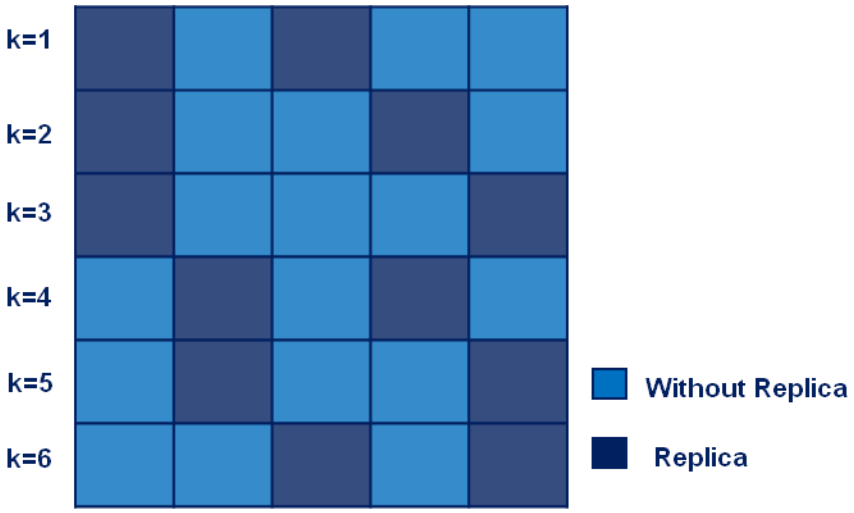

Figure 3.8: Possible patterns that a DI can choose from in a virtual frame of 5 slots and 2 available replicas.

In this example, the total amount of possible configurations is very low meaning that in a dense and uncoordinated network, a large number of DIs will choose the same configuration, so the occurrence of an extraordinary number of collisions is expected. So, the choice of the number of replicas and, again, the size of the virtual frame are two of the key design parameters that have to be considered. Another parameter that will be taking in consideration is the size of the set of possible configurations for transmission. For example, in the example exposed where there is 6 possible patterns, it is possible to pre-define a set with 1, 2, 3, 4, 5 or 6 possible patterns. The size of the set is defined before simulation and then the DIs choose a pattern for transmission from this pre-defined set, in a random way.

To send a certain message, a respective packet is created following the transmitter chain presented in Figure 3.9.

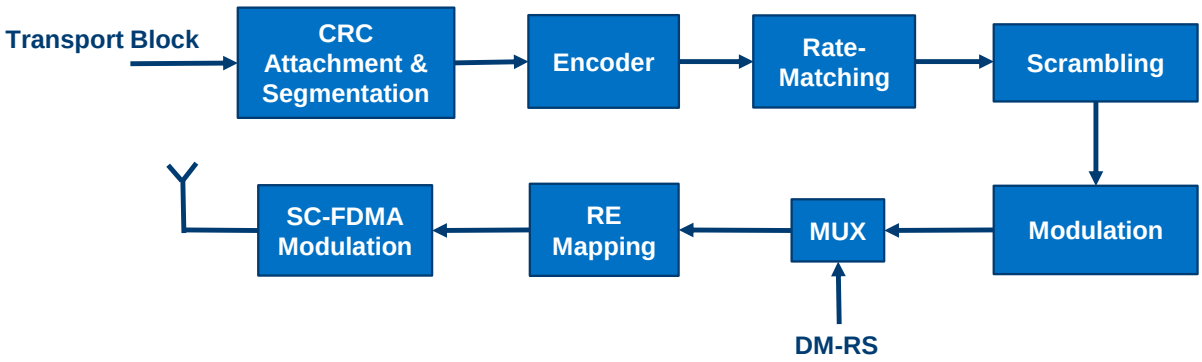

Figure 3.9: Transmitter chain.

For each payload, the process starts with a sequence of information bits, called transport block, where is accommodated the information that the user wants to transmit.

CRC Attachment and Segmentation

Then, a Cyclic Redundancy Check (CRC) block is appended at the end of the transport block. The purpose of this addition is the detection of errors done after a check value of this appendix in the receiver side. After, to ensure that the bit sequence entering in the turbo encoder is no larger than 6144 and it has a legal size in accordance with the 3GPP TS 36.212 [27], null filler bits can be added to solve the legal size problem and it can be applied segmentation forming code blocks, if the size of the transport block plus CRC is higher than 6144. An extra CRC is appended at the end of each code block. This extra CRC will allow an error early detection and it works has a double insurance. In the case where the size of the transport block is less than 6144 the segmentation is not applied, hence only the first CRC attached will be used for error detection. However, if it does not have a legal size, null filler bits are still added.

Encoder

With the intention of error correcting, each code block come into a turbo encoder, depicted in Figure 3.10. The encoder used is standardized in the chapter 5 of the 3GPP TS 36.212 [27] and has a rate of 1/3, meaning that for every bit with useful information, two redundant bits of data are created. For this reason, in the end of the encoder block, three sequences of bits will be acquired: the first one named systematic bit sequence, which is equal to the input code block, the second one that is a parity bit sequence obtained using the recursive systematic convolutional code 1 with the code block as input, and the third one, that is also a parity bit sequence but it was created using the recursive systematic convolutional code 2 with a permutation (an interleaved is applied) of the initial code block as input. Notice that both recursive systematic convolutional codes are equal.

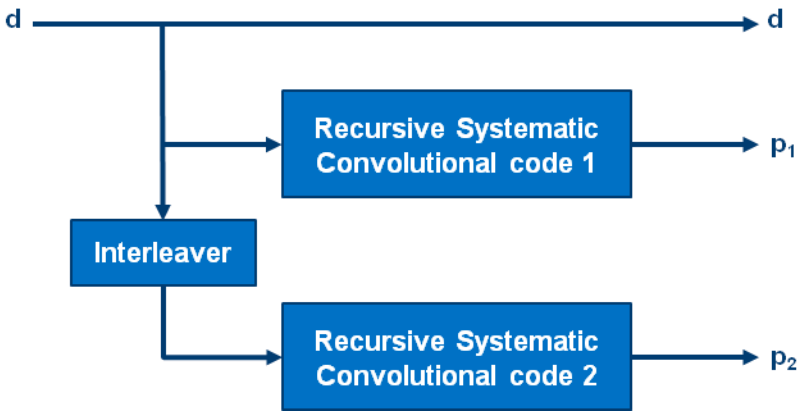

Figure 3.10: Turbo encoder block diagram.

Rate-Matching

After this, to match with the number of bits allocated for the transmission, which depends on the modulation and coding schemes defined by the transmitter device, rate matching is applied. The process of rate matching, which can be divided in three stages, is presented in Figure 3.11. In the first stage, called sub-block interleaver, as the name implies, the output of the turbo encoder (the coded bits) is

interleaved in accordance with the inter-column permutation pattern presented in Table 5.1.4-1 of 3GPP TS 36.212 [27]. In the second stage, the bit collection occurs. In here, the bits are arranged in a virtual circular buffer. The buffer presents first the interleaved systematic bits and then the interleaved parity bits in an interlaced way. Finally, in the last stage, named bit selection, the number of allocated bits are chosen from the virtual circular buffer starting from the point that corresponds to the redundancy version (RV) selected by the transmitter. In case the end of the buffer is reached, the selection will continue from the beginning of the virtual buffer, hence the term virtual circular buffer. At the end of this process, all the rate matched code blocks are concatenated forming a codeword.

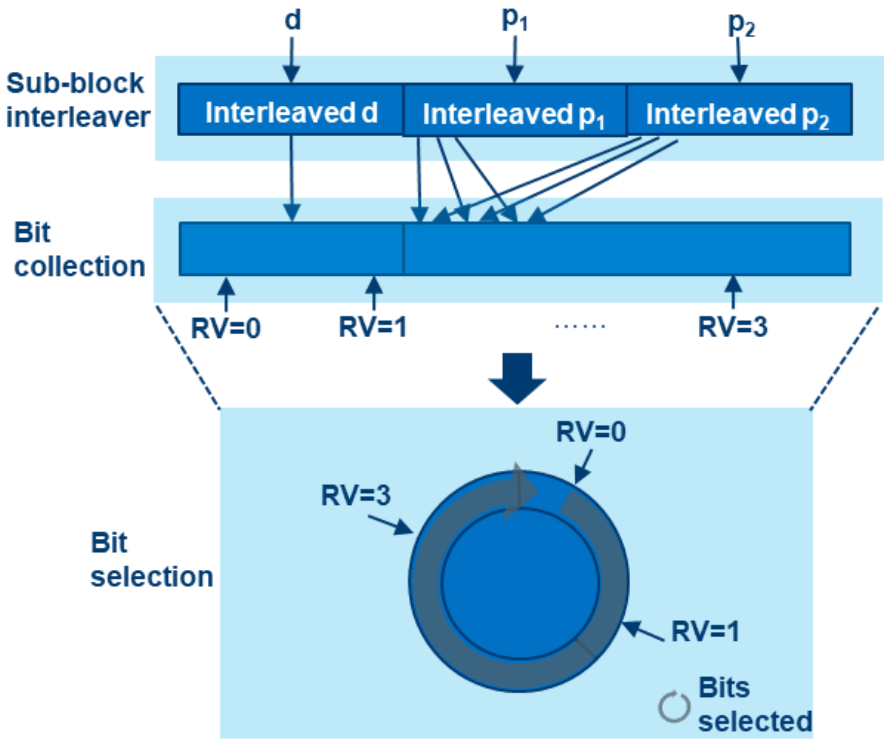

Figure 3.11: Rate-Matching block diagram.

Scrambling

Then, this codeword is scrambled with a pseudo-random bit sequence generated by the transmitter of the payload in consideration. This encrypts the signal, therefore only the devices that know this sequence can decode the information that is being transmitted. Here, it is considered that there is a common sequence for all devices so any device can decode any payload.

Modulation

Posteriorly, the scrambled bits are modulated creating symbols. It is assumed a quadrature phase shift keying (QPSK) modulation, meaning that one symbol corresponds to two bits. The constellation used is presented in Figure 3.12.

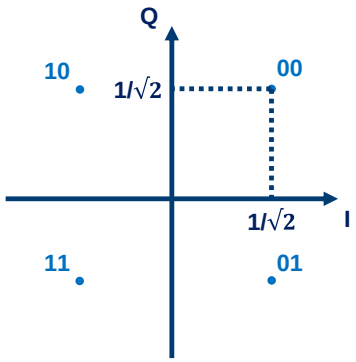

Figure 3.12: QPSK constellation used.

MUX and creation of Reference Signals

Now that the symbols that correspond to information were obtained, there is a need to create reference signals for posteriori execution of the channel estimation process. These pilot symbols, that together form a pilot sequence and are inserted in the payload of the transmitted message, as in Figure 3.13, are known by the transmitter and receiver.

Figure 3.13: Payload of MSGs1 and MSGs2.

As previously said, in the considered network, the devices establish communication links between each other through a random access scheme. As such, the number of contending devices is unknown to the receiver. To ensure that the receiver applies the appropriate decoding procedure (e.g. number of SIC rounds) knowledge of the number of contending devices is required. For that reason the use of multiple orthogonal pilot sequences is considered.

In a simpler LLS system, which is explained in more detail in section 5.1.1, the comparison between the use of a single pilot sequence and multiple orthogonal pilot sequences in different types of channel estimation is performed. In this system, two signals (one of interest and one interferer) were transmitted through a wireless medium having into account a Rayleigh fading channel and white Gaussian noise. At the receiver side, the signal of interest was decoded without any SIC technique and the block error rate (BLER) was calculated. It is possible to observe from the simulations presented in Figure 3.14 that in two different extremes of SIR (-15 dB and 15 dB), the best performances are obtained when the two signals use orthogonal pilot sequences. This is due to the fact that the receiver, with a pilot detection block which will be explained in the receiver side, can distinguish the two signals and so detect and decode the signal of interest more correctly. Also, it is possible to state that the use of MMSE-IRC improves the performance of the system.

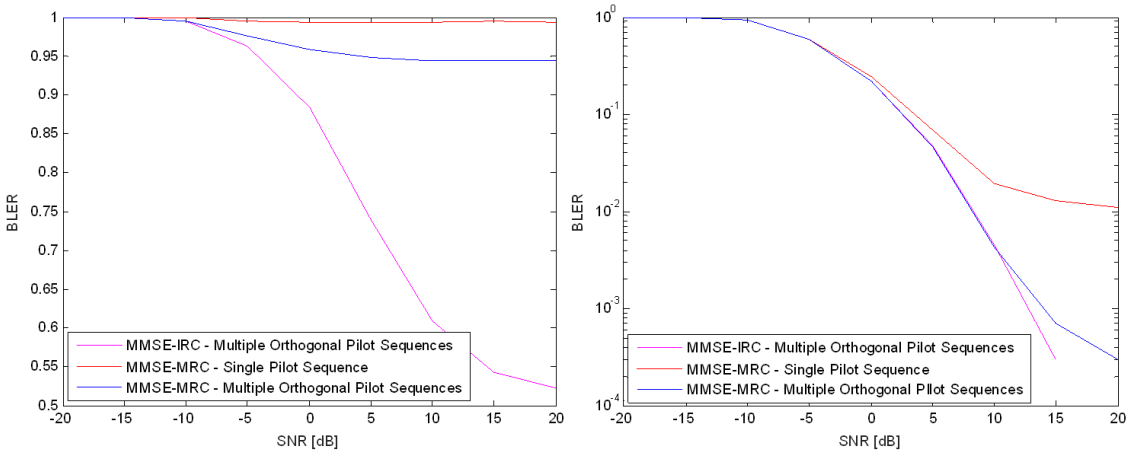

Figure 3.14: Comparison between the use of multiple orthogonal pilot sequences and a single one for different types of channel estimation in two different SIRs: -15 dB (left) and 15 dB (right).

Hence, one of the innovations of this solution is the design of a set of multiple orthogonal pilot sequences from where a user can choose from for its payload. The number of available orthogonal pilot sequences is a system design parameter. As the selection of the transmitted pilot sequences is done independently and randomly by each transmitter, then it is expected that with higher access loads there will be several pilot sequences used and that some of these have been selected by more than one transmitter. So, the size of this set is associated with the maximum supported load within a channel resource, meaning that when the network has to support higher loads, the number of available orthogonal pilot sequences should increase proportionally. In Figure 3.15 is presented how many orthogonal pilot sequences are required in a certain load to keep pilot collision below 1% and 10%.

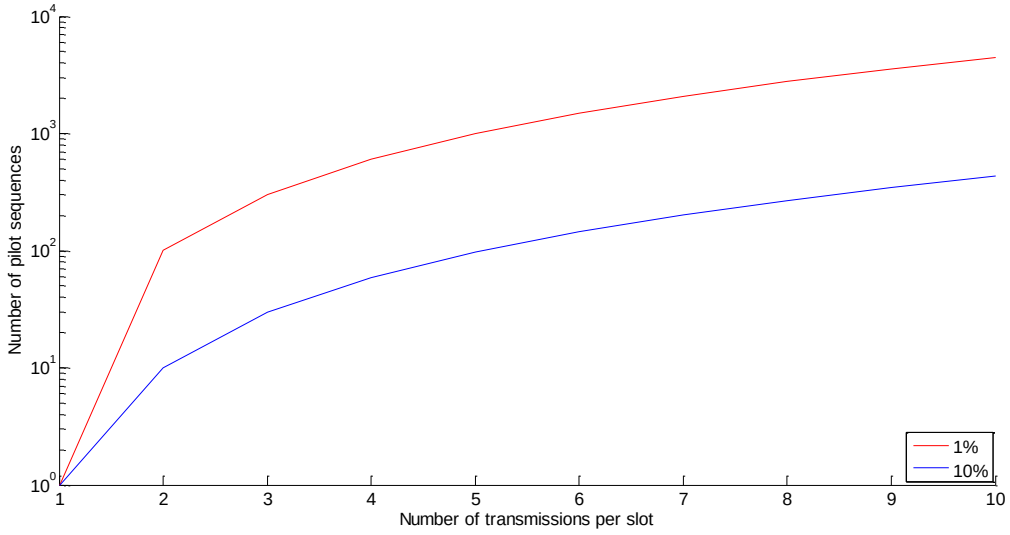

Figure 3.15: Number of pilot sequences associated with the supported load within a channel resource for a collision threshold.

An example of a set of 16 orthogonal pilot sequences with 16 pilot symbols that as said before, are generated according to the method described in the standard 3GPP TS 36.211 [21] is shown in Table 3.1.

Table 3.1: Example of a set of orthogonal pilot sequences.

Pilot Symbols

Multiple Orthogonal Pilot Sequences

	1	2	3	4	...	14	15	16
1	-0.7071-0.7071i	-0.7071-0.7071i	-0.7071-0.7071i	+0.7071+0.7071i		+0.7071+0.7071i	-0.7071-0.7071i	-0.7071-0.7071i
2	-0.7071-0.7071i	+0.7071+0.7071i	+0.7071+0.7071i	+0.7071+0.7071i		-0.7071-0.7071i	+0.7071+0.7071i	-0.7071-0.7071i
3	-0.7071-0.7071i	-0.7071-0.7071i	+0.7071+0.7071i	-0.7071-0.7071i		+0.7071+0.7071i	+0.7071+0.7071i	+0.7071+0.7071i
4	-0.7071-0.7071i	+0.7071+0.7071i	-0.7071-0.7071i	-0.7071-0.7071i		+0.7071+0.7071i	+0.7071+0.7071i	-0.7071-0.7071i
5	-0.7071-0.7071i	-0.7071-0.7071i	-0.7071-0.7071i	+0.7071+0.7071i		-0.7071-0.7071i	+0.7071+0.7071i	+0.7071+0.7071i
6	-0.7071-0.7071i	+0.7071+0.7071i	+0.7071+0.7071i	+0.7071+0.7071i		+0.7071+0.7071i	-0.7071-0.7071i	+0.7071+0.7071i
7	-0.7071-0.7071i	-0.7071-0.7071i	+0.7071+0.7071i	-0.7071-0.7071i		-0.7071-0.7071i	-0.7071-0.7071i	-0.7071-0.7071i
8	-0.7071-0.7071i	+0.7071+0.7071i	-0.7071-0.7071i	-0.7071-0.7071i		+0.7071+0.7071i	+0.7071+0.7071i	-0.7071-0.7071i
9	-0.7071-0.7071i	-0.7071-0.7071i	-0.7071-0.7071i	+0.7071+0.7071i		-0.7071-0.7071i	+0.7071+0.7071i	+0.7071+0.7071i
10	-0.7071-0.7071i	+0.7071+0.7071i	+0.7071+0.7071i	+0.7071+0.7071i		+0.7071+0.7071i	-0.7071-0.7071i	+0.7071+0.7071i
11	-0.7071-0.7071i	-0.7071-0.7071i	+0.7071+0.7071i	-0.7071-0.7071i		-0.7071-0.7071i	-0.7071-0.7071i	-0.7071-0.7071i
12	-0.7071-0.7071i	+0.7071+0.7071i	-0.7071-0.7071i	-0.7071-0.7071i		-0.7071-0.7071i	-0.7071-0.7071i	+0.7071+0.7071i
13	-0.7071-0.7071i	-0.7071-0.7071i	-0.7071-0.7071i	+0.7071+0.7071i		+0.7071+0.7071i	-0.7071-0.7071i	-0.7071-0.7071i
14	-0.7071-0.7071i	+0.7071+0.7071i	+0.7071+0.7071i	+0.7071+0.7071i		-0.7071-0.7071i	+0.7071+0.7071i	-0.7071-0.7071i
15	-0.7071-0.7071i	-0.7071-0.7071i	+0.7071+0.7071i	-0.7071-0.7071i		+0.7071+0.7071i	+0.7071+0.7071i	+0.7071+0.7071i
16	-0.7071-0.7071i	+0.7071+0.7071i	-0.7071-0.7071i	-0.7071-0.7071i		-0.7071-0.7071i	-0.7071-0.7071i	+0.7071+0.7071i

RE Mapping

After the creation of a pilot sequence and the insertion of it in the payload, the total amount of symbols is mapped in the time-frequency resource grid from chapter 10 of the standard in 3GPP TS 36.211 [21] presented in section 2.2.1.

SC-FDMA Modulation

To finish, the SC-FDMA signal generation is done, transforming the signal from frequency to time domain. As previously said, in the case here proposed in each slot of the resource grid there is only one subcarrier occupied with modulated symbols. Hence, in accordance with chapter 10 of the standard in 3GPP TS 36.211 [21], the time-continuous signal $s_{k,l}(t)$ for subcarrier index k in SC-FDMA symbol l in a slot is defined by

$$s_{k,l}(t) = a_{k^{(-)},l} \cdot e^{j\phi_{k,l}} \cdot e^{j2\pi(k+\frac{1}{2})\Delta f(t-N_{CP,l}T_s)} \tag{3.2}$$

$$k^{(-)} = k + \left\lfloor \frac{N_{SC}}{2} \right\rfloor \tag{3.3}$$

for $0 < t < (N_{CP,l} + N) \cdot T_s$, where $a_{k^{(-)},l}$is the modulated value of symbol l, N_{SC} is the number of subcarriers available, $\phi_{k,l}$ is a phase rotation, Δf is the subcarrier spacing, T_s is a basic time unit in seconds considered in the standard and N, $N_{CP,l}$ and k are parameters that depend on the value of the subcarrier spacing and are defined in the Table 10.1.5-1 of the standard. Finally, to be easier to work with, samples are obtained from the signal, considering a sampling rate of 1.92 MHz. For more details about the generation of the signal, for example how the phase rotation is calculated, consult section 10.1.5 of [21].

3.4. Receiver Side

The purpose of the receiver is, as depicted in Figure 3.16, recover the initial information sent by the devices, this is, the initial transport blocks.

Figure 3.16: Receiver chain.

SC-FDMA Demodulation

First, the SC-FDMA signal is demodulated, through the inversion of the signal generation process presented before and with the application of a Fast Fourier Transform, passing from time to frequency domain.

RE De-mapping

Then, the de-mapping from the resource grid is done, obtaining a total amount of symbols (y) composed with data and reference signals.

Receiver Advanced Techniques

After, the receiver has the possibility of using diverse and advanced decoding techniques. Here it is proposed an adaptive architecture that allows the use of two types of SIC, as depicted in Figure 3.17.

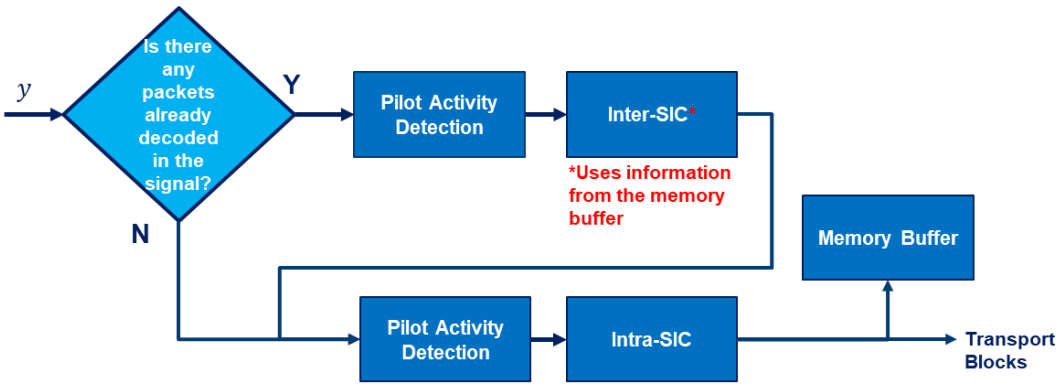

Figure 3.17: Proposed adaptive architecture for the receiver side.

As explained before, this architecture consists in the improvement of the decoding process in the following manner: when packets from the received signal that were not acquired yet, are decoded and the CRC checks, they are cancelled from the received signal (intra-SIC) and kept in a memory buffer. Later, if another signal comes with the same packet that was already decoded before, the receiver uses the information kept in the memory buffer to subtract its contribution from the received signal (inter-SIC) and try to decode the remaining packets. The information present in the memory buffer is deleted every time a VF starts since one of the reasons why the concept of VF arose is to keep both latency and

memory constraints reasonable. The data stored in the memory can be digital samples, modulation symbols, coded bits or uncoded bits. In this project it was considered that it keeps the uncoded bits of the packets decoded.

This architecture is considered adaptive since it is possible to choose between the use of only intra-SIC, or the use of intra-SIC and inter-SIC. In this architecture there are three important blocks:

- Pilot Activity Detection.
- Intra-SIC process.
- Inter-SIC process.

In the next sections, these three processes will be described in detail.

3.4.1.Pilot Activity Detection

The purpose of the pilot activity detection block is to derive the number of unique orthogonal pilot sequences activated by the transmitters, without any a priori information, based on the received signal y. Remember that in the transmitter side each user selects independently and randomly a pilot sequence from a set of orthogonal pilot sequences. With this information, the receiver can then decide an appropriate receiver architecture. Not only the receiver can choose the correct channel estimation, but also it can decide if the use of SIC should be considered or not. For example, as depicted in Figure 3.18, if only one of the pilot sequences is active, then the MMSE-MRC is used without SIC, while if multiple pilot sequences are active then the channel estimation MMSE-IRC and multiple SIC loops can be considered.

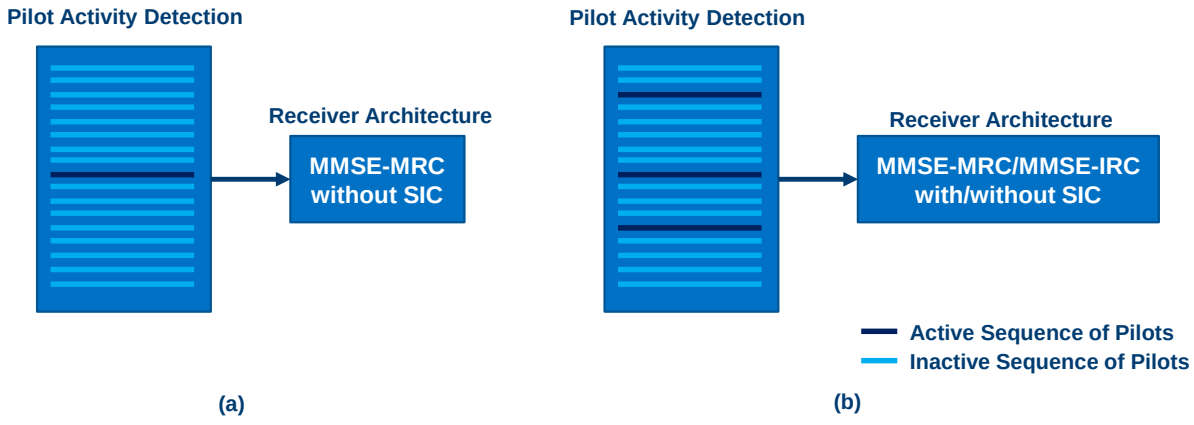

Figure 3.18: Receiver architecture for different results of pilot activity detection: (a) for when only one pilot sequence is detected; (b) for when multiple pilot sequences are detected.

Obviously, if only one pilot is detected, that does not mean directly that the receiver is only receiving one transmission – it can be receiving one or multiple transmissions where the transmitters selected the same pilot sequence. One advantage obtained from the use of the pilot activity detection block is in

terms of power consumption, since when the pilot activity detection block does not detect any pilot sequence, the device does not have to proceed with the reception process. Without the information given by this block, the power would have been spent attempting to decode a non-existing transmission. Also, the pilot activity detection block helps the creation of an adaptive receiver architecture that adapts, for example, the number of SIC rounds based on the pilot sequences detected. Hence, a suitable receiver complexity can be selected depending on the network conditions: in a case of low network activity, this translates to lower power consumption and lower receiver complexity; while in the case of high network activity, the power consumption and receiver complexity increases. The connection between this element of pilot activity detection and a receiver architecture with adaptive complexity gave rise to the first invention disclosure listed in section 1.5.

For the purpose of simulation, the pilot activity detection is genie aided (i.e. it is assumed a perfect detection). However, during the development of this project, different types of Pilot Activity Detection blocks were developed and tested. Since the pilot symbols are known to both transmitter and receiver, the receiver can estimate the distortion applied by the channel by comparing the received distorted pilot symbols with the non-distorted version of these same symbols. In the following, it will be described different types of pilot activity detection blocks architectures.

Parallel Matched Filter (baseline)

The baseline proposed is an architecture based on a matched filter as depicted in Figure 3.19.

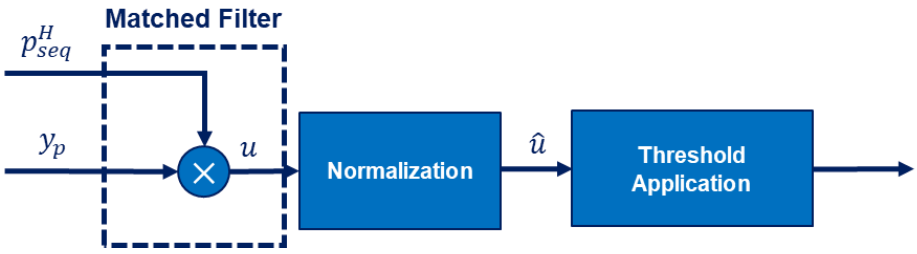

Figure 3.19: Matched filter baseline block diagram.

First, the receiver extracts the symbols that are located in the pilot positions from the received signal. Then, the extracted pilot sequence is multiplied with the conjugate transpose of all pilot sequences present in the set of multiple orthogonal pilot sequences, as follows:

$$u_i = |y_p \cdot p_{seq,i}^H| \qquad \forall\, i = 1, \dots, P \tag{3.4}$$

where y_p is the received signal corresponding to the pilot symbol positions, $p_{seq,i}$ is the i-th pre-defined pilot sequence from the set of size P, u_i is the statistic element that form the vector u and H is the conjugate transpose operation. Then, the obtained values are normalized by the largest element of u as follows:

$$\hat{u_i} = \frac{u_i}{u_{max}} \quad s.t. \quad u_{max} = \max_i \; u_i. \tag{3.5}$$

The greater is the value of $\hat{u}_i$, the greater the probability of a i-th pilot sequence being active. With these probabilities, it is also possible to order the signals so the SIC process can be done later in a descending order of signals power.

In the presence of multiple transmissions there is a need to put in place a mechanism to identify which of the pilot sequences are active. Hence, a hard decision mechanism is introduced based on a threshold. If a value $\hat{u}_i$ is above this threshold, then the system detects the i-th pilot sequence as active. So, one way to improve the performance of this block is to improve the reliability of the $\hat{u}_i$ values. For that reason, an improved architecture was developed.

Parallel Matched Filter with Adaptive Threshold via Common Neural Network

Now, another architecture, depicted in Figure 3.20, where the outputs of the parallel matched filter are inserted into a feedforward neural network is considered. In this architecture two configurations for the inputs of the feedforward neural network are considered:

- the inputs of the feedforward neural network are the outputs of the matched filter (Figure 3.20a);
- the inputs of the feedforward neural network are the outputs of the matched filter plus the original received signal in pilot positions (Figure 3.20b).

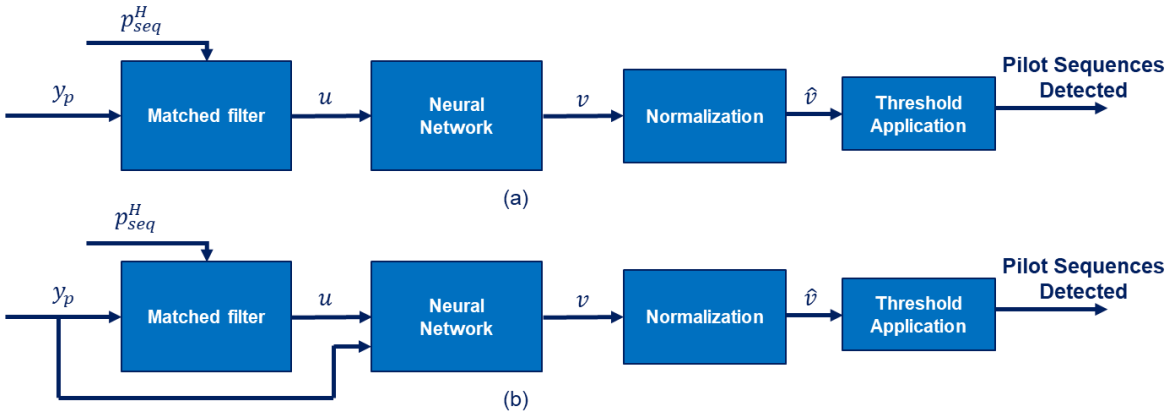

Figure 3.20: Parallel matched filter with adaptive threshold via common neural network.

The main difference between this architecture and the previous one is the place where the normalization process and the threshold application are done. In this new case these operations are performed at the output of the feedforward neural network, and not at the output of the parallel matched filter. The addition of a neural network allows to refine the estimation of the activation probabilities.

The general architecture of the feedforward neural network used in the solution is depicted in Figure 3.21. The feedforward network is composed by an input layer with N inputs (denoted from q_1 to q_N), M hidden layers (each with l_M hidden nodes) and an output layer with P outputs (denoted from s_1 to s_P). The input of the feedforward neural network is a vector composed by N elements. This vector is fed into the input layer. In turn these inputs are combined into each of the nodes of the first hidden layer with a

scaling and offset factors (these factors are specific for each connection, and are discovered during the training phase of the neural network, based on the well-known backpropagation algorithm).

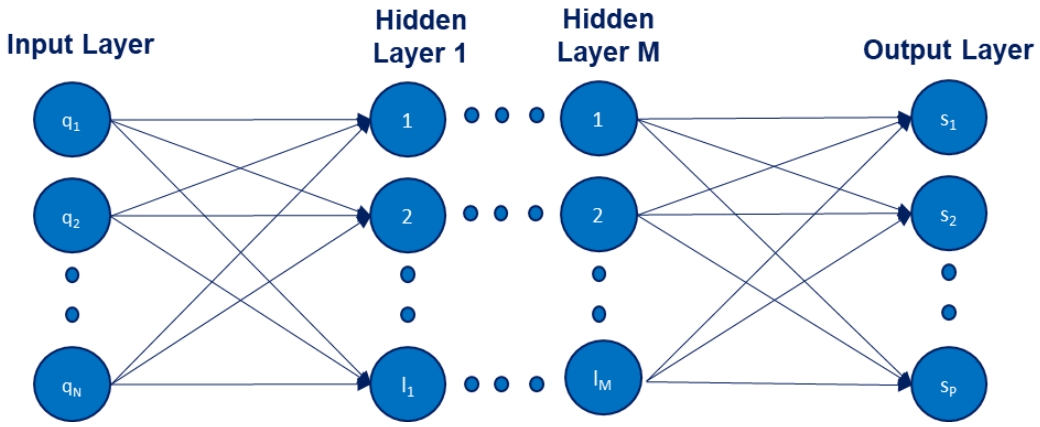

Figure 3.21: Feedforward neural network architecture.

This process occurs between all hidden layers until it is propagated to the P nodes in the output layer, where each node has then soft values. Each node in the output layer is then associated with a value v_i and correspond each to a class (or in this example to a specific pilot sequence).

Parallel Matched Filter with Adaptive Threshold via Individual Neural Network

Finally, a third architecture is proposed, where each pilot sequence is assigned to a dedicated neural network as depicted in Figure 3.22.

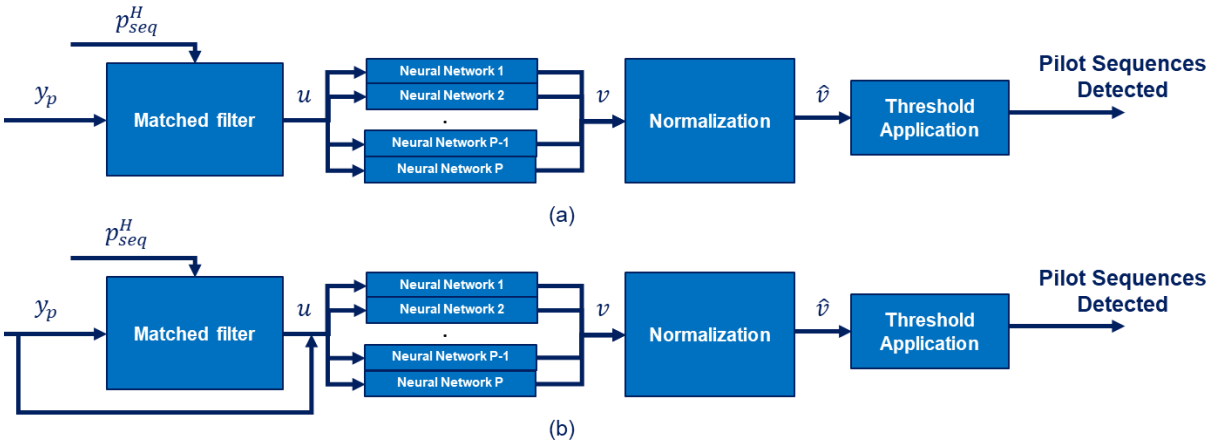

Figure 3.22: Parallel matched filter with adaptive threshold via individual neural network.

This architecture is very similar to the previous one. The only difference is that instead of having only one neural network responsible for the soft values of all pilot sequences, it has P separate neural networks, each trained to detect the activity of a single pilot sequence.

A performance comparison between these three architectures is presented in section 5.1.2. These different architectures for the pilot activity detection block gave rise to the third invention disclosure report presented in section 1.5.

3.4.2.Intra-SIC process

With the information of the number of pilot sequences active in the received signal given by the pilot activity detection block, the intra-SIC process consists in the application of a certain number of SIC loops, in order to decode as many packets as possible. The packets that are decoded and the CRC checks are kept in a memory buffer for posterior use. In Figure 3.23 is presented this process diagram.

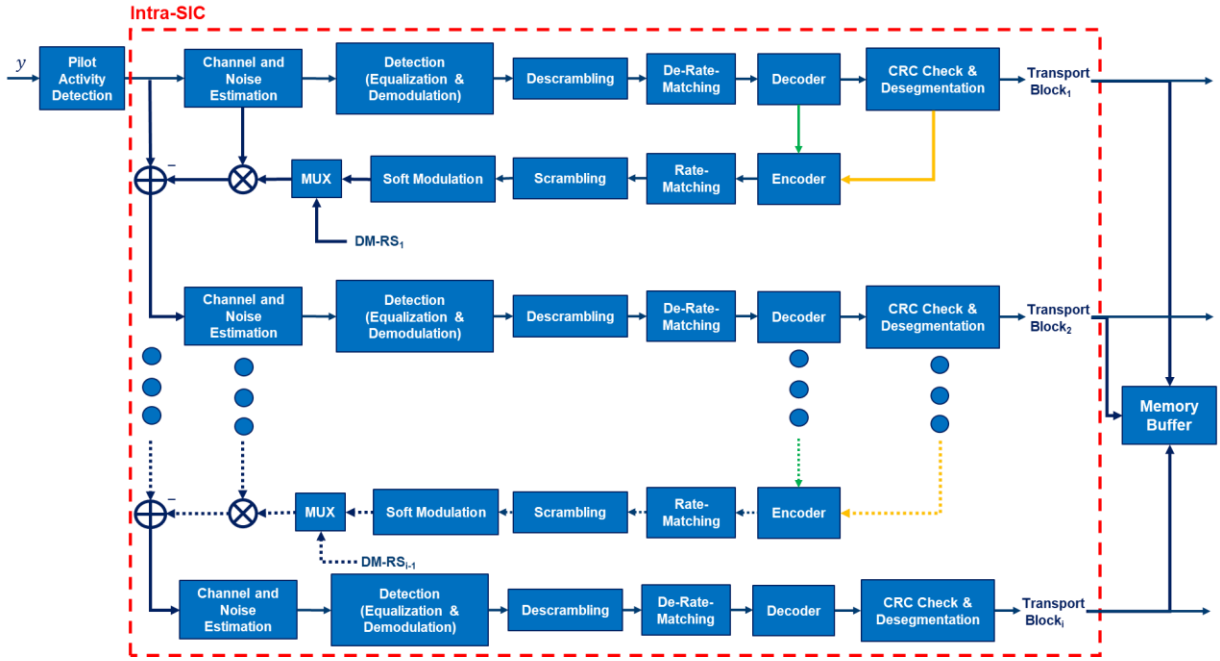

Figure 3.23: Intra-SIC block diagram.

The purpose of the SIC loop, as depicted in Figure 3.24, is to detect and decode a signal from the received signal and then re-estimate it so its contribution can be cancelled from the received signal.

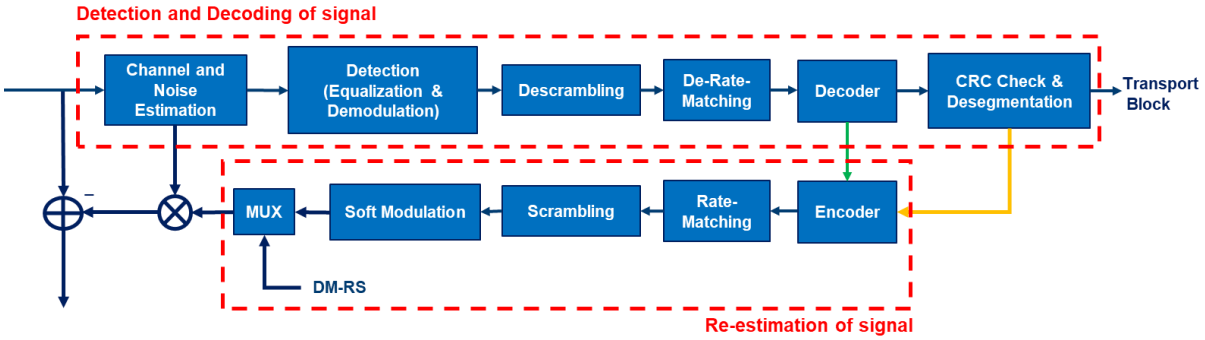

Figure 3.24: SIC loop process.

In respect to the SIC loop, it was used a configuration that enables codeword-level interference cancellation, i.e. the signals are decoded and re-encoded before the subtraction. In here, two options were considered:

- a signal tries to be acquired by the receiver and it is withdrawn from the received signal every time, even if its CRC does not check (green line in the diagram);

- a signal tries to be acquired by the receiver and it can only be withdrawn from the received signal if its CRC checks (yellow line of the diagram).

Next, each block that constitutes a SIC loop will be described, except for the rate-matching, scrambling, MUX and creation of reference signals that are reused from the transmitter chain.

Channel and Noise Estimation

After the pilot sequences being detected, the signal enters the channel estimation block. As said before, the channel estimators used are MMSE based – MMSE-MRC and MMSE-IRC. Both were done in an iterative manner. Starting with the simplest one, MMSE-MRC, and having into account section 2.2.2, the mechanism used is presented in Figure 3.25.

It is possible to observe that in this process it is not taken into account any interfering signal and that it is done with the application of a loop which allows to get a better accuracy of results in the calculation of the MMSE channel estimation, $\widehat{H_{MMSE0}}$, and of the noise covariance matrix, R_{r0}, of a signal of interest. To start the process, in the first iteration an initial condition of the noise covariance matrix is used. This loop is executed a fixed number of times, which is the number where, through simulations, it was found that the precision of results does not change significantly anymore.

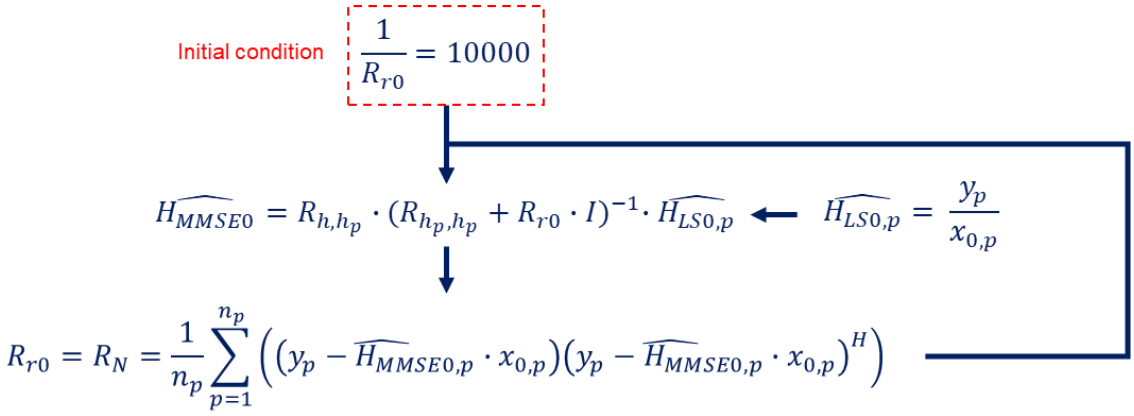

Figure 3.25: Mechanism of MMSE-MRC with pilot symbols.

In respect to the process of MMSE-IRC, depicted in Figure 3.26, it is possible to observe that this procedure is similar to the scheme presented before. Note that this figure shows an example where there are two signals present in the received signal.

Here, it also functions as a loop where the initial conditions are the noise covariance matrix of a signal of interest, R_{r0}, and of an interfering signal, R_{r1}. Hence, contrary to what happens in MMSE-MRC, in this channel estimation, the effect of interfering signals is taken into consideration. Assuming that there

is only one interfering signal, its channel, $\widehat{H_{MMSE1}}$, has to be calculated as well, so it can be considered in the R_N and later in the R_{r0}.

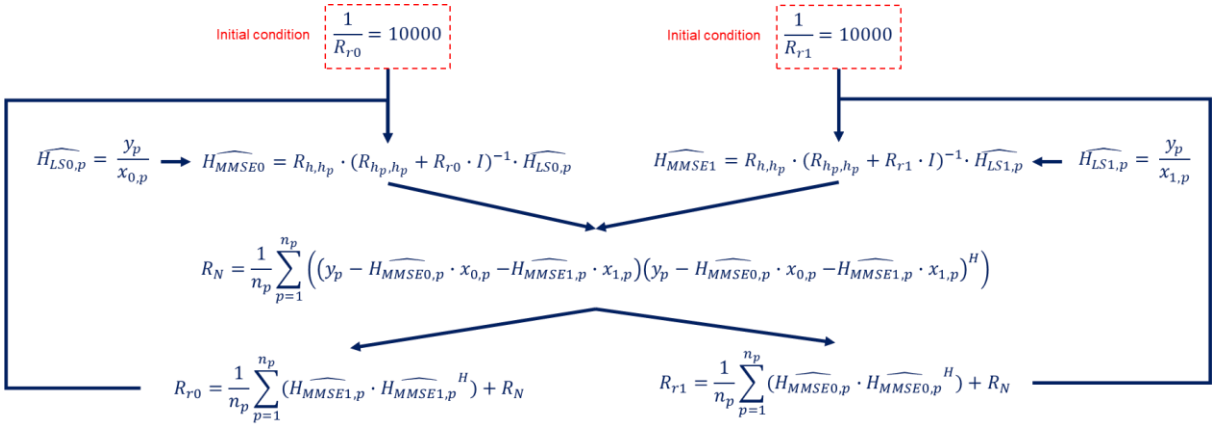

Figure 3.26: Mechanism of MMSE-IRC with pilot symbols.

Independently of which channel estimation is used, at the end of this block, the channel of the signal of interest, $\widehat{H_{MMSE0}}$ and the noise covariance matrix R_{r0} are obtained.

Equalization

With the outputs of the channel and noise estimation block and the data symbols from the received signal, the signal enters the detection block and it is equalized using the following

$$y_{d,MMSE} = \widehat{H_{MMSE0,d}}^H \cdot (\widehat{H_{MMSE0,d}} \cdot \widehat{H_{MMSE0,d}}^H + R_{r0} \cdot I)^{-1} \cdot y_d \tag{3.6}$$

where $\widehat{H_{MMSE0,d}}$ is the channel estimation of the signal of interest in data positions, R_{r0} is the noise covariance matrix, y_d is the received signal in data positions, $y_{d,MMSE}$ is the signal detected, H is the conjugate transpose operation and I is the identity matrix.

Demodulation

Then, still on the detection block, the signal is soft demodulated. In a demodulation process, the goal is to pass from symbols to bits. Since it is “soft”, instead of bits, the output are soft bits named Logarithm Likelihood Ratio (LLR). With the LLR it is possible to know how much certainty there is that a bit is 0 or 1. The formula of a LLR of a certain bit b_i is the following

$$LLR(b_i) = log \frac{Pr(b_i = 1)}{Pr(b_i = 0)} \tag{3.7}$$

where $\Pr$ represents probability. With the formula, it is possible to observe that if $LLR(b_i) < 0$, it is more likely that the bit is 0 and if $LLR(b_i) > 0$, it is likely that the bit is 1. However, if $LLR(b_i) = 0$, there is complete uncertanty of whether the bit is 0 or 1. Note that, its magnitude is the level of certainty.

For ease of exposure, an example will be demostrated to illustrate how the soft demodulation works. The first step when doing this process is to compare the obtain symbols, for example $0.7542 + 0.2881i$, with the symbols from the QPSK constellation,

$$0.7542 + 0.2881i \overset{-}{\Leftrightarrow} 0.7071 + 0.7071i \overset{|\ |^2}{\Leftrightarrow} 0.1778 \tag{3.8}$$

$$0.7542 + 0.2881i \overset{-}{\Leftrightarrow} 0.7071 - 0.7071i \overset{|\ |^2}{\Leftrightarrow} 0.9926 \tag{3.9}$$

$$0.7542 + 0.2881i \overset{-}{\Leftrightarrow} -0.7071 + 0.7071i \overset{|\ |^2}{\Leftrightarrow} 2.3108 \tag{3.10}$$

$$0.7542 + 0.2881i \overset{-}{\Leftrightarrow} -0.7071 - 0.7071i \overset{|\ |^2}{\Leftrightarrow} 3.1257. \tag{3.11}$$

Then, having into account the bits associated with the symbols from the QPSK constellation, as shown in Table 3.2, it is done the subtraction between the minimum comparison that correspond to bits 0 and 1 for the corresponding bit, as following

$$b_1 = \min(0) - \min(1) = 0.1778 - 2.3108 = -2.1330 \tag{3.12}$$

$$b_2 = \min(0) - \min(1) = 0.1778 - 0.9926 = -0.8148. \tag{3.13}$$

Table 3.2: Correspondent bits to QPSK symbols.

b_1	b_2	symbols
0	0	0.7071+0.7071i
0	1	0.7071-0.7071i
1	0	-0.7071+0.7071i
1	1	-0.7071-0.7071i

Hence, since the LLR for both bits is negative, having into consideration the LLR formula exposed above, it is possible to conclude that there is a certain probability that both bits of this symbol are 0. Also, in accordance with the magnitute there is more certainty that b_1 is 0 than b_2 is 0.

Descrambling

After obtaining the LLRs for all data symbols of the equalized signal, the sequence is descrambled. The receiver has knowledge of the pseudo-random bit sequence used in the transmitter phase, so it inverts this sequence and applies to the LLRs. Remember that in this case, there is a common sequence for all transmissions, so a device can decode any payload.

De-Rate-Matching

Later, it is time to apply the de-rate-matching. To invert the process of rate matching, first some preparation is needed. Knowing the size of the encoder output which is composed by three sequences of bits (one systematic and two parity) and assuming that its values are a sequence of known indexes, applying rate matching to it, it is possible to observe in which positions each bit end up after the process. With this information it is possible to de-rate-match the LLR sequence, obtaining three sequences of soft bits corresponding to a systematic, $LLR_c(d)$, and two parity, $LLR_c(p_1)$ and $LLR_c(p_2)$, bit sequences.

Decoder/Encoder

Later on, these three sequences enter in a turbo decoder block. Due to a special feature of this decoder, that simplifies the process of decoder and encoder, a decoder block that was studied and implemented by a former intern at Intel was used. The turbo decoder/encoder block diagram is exposed in Figure 3.27.

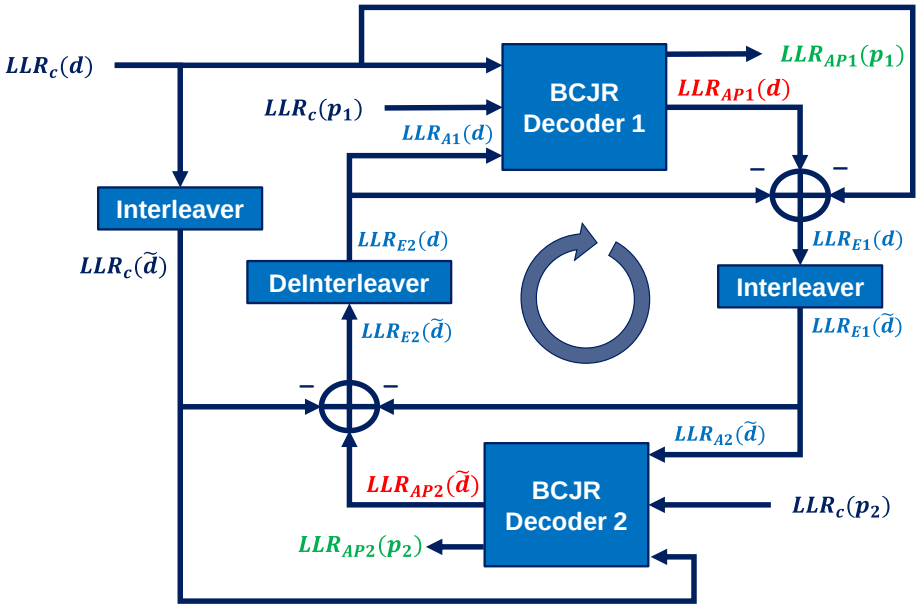

Figure 3.27: Turbo decoder/encoder block diagram.

First, the usual decoding process is explained. The main goal of the decoding process is to refine the LLR of the systematic bits, since it corresponds to the initial input of the system. This is possible with the application of a loop and working in an iterative manner. In the first iteration, and having as input the LLR of the systematic bits, $LLR_c(d)$, the LLR of the first parity bits, $LLR_c(p_1)$, and with an a priori LLR, $LLR_{A1}(d)$, equal to 0, the decoder 1 applies the Bahl Cocke Jelinek Raviv (BCJR) algorithm and with the help of the information from the parity bits, it is possible to increase or decrease the magnitude of the LLR of the systematic bits depending if there is more or less certainty about their values. After this process, the decoder 1 output is the following

$$LLR_{AP1}(d) = LLR_c(d) + LLR_{A1}(d) + LLR_{E1}(d) \tag{3.14}$$

where $LLR_{AP1}(d)$ corresponds to the a posteriori LLR from decoder 1 and $LLR_{E1}(d)$ represents the extrinsic information obtained from decoder 1 which is the real information contribution obtained from this decoder. This information, $LLR_{E1}(d)$, is then interleaved and inserted as a priori information, $LLR_{A2}(\tilde{d})$, in decoder 2. This interleaver corresponds to the same used in the encoder block in the transmission phase. After, having as input the interleaved LLR of the systematic bits, $LLR_c(\tilde{d})$, the LLR of the second parity bits, $LLR_c(p_2)$, and the a priori LLR, $LLR_{A2}(\tilde{d})$, obtained by decoded 1, decoder 2 applies the BCJR algorithm, and the information certainty is updated once again. From here, the a posteriori LLR from decoder 2, $LLR_{AP2}(\tilde{d})$, is obtained and the real contribution,$LLR_{E2}(\tilde{d})$, is then de-interleaved and inserted as a priori information, $LLR_{A1}(d)$, in decoder 1. At this point, the first iteration is completed. After a certain amount of iterations, with the constant exchange of information, the two decoders tend to converge their information. At the end of the last iteration, $LLR_{AP2}(\tilde{d})$ is de-interleaved obtaining the final LLR corresponding to the systematic bit sequence.

In the end of the conventional encoder it would be expected three LLRs: one for the systematic bits and two for the parity bits. Hence, the conventional turbo decoder is modified so that during the last turbo iteration not only the LLR for the systematic bits is obtained but also the LLRs corresponding to the parity bits. For this to occur, in the last turbo iteration, each BCJR decoder runs twice, obtaining the usual LLR for the systematic bits in the first run, and in the second run, in parallel, the LLR for the correspondent parity bits. In the process of the parallel run, the LLR for the systematic bits and the LLR for the parity bits basically have their role swapped. The reason why the parity LLRs are only obtained in one iteration is because, contrary to what happens with the systematic bits, each parity bits sequence is only associated with one of the BCJR decoders, so the decoders cannot change information between each other. With this feature the computational work of the decoder and encoder is simplified.

Then, on top of the LLR for the systematic bits sequence, hard decision is applied, meaning that if the LLR of a bit is negative, that bit is considered 0, while if it is positive, it is considered 1; and the final bit sequence can proceed for the CRC check and de-segmentation block. Then, depending of which option of receiver is being analyse and of the result of the CRC check, the LLRs for the parity bits can be used in the continuation of that SIC loop process.

CRC Check and De-segmentation

After the decoding process, if the bit sequence is divided in code blocks, each CRC of each code block is checked and if the check is successful for all code blocks, each CRC is detach and the code blocks are concatenated together forming a bit sequence composed with a transport block and a CRC. Also if initially null filler bits were inserted, now they have to be removed. Finally, the CRC from the transport block is checked as a double insurance and detach from the transport block. In the other hand, if the signal did not went through the segmentation process in the transmission phase, first if initially null filler bits were inserted, now they have to be removed. Then, the CRC initially inserted is checked and if the check is done successfully, it is detach from the bit sequence, resulting in a successful reception of the initial transport block.

Soft Modulation

Remember that in the transmitter chain there is a modulation block which purpose is pass from bits to symbols in the QPSK constellation. However, in this case the input is a sequence of soft bits (LLRs) which requires a more complex block process. To explain this, an example will be illustrated. Imagine that the block is receiving two soft bits as depicted in Table 3.3.

Table 3.3: Example of LLRs for two bits.

LLR	
b_1	b_2
-32.1129	35.9448

By the high magnitude of the LLRs, it is possible to note that the symbol will be very close to one of the QPSK constellation symbols. The formulas that will be used to calculate the symbol are the following

$$\Pr(b_i = 1) + \Pr(b_i = 0) = 1 \tag{3.15}$$

$$\Pr(b_i = 1) = \frac{e^{LLR(b_i)}}{1 + e^{LLR(b_i)}} \tag{3.16}$$

$$\Pr(b_i = 0) = \frac{1}{1 + e^{LLR(b_i)}} \tag{3.17}$$

$$\begin{aligned}\hat{x} = {} & \Pr(b_1 = 0) \cdot \Pr(b_2 = 0) \cdot f_{map}([0,0]) + \Pr(b_1 = 0) \cdot \Pr(b_2 = 1) \cdot f_{map}([0,1]) \\ & + \Pr(b_1 = 1) \cdot \Pr(b_2 = 0) \cdot f_{map}([1,0]) + \Pr(b_1 = 1) \cdot \Pr(b_2 = 1) \cdot f_{map}([1,1])\end{aligned} \tag{3.18}$$

where $\Pr$ represents probability, b_i represents the bit number i, LLR is the value of the soft bit, f_{map} represents the mapping of the bits to QPSK symbols and $\hat{x}$ represents the obtained symbol. First, the probabilities of a bit being 0 or 1 are calculated as following

$$\Pr(b_1 = 1) = \frac{e^{-32.1129}}{1 + e^{-32.1129}} = 0 \tag{3.19}$$

$$\Pr(b_1 = 0) = \frac{1}{1 + e^{-32.1129}} = 1 \tag{3.20}$$

$$\Pr(b_2 = 1) = \frac{e^{35.9448}}{1 + e^{35.9448}} = 1 \tag{3.21}$$

$$\Pr(b_2 = 0) = \frac{1}{1 + e^{35.9448}} = 0. \tag{3.22}$$

Finally, with this information, the symbol is calculated as follows

$$\begin{aligned}\hat{x} &= 1 \cdot 0 \cdot (0.7071 + 0.7071i) + 1 \cdot 1 \cdot (0.7071 - 0.7071i) \\ &+ 0 \cdot 0 \cdot (-0.7071 + 0.7071i) + 0 \cdot 1 \cdot (-0.7071 - 0.7071i) \\ &= 0.7071 - 0.7071i\end{aligned} \tag{3.23}$$

and, as predicted, it is on top of one of the QPSK constellation symbols, Figure 3.28.

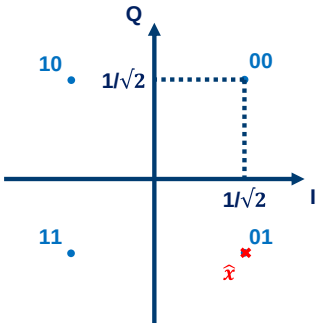

Figure 3.28: Localization of the obtained symbol in the QPSK constellation.

3.4.3.Inter-SIC process

This process consists in cancellation of signals, from the received signal, that were already decoded before in the current virtual frame in consideration and hence its information is being kept in the memory buffer. Therefore, when a receiver is performing inter-SIC, it already knows the generating id, the associated pilot sequence and the transport block of the packet already decoded in consideration. The process diagram is depicted in Figure 3.29.

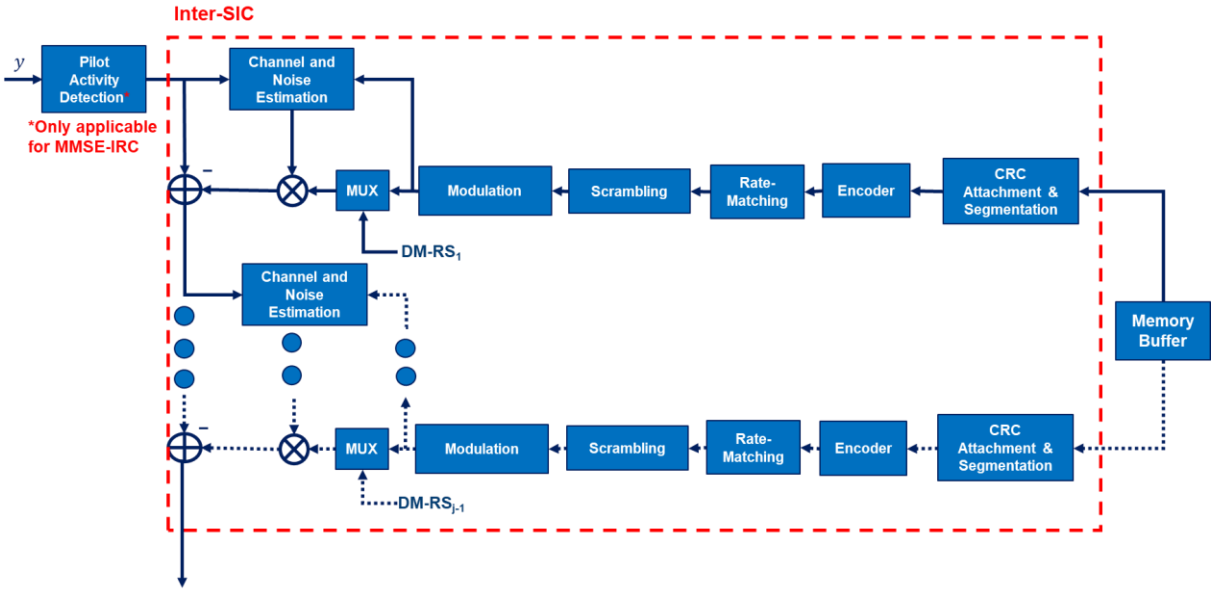

Figure 3.29: Inter-SIC block diagram.

To subtract the already decoded packet, the channel and the symbols of the signal have to be estimated. In respect to the symbols, since the receiver already has information about the transport block and the pilot sequence of the signal, it proceeds reusing the blocks from the transmitter chain: CRC attachment

and segmentation, encoder, rate-matching, scrambling, modulation and MUX with the correspondent pilot symbols. To determine the channel, there are two options as before: MMSE-MRC and MMSE-IRC.

Channel Estimation

In the case where MMSE-MRC is applied, the process is very similar to the one presented in the previous architectures. However, instead of using just pilot symbols, because the transport block of the signal that is going to be subtracted is known, its data symbols will be also used as “extra” pilots in the channel estimation process, as depicted in Figure 3.30. Note that in this case, the pilot activity detection block is not needed.

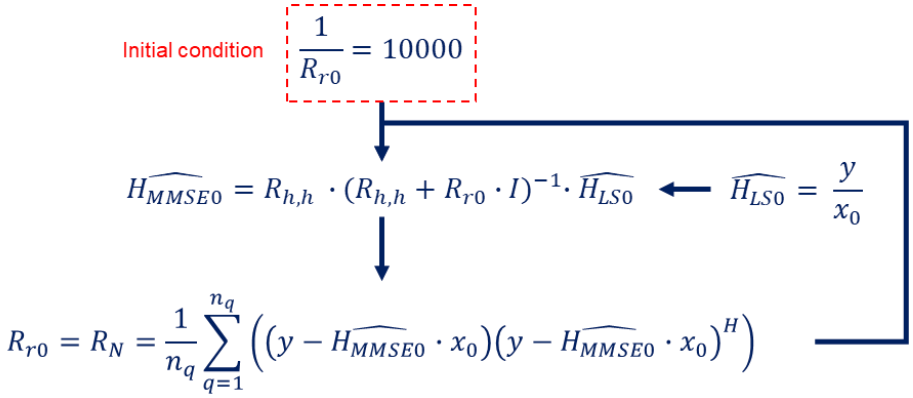

Figure 3.30: Mechanism of MMSE-MRC with pilot and data symbols.

The MMSE-IRC case, depicted in Figure 3.31, is also similar to what was shown in previous architectures, this is, it takes into account interfering signals. Hence, a receiver needs to know the pilot sequences of the interfering signals that could have been decoded before or not. The ones that had been decoded before, it has knowledge of their pilot sequences, however, for the ones that were not decoded yet, it does not know their pilot sequences. For that reason, pilot activity detection in inter-SIC needs to be used in this type of channel estimation.

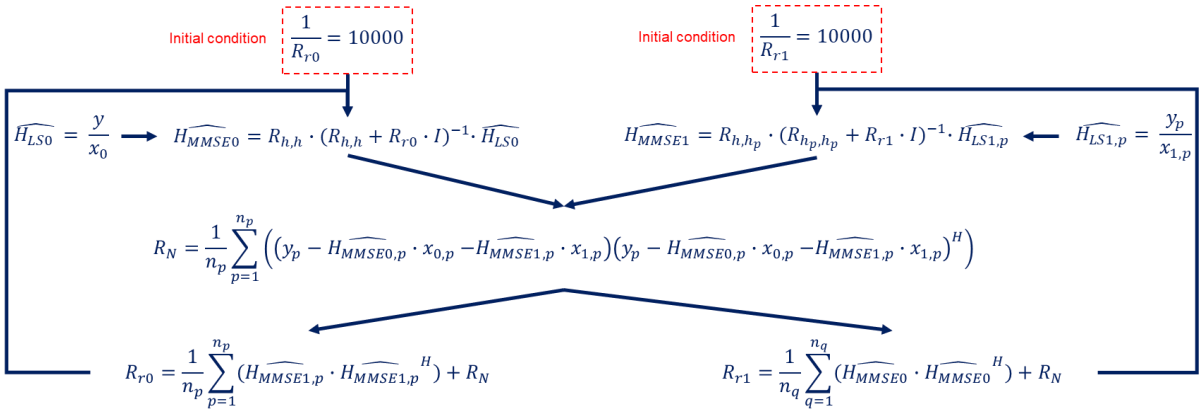

Figure 3.31: Mechanism of MMSE-IRC with pilot and data symbols.

In Figure 3.31 it is presented a case where the purpose is to obtain the channel estimation of a signal of interest $\widehat{H_{MMSE0}}$, having into consideration another signal which was not decoded by the receiver yet. As it is possible to see, in this process it is taking into account the data and pilot symbols from the signal of interest, because it was already decoded, and only the symbols in pilot positions of the interfering signal.

4. Implementation

To analyse the proposed solution, simulations were done through the construction of a system composed by a Link Level Simulator (LLS) that is focused on the PHY layer, and a System Level Simulator (SLS) focused on the MAC layer. In the following, the way that the system and simulators were implemented is described. The description will start with the SLS.

4.1. System Level Simulator

First, a determinant number of parameters were chosen, for example, the number of arrivals per 30 seconds, the number of frames (equal to the number of discovery slots) being simulated, the number of replicas that a DI can use per virtual frame, the number of slots of a virtual frame, a counter to know in which slot of the virtual frame the simulation currently is, a counter that keeps track of the current number of VFs, the size of the subset with the possible patterns for transmission, the size of the subset with multiple orthogonal pilot sequences, the maximum number of attempts of decoding allowed and the maximum back off interval that can exist between a VF where a device is currently transmitting and a VF where a device will transmit again in case of failure. Also, the subset with the possible patterns for the replicas transmissions is created. Notice that as said before, all the process explained in the following is focused on the discovery slots.

Then, it starts with the construction of the structure of each User Equipment (UE). Each UE has an associated id, pilot sequence id, number of receiving antennas, type, state and a list of associated UEs. For example an UE can have an id 1, pilot sequence id 8, 2 receiving antennas, be a DI, be Inactive and be associated with UE with id 2. To be associated means that, if the UE is a DI, the list of associated UEs is the list of DRs for which the DI wants to send its message, and vice versa. In respect to the pilot sequence id, it is chosen based on the size of the subset with multiple orthogonal pilot sequences. Also, it is considered that all devices have 1 transmitting and 2 receiving antennas. In the reception, due to the use of the 2 antennas, it is considered an antenna gain of 3 dB, from the spatial diversity process and a 8 dB of antenna losses. Furthermore, to allow the development of the system each UE has to have a memory buffer associated, and if it is of type “DI” it also has parameters saying which configuration for transmission of replicas was chosen from the subset, how many replicas were already used in the current virtual frame and the number of times it already tried the decoding process.

After this and considering a certain number of DIs per km^2 and only 1 DR per DI, the deployment of the system was computed. Here it was considered a circle cluster coupling loss based deployment and for each UE it was calculated its Cartesian coordinates and the distance and the path loss and shadowing between them and the associated UE. For more information about the approach that was used in these calculations, consult Appendix A.

So, with Figure 4.1 that represents the state machine of a DI, let us analyse the simulator in more detail.

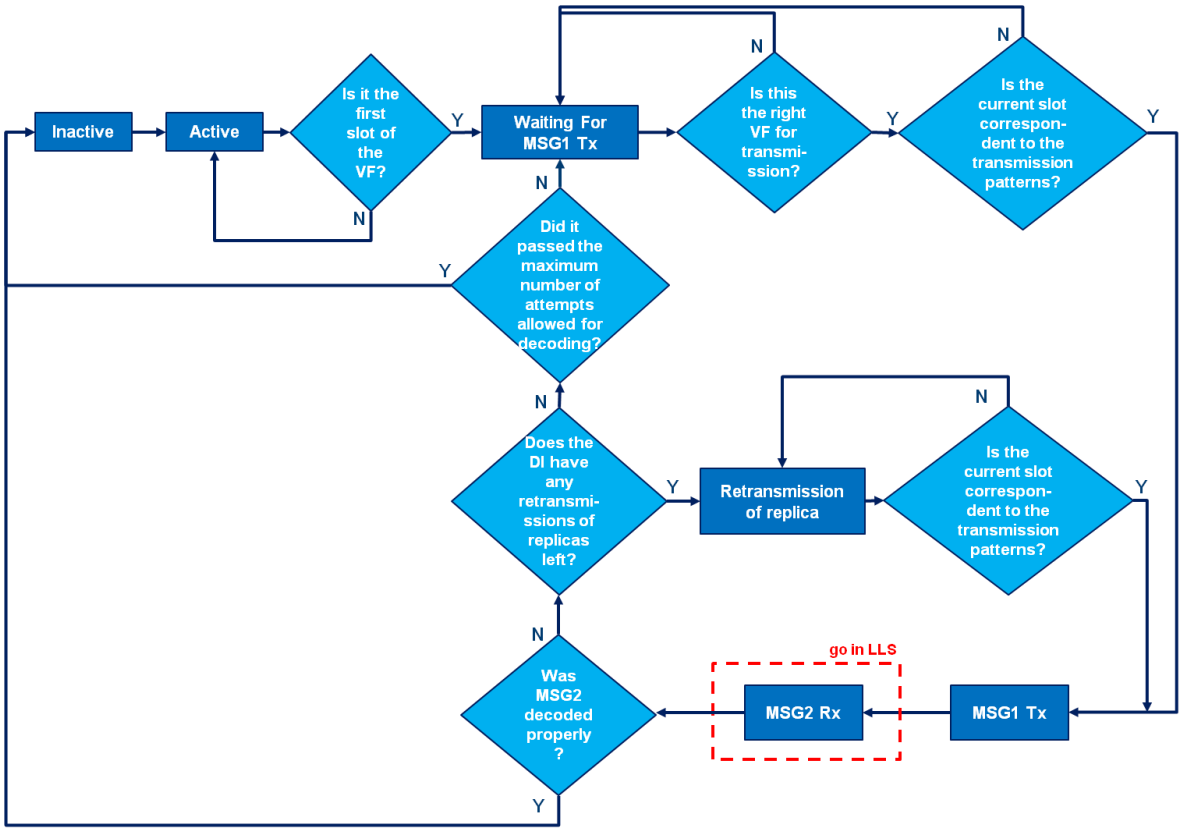

Figure 4.1: State machine of a DI in the SLS system.

In the beginning of the process, all UE devices are inactive, and obviously the number of replicas used, number of virtual frames where there was attempt of decoding and the memory buffer are initialized. Note that every time a new VF starts, the variable with the number of replicas used and the memory buffer of each device are initialized. Hence, the size of a virtual frame directly affects the size of the memory buffer required for the execution of this process.

Then, depending on the MSG1 access probability, associated with the number of arrivals per 30 seconds, a DI can go from “Inactive” to “Active". When this happens, the associated DRs are also activated.

If the DI is in state “Active” and it is the beginning of a VF, its state changes to “Waiting for MSG1 Tx”, otherwise it stays in the same state. This means that all DIs that become “Active” during a VF process will pass to the “Waiting for MSG1 Tx” state in the beginning of the next VF.

When the DI is in the “Waiting for MSG1 Tx” state, if it is in the right VF and it is in the right slot of the VF for the transmission, its state changes to “MSG1 Tx”, otherwise it stays in the same state. The first decision block, related with if it is the right VF or not, is needed since in the case where a VF is processed but the DI could not receive MSG2 successfully, there is a random back off interval between the current VF and the next one where the DI will try the decoding process again. The second decision block is also needed since the current slot of the virtual frame being processed can or cannot be the slot

correspondent to the pattern of transmissions chosen by the DI. This is done taking advantage of the counter that keeps track of which slot in the VF the simulation currently is.

After, in the “MSG1 Tx” state, the creation and transmission of the MSG1 payload is done. Each payload is constituted by the generating id, the state of the message, the pilot sequence id and the transmitted power. Remember that the pilot sequence was chosen initially by the device from a pre-defined set of multiple orthogonal pilot sequences known by the transmitter and the receiver. Also, it is considered that the transmission power of all MSG1 payloads is 30 dBm. So, for example, a payload could have been generated by the UE of id 1, the state of the message can be “Not received yet”, the pilot sequence id can be 6 and the transmitted power is 30 dBm. It is also in this state that the device chooses in each subcarrier resource it wants to transmit its message. In the case of MSG1 transmissions, the only subcarrier available is subcarrier 1. Finally, the variable containing the number of replicas already used in a virtual frame is incremented. Afterwards, the state changes to “MSG2 Rx” and because this last is a reception state and the device is half-duplex, the continuation of the process is done in the next discovery slot.

In the “MSG2 Rx” state, the introduction of the LLS and its processing starts. In this process, with techniques such as intra and inter-SIC, the DI tries to decode as many MSG2 payloads as it can and in the case where inter-SIC is used, it keeps the ones decoded correctly in a memory buffer. So, essentially, the output of the LLS, which will be explained later on, are the payloads that were decoded.

If between the payloads decoded, the MSG2 generated by the associated DR of this DI is present, both DI and DR become inactive, the variable counting the number of attempts of decoding is initialized and the DI state changes to “Inactive”. Otherwise, there are two options:

- If there are still replicas to transmit in this VF, the DI state changes for “Retransmission of replica” and stays in this state waiting for the right slot of this VF to change its state to “MSG1 Tx” and transmit its payload again.

- If it does not have any transmission of replica left to do in this VF, increments the variable of the number of attempts of decoding, and:

    (i) If this variable is higher than the maximum number of attempts allowed, the DR and DI become inactive, the variable that keeps track of the number of attempts of decoding is initialized and the DI state is changed to “Inactive”.

    (ii) If this variable is equal or less than the number of attempts allowed, the DI state changes to “Waiting for MSG1 Tx” and because there is a random back off interval between this VF and the next one in which the decoding process will occur, the device stays in this state until the right virtual frame is reached.

Now, let us see Figure 4.2, where it is exposed a much simpler scheme that corresponds to the state machine of the DRs.

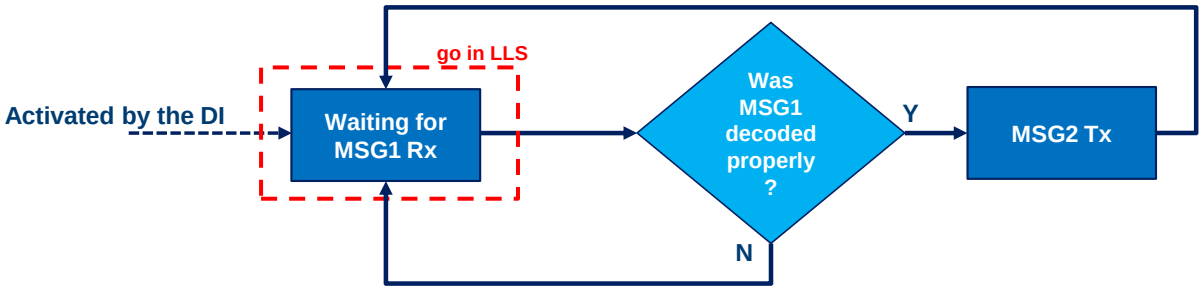

Figure 4.2: State machine of a DR in the SLS system.

As said before a DR is activated when the associated DI is also activated. From the moment that a DR is activated, its state is “Waiting for MSG1 Rx” and the process in the LLS starts. In a discovery slot, with the LLS process the device tries to decode as many MSG1 as possible and, alike to what happens in the DIs, if inter-SIC is being considered, the ones decoded correctly are stored in the memory buffer of the DR. This process will be explained later. If, in the decoded payloads, the one from the associated DI is not present, it continues in this state until this MSG1 payload of interest is decoded or until it becomes inactive. In case of decoding of the MSG1 payload of interest, the DR changes to “MSG2 Tx”. Again, because it is passing from a reception state to a transmitting state and because is half-duplex, the “MSG2 Tx” state is done in the next discovery slot of a virtual frame.

The “MSG2 Tx” state is very similar to the “MSG1 Tx” of the DI state machine. Here it is done the creation and transmission of the MSG2 payloads. Also, in this case a MSG2 payload is constitute by the generating id, the state of the message, the pilot sequence id and the transmitted power. However, the transmitted power is not a priori defined as before. To assign a transmitted power to the MSG2 payloads, the power control technique was used. Knowing the transmitted power and calculating the received power of MSG1, with the path losses and shadowing between the 2 devices, antenna gains and losses, and assuming -133 dBm for the thermal noise of the receiver, it is possible to calculate and invert the channel between the two devices in a way that allows knowing the transmitted power required for MSG2 to get a certain SNR target in the receiver. It was considered for means of simulation a 0 dB SNR target and a maximum transmitted power threshold of 30 dBm. In the use of this technique, for simplification of simulation and decrease of computational time, it was not considered the use of fading since it depends on the time of transmission. Finally, in the case of MSG2 transmissions, there are 20 subcarriers available from which the DR can randomly choose to send its message. After MSG2 payload transmission, the state of the DR changes to “Waiting for MSG1 Tx” and it will continue in this state until it receives again a MSG1 payload of interest or until it becomes inactive.

Next, it will be exposed the LLS process inserted in the two state machines presented before.

4.2. Link Level Simulator

As said before, the LLS process begins when a device is trying to receive a message. Having into account the payloads that it is receiving in the current discovery slot, the function of the LLS is

- to re-create the payloads of the subcarrier that it is taking in consideration;
- pass them through a wireless medium;
- try to decode them in the reception;

, while payloads from other subcarriers are considered as noise. So, in the case where a DI is trying to decode MSG2, it has to do this process for every subcarrier occupied with MSGs2 considering the payloads present in the others subcarriers as noise, and for the case where a DR is trying to decode MSG1, this process is done for the payloads in the first subcarrier and considering the payloads from the other subcarriers as noise.

Starting with the first point, each payload of the subcarrier in consideration is re-created with the transmitter chain presented in the last section, beginning with a random generation of a sequence of bits – transport block. Note that from the SLS, it is possible to obtain information about the pilot sequence id of each payload so then the right DM-RS can be created and multiplexed. The implementation of the transmitter chain in the LLS system is done as shown in Figure 4.3.

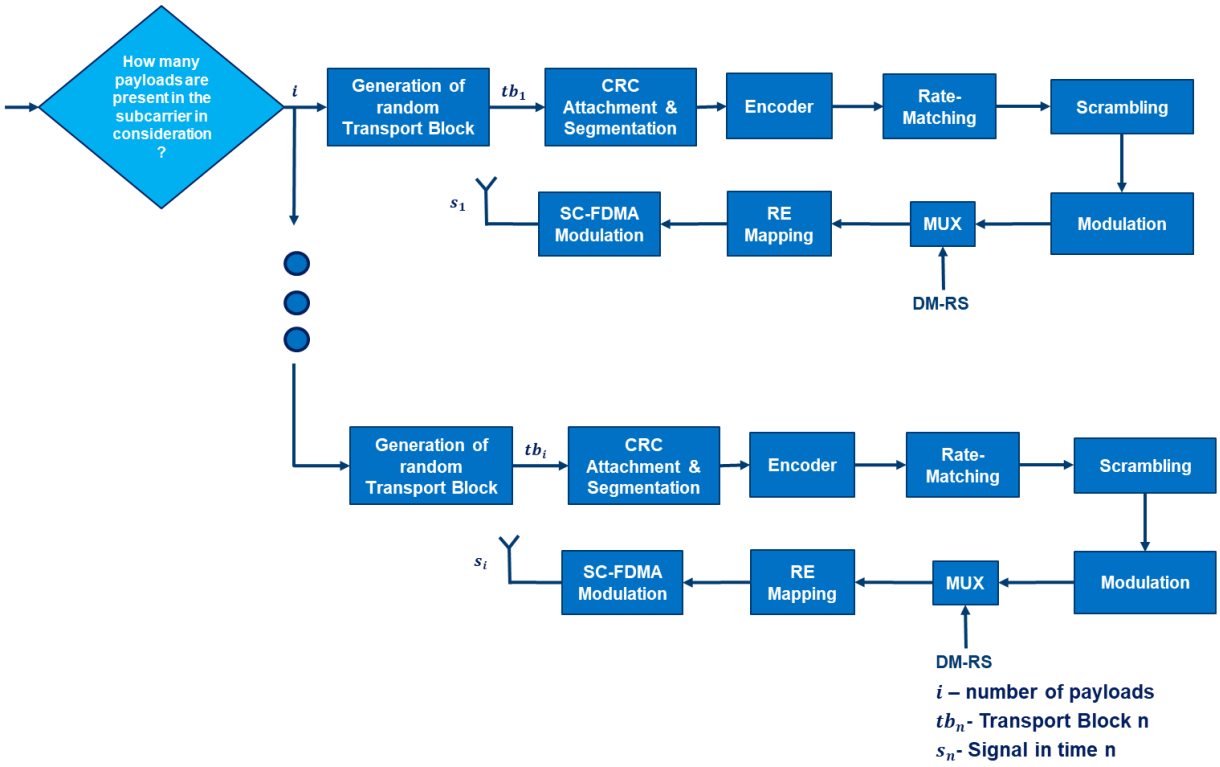

Figure 4.3: Transmitter chain in the LLS system.

After the creation of all payloads of a specific subcarrier in the LLS, it is time to pass them through a wireless medium. At this time all signals have linear power of 1, or 0 dB. This procedure starts by passing each signal by a multi-path Rayleigh fading environment created with the assistance of the function lteFadingChannel, offered by Matlab. To configure this function, it was considered the Extended

Pedestrian A (EPA) model with a maximum Doppler frequency of 5 Hz, a sampling rate of 1.92 MHz, 2 receiving antennas (all devices have this configuration), a medium MIMO correlation, an initial time that varies depending on which discovery slot is currently being simulated and a seed that is reciprocal and depends on the transmitter and receiver id for each payload. After applying the fading channel, some payload characteristics recover from the SLS such as transmitted power, path loss and shadowing and antenna gains and losses were also applied to each payload. Note that the transmitted power for each payload was calculated in its formation, path loss and shadowing for devices in the list of associated UEs was calculated in the computation of deployment but it can be calculated also for devices outside that list, and it is considered a total antenna gain of 3 dB and losses of 8 dB. At this moment, all aspects related with the payloads that will be submitted to the decoding process are handled. The only thing left to do in the second point of the LLS process is the noise generation. Hence, to the sum of the payloads generated before, a white Gaussian noise is added. The power of the noise is composed by the thermal noise (-133 dBm) plus the sum of the received powers of the payloads from the other subcarriers, since, as said before, they will be considered as noise. Each of these payload powers is calculated with the following expression

$$P_{payload} = P_{tx} - A_{pathloss} + G_{antennas} - A_{antennas} - A_{crossSubBand} \quad (4.1)$$

where $P_{payload}$ is the received power of a specific payload, P_{tx} is the transmitted power of that payload, $G_{antennas}$ is the antenna gain and $A_{pathloss}$, $A_{antennas}$ and $A_{crossSubBand}$ are attenuations due to pathloss and shadowing, antennas and because it is not the subcarrier in consideration, respectively. In the LLS it is considered a cross sub band attenuation of 40 dB.

After passing through the channel, the signal reaches the receiver and has opportunity of using different types of techniques for decoding as many payloads as possible. In the simulations, three types of architectures were studied considering:

- no use of any type of SIC;
- use of intra-SIC;
- use of intra and inter-SIC.

Next, the three above architectures will be illustrated and briefly discussed. Note that all the blocks presented in the diagrams of these architectures were already explained in the last section.

4.2.1.No SIC

The first architecture, which does not use any type of SIC, is depicted in Figure 4.4. It is expected that this receiver architecture is the one that has the worst performance, since there is no application of any kind of SIC technique in the decoding process.

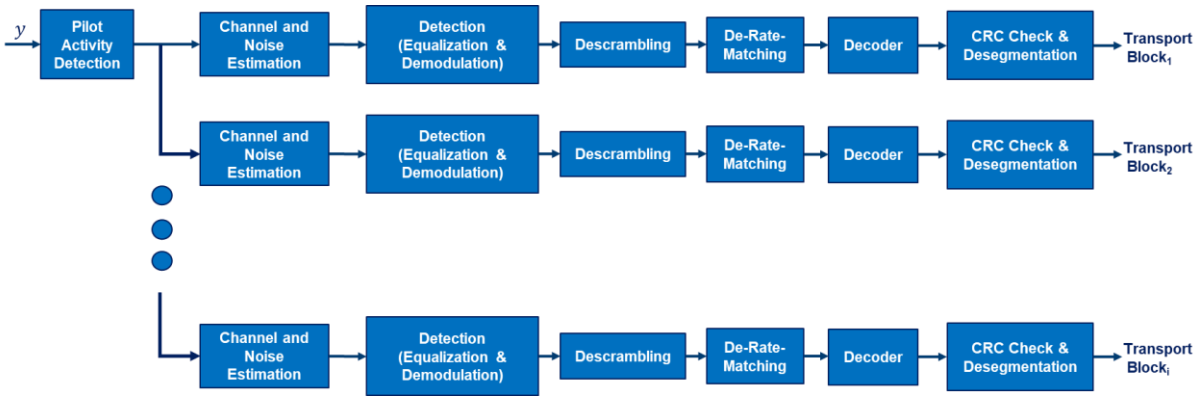

Figure 4.4: Receiver architecture without SIC in the LLS system.

4.2.2.Intra-SIC

Let us analyse now the structure of a receiver architecture that applies intra-SIC. The block diagram of this architecture is presented in Figure 4.5. Remember that its process consists in the application of SIC loops, allowing a continuous cancellation of signals from the received signal. It is expected that this receiver architecture is better than the last one, since if the channel and noise estimations are good and the decoding process is correctly done, each cancellation of signal will allow better circumstances for decoding the remaining packets in the received signal. This will allow a higher number of discovery sessions during the process.

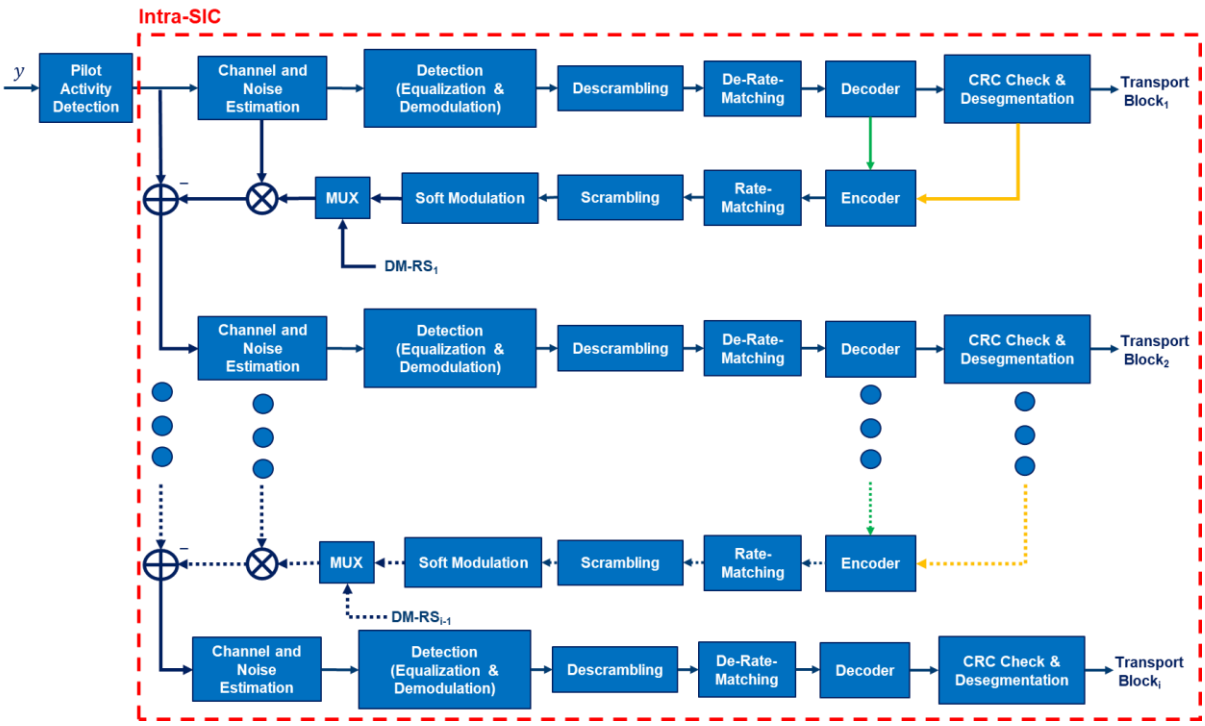

Figure 4.5: Receiver architecture with intra-SIC in the LLS system.

4.2.3.Intra and Inter-SIC

Finally, the last receiver architecture for decoding the payloads is depicted in Figure 4.6. As mentioned before, in this architecture it is taken in consideration two types of SIC – intra and inter. The great advantage of this technique over the last two is that it uses information obtained from previous slots to apply SIC and ease the decoding process in posterior slots. Remember that this is only possible because the packets sent by a user in a virtual frame are replicas. It is expected that this receiver architecture will be the one with the best performance, since it applies two different manners of SIC, which will boost the increase of discovery sessions.

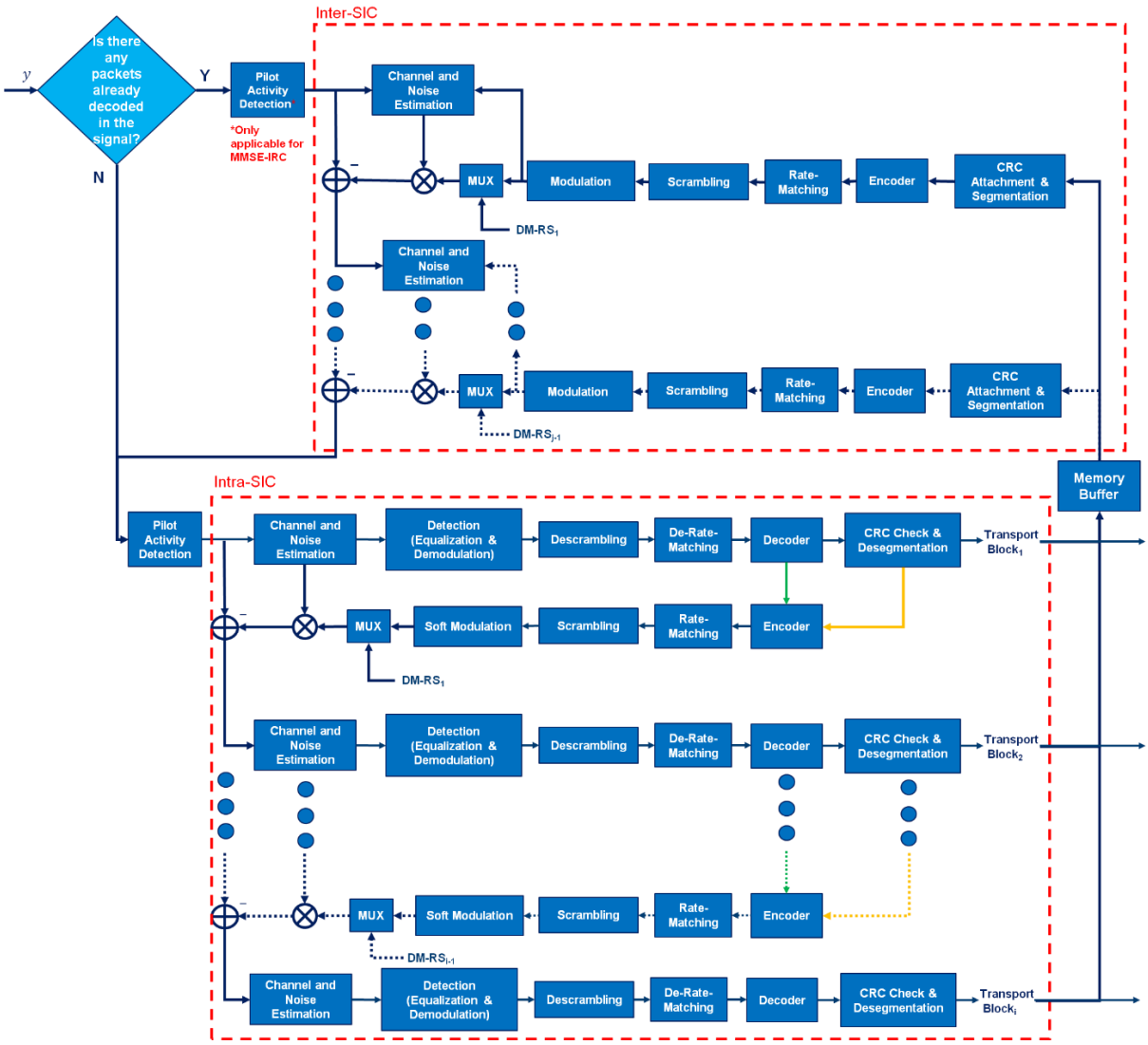

Figure 4.6: Receiver architecture with intra and inter-SIC in the LLS system.

5. Results Analysis

In this chapter, several results will be discussed, in terms of performance and complexity.

5.1. Performance

Before starting the construction of the full system, preliminary simulations at physical level (LLS) were performed.

5.1.1. Preliminary Results

A simpler LLS was implemented where two signals (one signal of interest and one interferer) were constructed, passed through a wireless medium and received. The system parameters used in the following simulations are presented in Table 5.1.

Table 5.1: System parameters for preliminary simulations.

LLS parameters	Value
Size of Transport Block	40
Δf [Hz]	3750
Modulation	QPSK
Turbo iterations	8
Channel	Rayleigh Fading EPA 5Hz
Noise	White Gaussian
SNR [dB]	-20/-15/-10/-5/0/5/10/15/20
SIR [dB]	-20/-15/-10/-5/0/5/10/15/20
Channel Estimation	MMSE-MRC/MMSE-IRC
Periods	10 000

The construction of the signals was done with the transmission chain presented in Figure 3.9. Then, each signal was affected by a multipath Rayleigh fading channel EPA 5 Hz implemented with the lteFadingChannel from Matlab. In order to get results for different magnitudes of interference, the power of the interfering signal was modified depending on a pre-defined signal-to-interference ratio (SIR). Also, both signals use different orthogonal pilot sequences, because as seen before there is an advantage of using this instead of a single one. After, the two signals and a White Gaussian noise, also modified

having into account a signal-to-noise ratio (SNR), are added. Hence, each simulation run which does the transceiver process a certain number of periods, is composed by a pair (SIR, SNR). Finally, the signal reaches the receiver and after applying SIC or just the simple decoding process, it checks the CRC and compares the final transport block of the signal of interest with its initial. If the blocks match and the CRC checks, the BLER is 0, otherwise is 1. After all the periods, a mean is done over these values, presenting the mean value of the BLER for a pair (SIR, SNR).

Now that the preliminary LLS process was described, the simulations performed with this simulator will be presented.

In the first simulation, Figure 5.1, it is simulated the two types of channel estimation – MMSE-MRC and MMSE-IRC – in presence of interference and without the use of SIC.

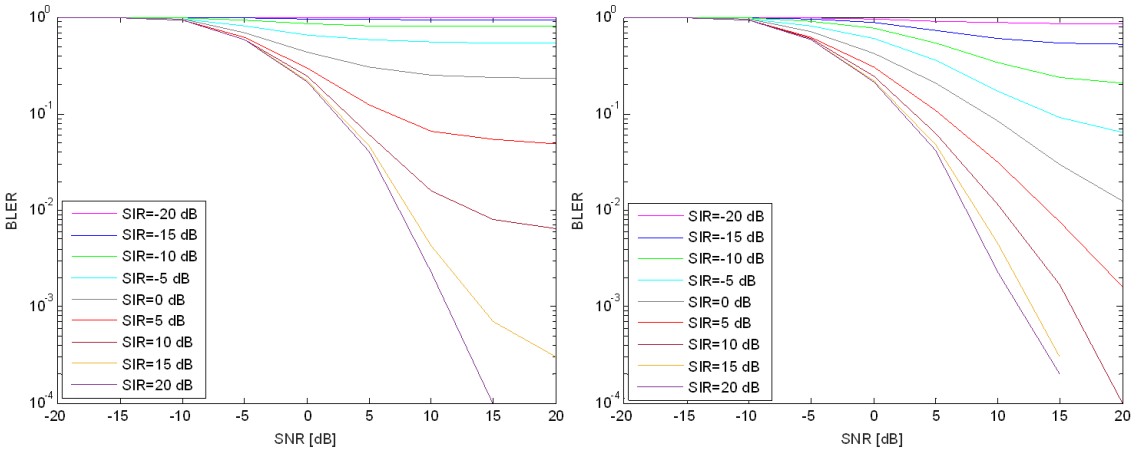

Figure 5.1: Comparison between two types of channel estimation in presence of interference: MMSE-MRC (left) and MMSE-IRC (right).

Figure 5.1 shows that when the amount of interference increases (SIR decreases), in both types of channel estimation, the performance of the system decreases. Also, it is possible to observe that in general, MMSE-IRC presents better performance than MMSE-MRC. Note that for cases where the SIR is very high (20 dB), due to the small amount of interference, the performance of both channel estimations is expected to be very similar. In this circumstances and in this simulation, the MMSE-MRC shows slightly better performance than MMSE-IRC, due to the randomness of the system.

In the second simulation, Figure 5.2, the use of SIC was tested. Here the difference in terms of performance of not using and using SIC is presented for both channel estimations and for different amounts of interference.

It is possible to observe that SIC improves the performance of the system especially in cases with high amount of interference while in cases with low amount of interference the performance is very similar to the one in which SIC is not used. Again here, the MMSE-IRC channel estimation presents better performance than MMSE-MRC in cases where there is a high amount of interference and they are very similar for cases where there is low quantity of interference.

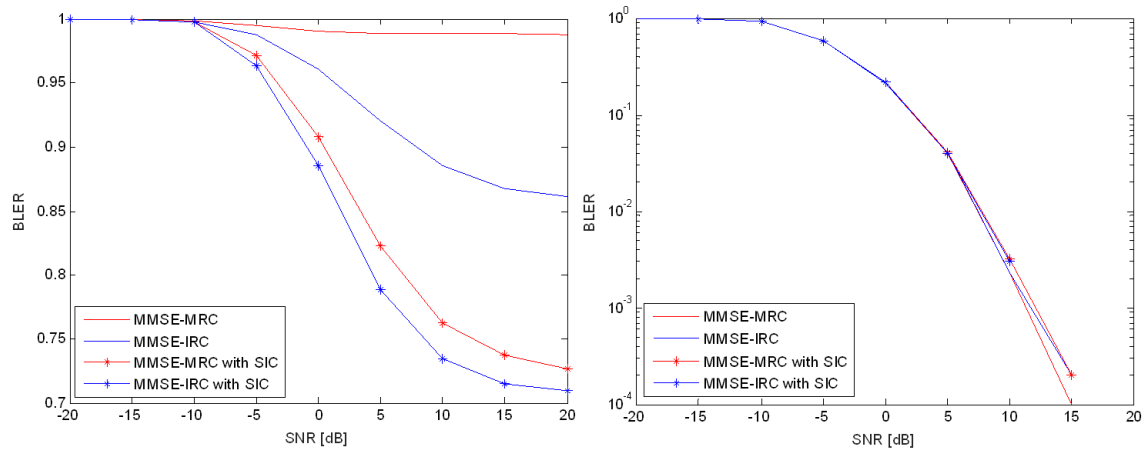

Figure 5.2: Comparison between no use of SIC and use of SIC for two types of channel estimation in different amounts of interference: SIR=-20 dB (left) and SIR=20 dB (right).

Now that some preliminary results were analysed, results from the proposed solution in consideration will be shown, starting by analysing the difference, in terms of performance, of the different architectures for pilot activity detection.

5.1.2.Pilot Activity Detection

The system used for simulation of the different architectures is very similar to the preliminary LLS. The greater differences are that instead of using SNR and SIR parameters, the two signals and noise have specific powers and also, instead of the two signals have different orthogonal pilot sequences, in here there are a certain number of available orthogonal pilot sequences from which the two devices randomly choose one of them. Hence, they can transmit different orthogonal pilot sequences or the same one. Then, in the reception, there is no need to simulate the full receiver chain and decode one of the signals since after applying the different pilot activity detection architectures, the pilot sequences are detected, or not, which is what is being studied now. This process is done a certain number of times to test the different architectures. These changes were made so the system becomes more close to the real system implementation in consideration. The system parameters used in these simulations are presented in Table 5.2.

To evaluate the performance of the proposed architectures, the received pilot sequences can be classified as follows:

- If a pilot sequence is detected but it was not transmitted by any of the devices, it is a false positive.
- If a pilot sequence is detected and was transmitted by at least one device, it is a true positive.
- If a pilot sequence is not detected but was transmitted by at least one device, it is a false negative.

- If a pilot sequence is not detected and it was not transmitted by any of the devices, it is a true negative.

Table 5.2: System parameters for simulation of different pilot activity detection architectures.

LLS parameters	Value
Size of Transport Block	40
Δf [Hz]	15 000
Modulation	QPSK
Turbo iterations	8
Channel	Rayleigh Fading EPA 5Hz
Noise	White Gaussian
P_{noise} [dBm]	-133
$P_{signals}$ [dBm]	Random from -200 to 0
Available Orthogonal Pilot Sequences	16
Samples for network training	55 000
Samples for testing the architectures	10 000

The performance evaluation is done with the calculation of the false positive and true positive when different threshold values are applied; an increase of the threshold value brings a reduction of true positive and false positive values, contrariwise a decrease of the threshold value brings an increment of false positive and true positive. Figure 5.3 shows the comparison between the three proposed solutions where:

- Case 1: Parallel Matched Filter (Baseline).
- Case 2a: Parallel Matched Filter with Adaptive Threshold via common Neural Network, with the outputs of the matched filter as input of the neural feedforward network.
- Case 2b: Parallel Matched Filter with Adaptive Threshold via common Neural Network, with the outputs of the matched filter plus the original received signal as input of the neural feedforward network.

- Case 3a: Parallel Matched Filter with Adaptive Threshold via individual Neural Network, with the outputs of the matched filter as input of the neural feedforward networks.

- Case 3b: Parallel Matched Filter with Adaptive Threshold via individual Neural Network, with the outputs of the matched filter plus the original received signal as input of the neural feedforward networks.

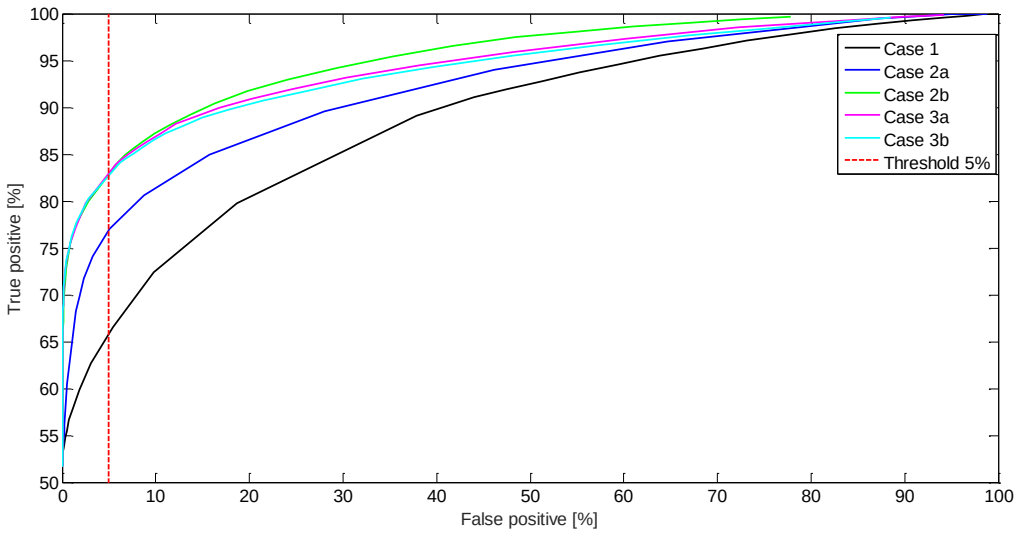

Figure 5.3: Percentage of true positives for different pilot activity detection architectures.

As it is possible to see, when operating at a maximum value of false positives equal to 5%, introducing the neural network allows to significantly increase the number of true positives compared to the naïve (Parallel Matched Filter only) solution. A further gain in the performance is obtained by either providing extended input vectors (2a vs 2b) or by switching to separate neural networks.

A summary of different characteristics for the different cases is show in Table 5.3.

Table 5.3: Summary of characteristics and results obtained from different pilot activity detection architectures.

Proposed Pilot Activity Detection Architecture	Number of neural network inputs	Number of networks	Number of layers	Number of nodes	False positive	True positive
1	-	-	-	-	5%	65.81%
2a	16	1	1	50	5%	76.85%
2b	80	1	1	50	5%	82.82%
3a	16	16	1	50	5%	82.97%
3b	80	16	1	50	5%	82.77%

5.1.3.Receiver Architectures

Finally, it will be shown the results obtained for different receiver architectures – no SIC, intra-SIC, and intra-SIC and inter-SIC – in the system proposed. Here it was used the SLS and LLS systems presented in chapter 4. The general system parameters used are presented in Table 5.4 and Table 5.5.

Table 5.4: System parameters used in SLS.

SLS parameters	Value
Number of frames	4000
Time of a frame [ms]	1000
Number of DIs per km^2	200
Number of DRs per DI	1
Size of set with orthogonal pilot sequences	16
Max attempts of decoding allowed	8
Max back off interval between VFs	8

Table 5.5: System parameters used in LLS.

LLS parameters	Value
Size of Transport Block	40
Δf [Hz]	15 000
Modulation	QPSK
Turbo iterations	8
Channel	Rayleigh Fading EPA 5Hz
Noise	White Gaussian
Account for Cross Sub-Band Attenuation	Yes
Channel Estimation	MMSE-MRC/MMSE-IRC

Note that parameters such as number of replicas per packet, size of the virtual frame and size of the set with the possible transmission patterns will be defined later since they change depending on the receiver

architecture in consideration. However, in the case of “no SIC” and “intra-SIC” there is no advantage of using replicas, since there is nothing helping the communication between them, so it is used slotted ALOHA which is equivalent to the use of one replica, a virtual frame of size one and a set with only one possible transmission pattern. Also, it is important to comment that the following results are an upper bound in respect to the pilot activity detection, since this one is considered perfect.

No SIC

So, let us start the evaluation of the total system considering no use of SIC in the reception of MSG1 and no use of SIC in the reception of MSG2. In Figure 5.4 it is presented the average number of completed discovery sessions per minute for this system, for different channel estimations. Remember that a discovery session is initiated when a DI sends an initial MSG1 and it is completed when it receives the correspondent MSG2.

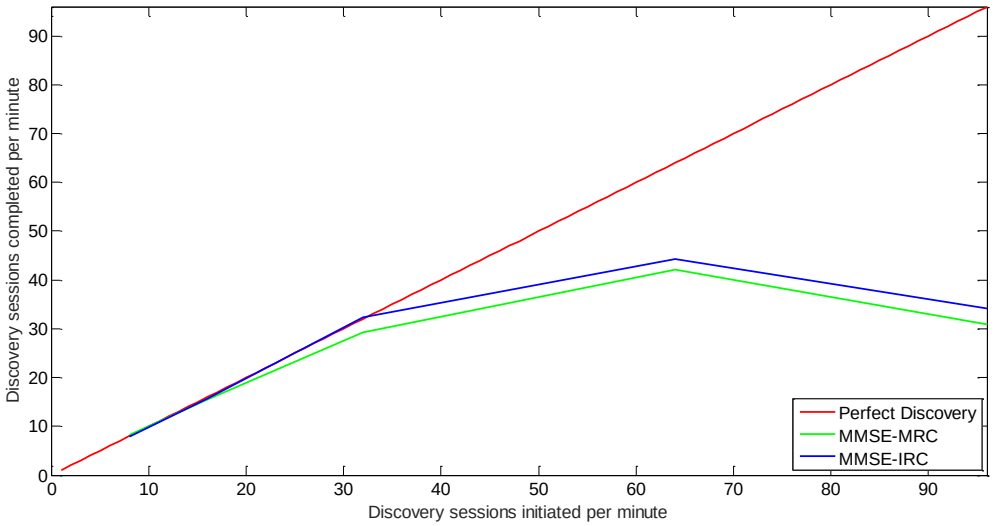

Figure 5.4: Comparison between the two types of channel estimation for a system with no SIC in both MSGs.

It is possible to see, once again that MMSE-IRC presents better performance than MMSE-MRC. In respect to the overall system, its performance starts to decrease when the number of discovery sessions initiated per minute increases, which is expected.

Intra-SIC

Now, results to evaluate the performance of the process intra-SIC will be showed. Remember that there are two manners of executing this process: one where the subtraction of signals is always done even if the CRC does not check, and the second one where the subtraction is only done if the CRC checks. Here, it is possible to explore three different systems: use of intra-SIC only in MSG1, use of intra-SIC only in MSG2 and use of intra-SIC in MSG1 and MSG2. To discover which of these systems have better trade-off between performance/complexity, the three systems are simulated using the simplest channel estimation, MMSE-MRC.

In Figure 5.5 the average number of completed discovery sessions per minute for the first system in consideration is exposed.

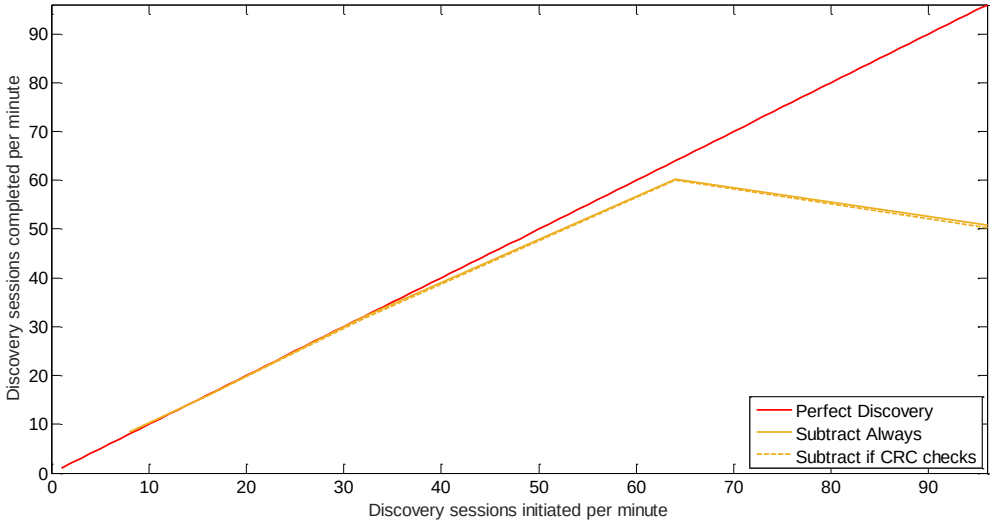

Figure 5.5: Average number of discovery sessions completed per minute for a system with intra-SIC only in MSG1 and applying MMSE-MRC.

In the system where intra-SIC only occurs in MSG1, it is possible to see that the two options of intra-SIC have a similar performance.

Then, in Figure 5.6, the results obtained for the second system are shown.

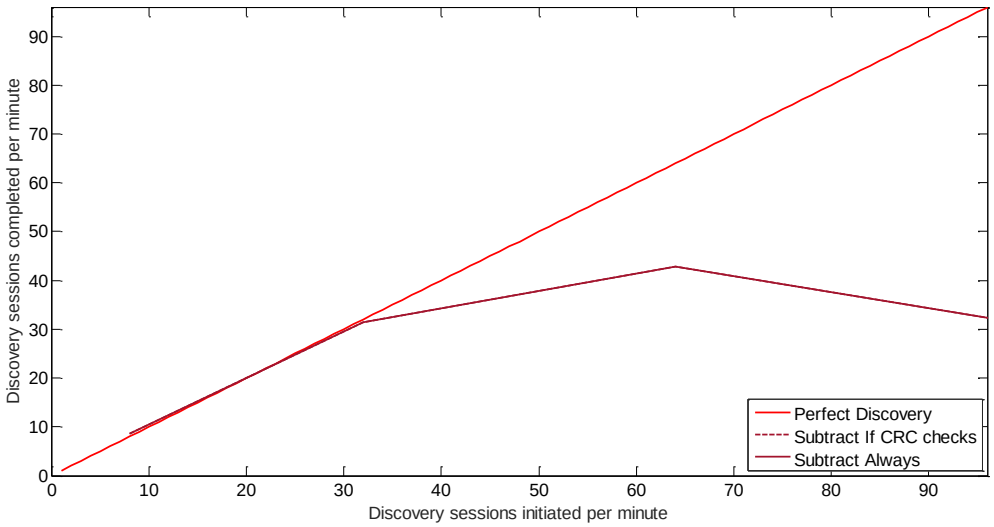

Figure 5.6: Average number of discovery sessions completed per minute for a system with intra-SIC only in MSG2 and applying MMSE-MRC.

In this system, where intra-SIC is only applied to MSG2, the performance between the two options of intra-SIC matches perfectly. This is probably due to the fact that MSG2 have 20 subcarriers available for transmission, so the interference within a subcarrier is low and every time a packet is decoded, its CRC checks.

And finally in Figure 5.7, the results obtained for the third system are presented.

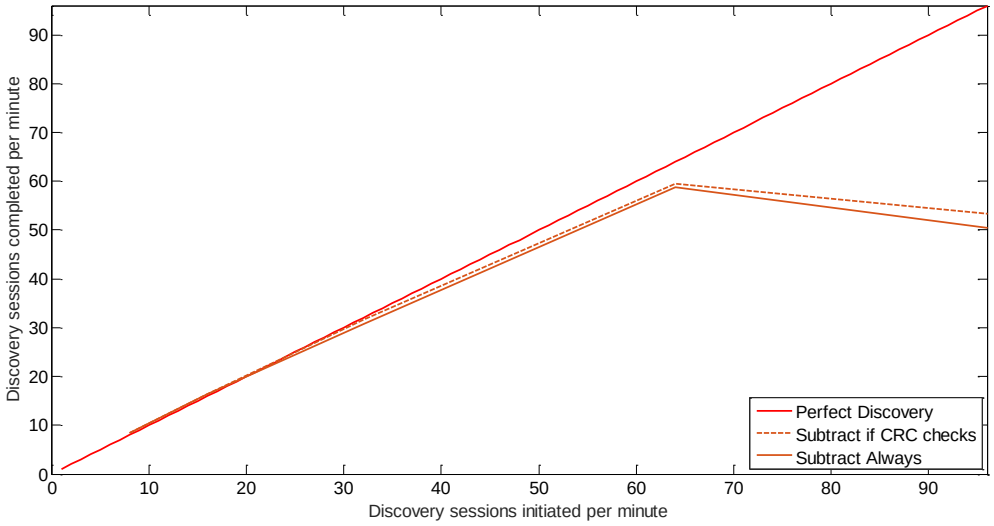

Figure 5.7: Average number of discovery sessions completed per minute for a system with intra-SIC in both MSGs and applying MMSE-MRC.

In this system where intra-SIC is applied in the two messages, it is shown that it obtains the best performance when only the packets that were correctly decoded are removed from the system.

In Figure 5.8 it is shown a comparison between the three systems, having in consideration the best option of intra-SIC in each one of them.

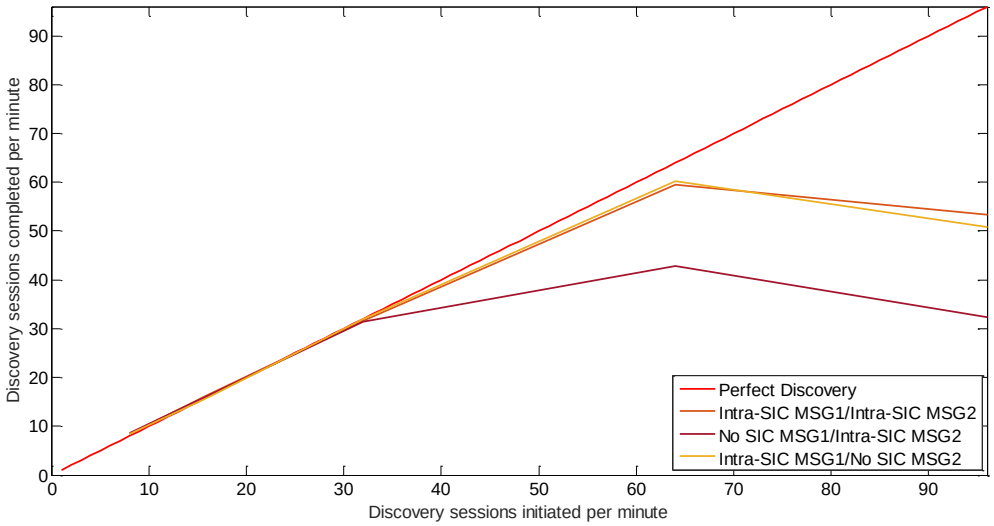

Figure 5.8: Comparison between the three systems where intra-SIC can be applied.

It is possible to say that the result of doing intra-SIC only in MSG1 gives almost the same performance as using intra-SIC in both messages. This is due to the fact that MSG1 has only one available subcarrier for its transmission/reception, hence the majority of the collision problem comes from there. For that reason, from now on the focus will be in the application of the different types of SIC only in MSG1.

So, since it was already exposed in Figure 5.5 the performance of the system where it is applied only intra-SIC in MSG1 for the MMSE-MRC channel estimation, now in Figure 5.9 it is showed for MMSE-IRC.

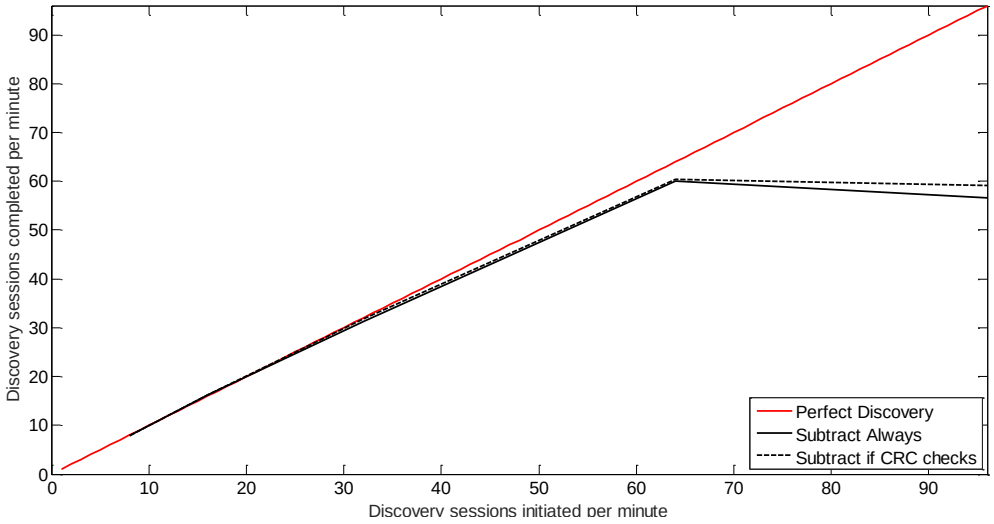

Figure 5.9: Average number of discovery sessions completed per minute for a system with intra-SIC only in MSG1 and applying MMSE-IRC.

For this system and applying MMSE-IRC, it is possible to see that both options for the use of intra-SIC are very similar, however when the number of discovery sessions initiated per minute starts to increase, the option where the packets are always subtracted seems to become more affected by the system interference than the other option.

In Figure 5.10 is presented the comparison between the two channel estimations, considering the best option for the intra-SIC, in a system where intra-SIC is only applied in MSG1.

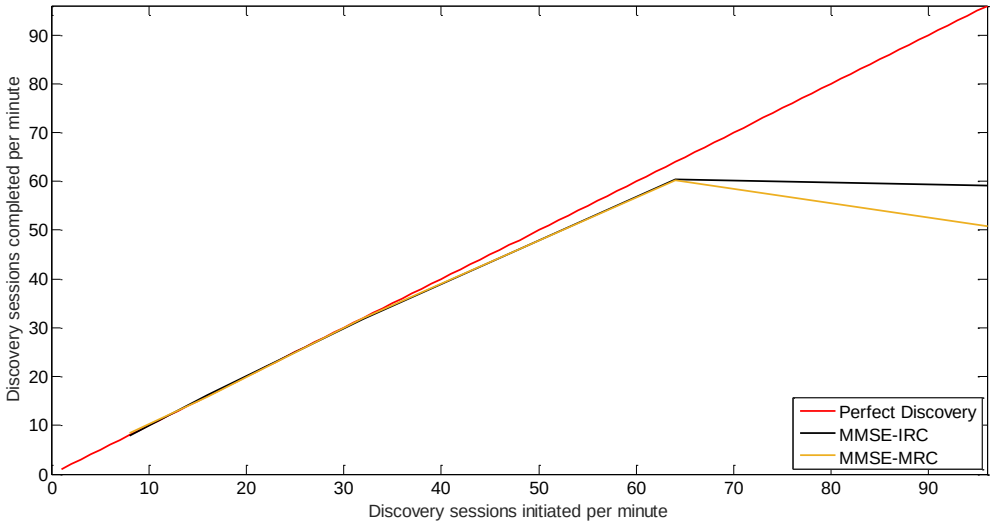

Figure 5.10: Comparison between the two types of channel estimation for a system where intra-SIC is applied only in MSG1.

Here it is possible to observe that again MMSE-IRC presents better performance than MMSE-MRC.

Intra and Inter-SIC

Finally, the system with application of inter-SIC and intra-SIC in MSG1, and with no use of SIC in MSG2, is studied. It is in this system, which uses the inter-SIC process, that the replicas and the virtual frame will fulfil their purpose. Hence, for each one of the receiver architectures depicted in Table 5.6, and considering a virtual frame with size 10, it was found the number of replicas and the size of the set with the possible transmissions patterns that maximizes the performance of every one of these architectures. Those parameters are presented in Table 5.6.

Table 5.6: Parameters for simulation of inter-SIC/intra-SIC architecture for channel estimations MMSE-MRC and MMSE-IRC.

	Inter-SIC and Intra-SIC MSG1/No SIC MSG2			
	MRC		IRC	
	Subtract Always	Subtract if CRC checks	Subtract Always	Subtract if CRC checks
Number of replicas	2	2	3	2
Size of the VF	10	10	10	10
Size of the set with the possible transmission patterns	30	30	50	30

Next, it will be exposed in Figure 5.11, the average number of completed discovery sessions per minute for the different architectures, starting with the ones that apply MMSE-MRC.

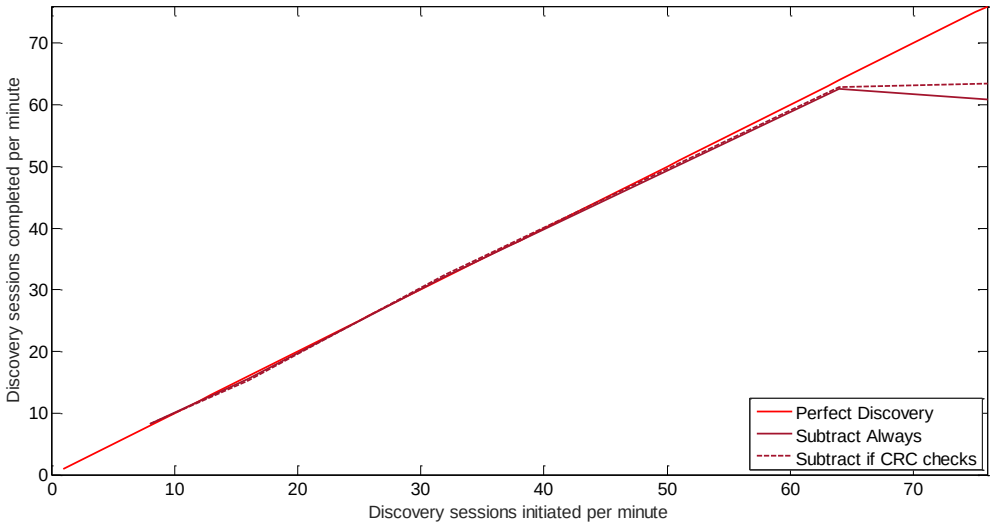

Figure 5.11: Average number of discovery sessions completed per minute for a system with intra-SIC and inter-SIC only in MSG1 and applying MMSE-MRC.

In this type of architecture seems that when the number of discovery sessions initiated per minute increases, to get better performance, the subtraction should only be done if the CRC of the packets being decoded checks.

Now, it is exposed in Figure 5.12, the average number of completed discovery sessions per minute for the case where the whole system uses MMSE-IRC.

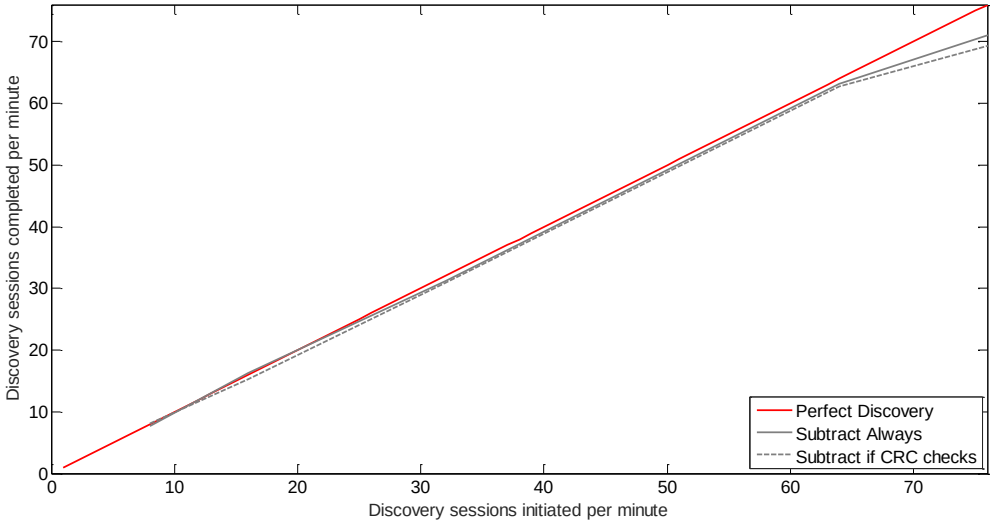

Figure 5.12: Average number of discovery sessions completed per minute for a system with intra-SIC and inter-SIC only in MSG1 and applying MMSE-IRC.

As it is possible to see, the performance of the two options using MMSE-IRC is very similar, however, contrary to the case of MMSE-MRC, a little gain is obtained if the subtraction is done always even if the CRC of the packets being decoded does not check.

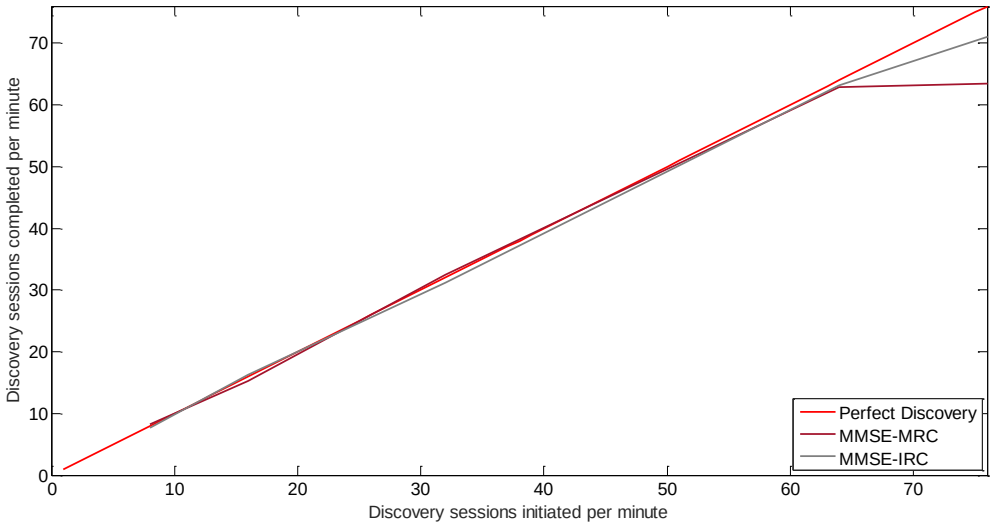

Figure 5.13: Comparison between the two types of channel estimation for a system where intra-SIC and inter-SIC are applied only in MSG1.

In Figure 5.13 is presented the comparison between the two channel estimations, considering the best option for the intra-SIC, in a system where intra-SIC and inter-SIC are applied in MSG1.

It is possible to see that also in this architecture, the MMSE-IRC continuous to present better performance compared to MMSE-MRC.

One question that caught the attention when the project was being developed was if in a system where MMSE-IRC is used, a channel estimation with such complexity was really needed in the process of inter-SIC, since in this process the channel estimation already has the advantage of using the data symbols. For that reason it was also tested a system with MMSE-IRC but with MMSE-MRC in the inter-SIC process. Also, for sake of results it was simulated the case where MMSE-MRC is used but with MMSE-IRC in the inter-SIC process. The parameters used that gave the best results for these architectures are presented in Table 5.7.

Table 5.7: Parameters for simulation of inter-SIC/intra-SIC architecture for channel estimations MMSE-MRC with MMSE-IRC in the inter-SIC process and MMSE-IRC with MMSE-MRC in the inter-SIC process.

	Inter-SIC and Intra-SIC MSG1/No SIC MSG2			
	MRC with IRC in inter-SIC		IRC with MRC in inter-SIC	
	Subtract Always	Subtract if CRC checks	Subtract Always	Subtract if CRC checks
Number of replicas	2	2	2	3
Size of the VF	10	10	10	10
Size of the set with the possible transmission patterns	30	20	20	30

First, it is presented in Figure 5.14 the two simulations for the case where MMSE-MRC is applied in the whole system except in the process of inter-SIC where MMSE-IRC is applied.

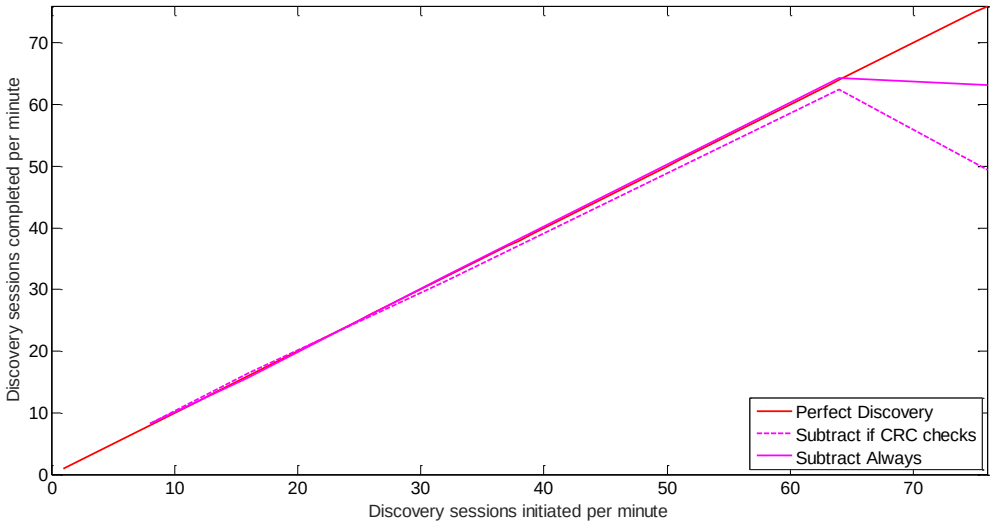

Figure 5.14: Average number of discovery sessions completed per minute for a system with intra-SIC and inter-SIC only in MSG1 and applying MMSE-MRC except in the process of inter-SIC where MMSE-IRC is applied.

In this case, as it is possible to observe, there is a big difference in terms of performance between the two architectures of intra-SIC, presenting the best one when the cancellation of the signals is always done.

Next, Figure 5.15 presents the two simulation for the case where MMSE-IRC is used in the system except in the inter-SIC process where MMSE-MRC is used instead.

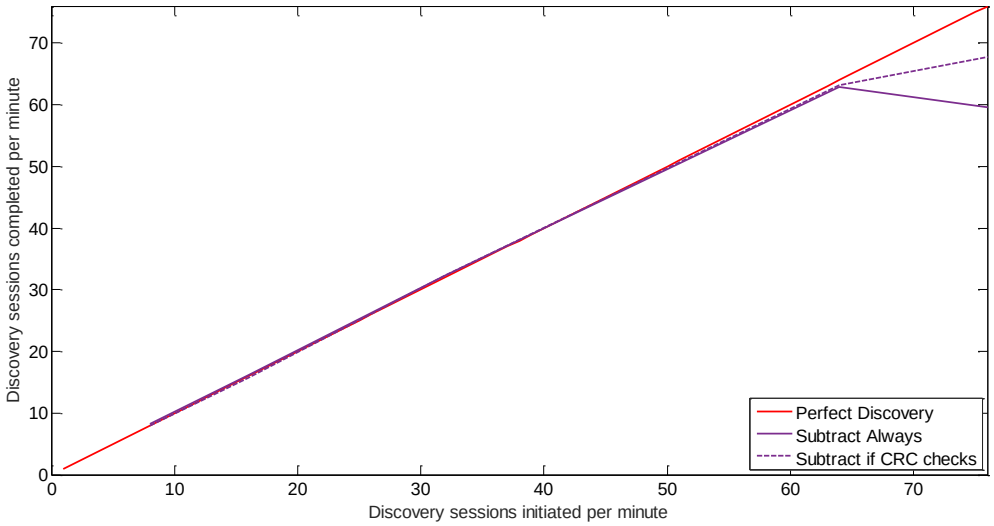

Figure 5.15: Average number of discovery sessions completed per minute for a system with intra-SIC and inter-SIC only in MSG1 and applying MMSE-IRC except in the process of inter-SIC where MMSE-MRC is applied.

Here, there is also a big difference in terms of performance between the two architectures of intra-SIC, presenting the best one when the cancellation of the signals is only done when the packets are correctly decoded.

So, in Figure 5.16, a comparison between the four inter plus intra architectures, considering the best option for the process of intra-SIC in each one of them, is done.

Here it is possible to observe that when MMSE-MRC is used in the system, for the two types of channel estimation in the inter-SIC process, the performance is very similar. However, when MMSE-IRC is used and instead of using MMSE-IRC, it is used MMSE-MRC in the inter-SIC process, the performance decreases approximately 5%.

Finally, in Figure 5.17 is presented the comparison between all systems – no SIC in MSG1 and no SIC in MSG2, intra-SIC in MSG1 and no SIC in MSG2, inter-SIC/intra-SIC in MSG1 and no SIC in MSG2 – for the two types of channel estimation in consideration – MMSE-MRC and MMSE-IRC.

As expected the system with lower performance is when no type of SIC is applied in MSG1. The use of intra-SIC increases a lot the system performance but the one that has the highest performance is when the two types of SIC are applied. In each system, and as said before, the use of MMSE-IRC has always performance benefits in respect to the less complex channel estimation MMSE-MRC.

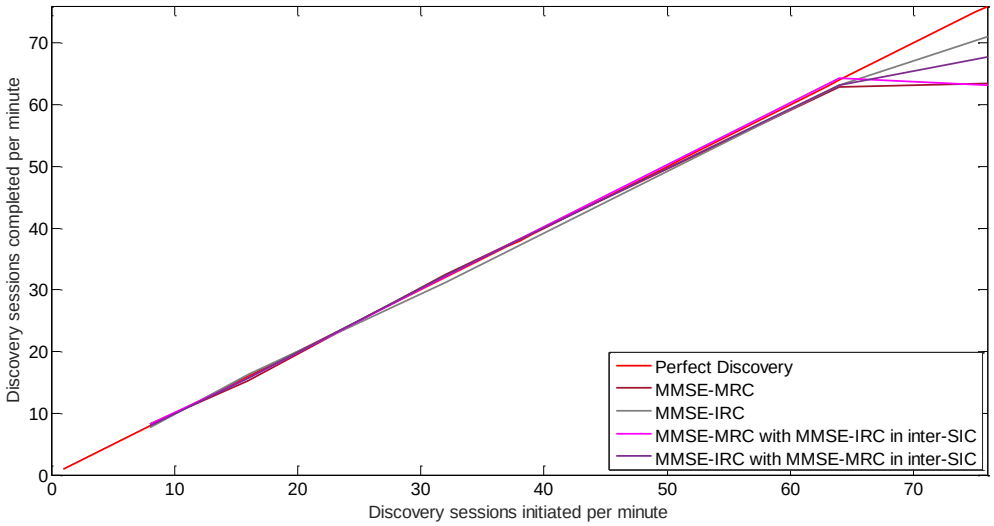

Figure 5.16: Comparison between the different architectures when intra-SIC and inter-SIC are applied only in MSG1.

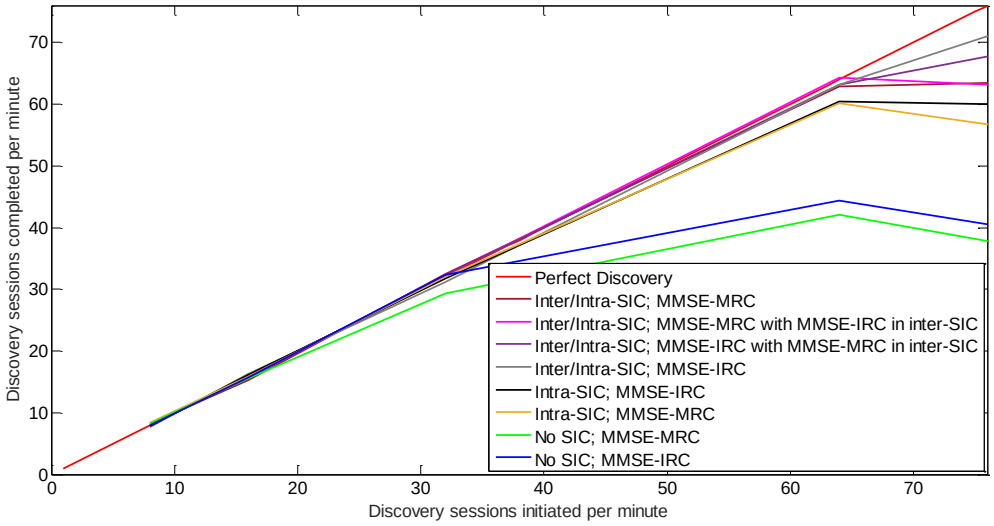

Figure 5.17: Comparison between all systems for the two types of channel estimation in consideration.

5.2. Complexity

To evaluate the complexity of the proposed solution, the three systems in consideration are compared:

- No SIC in MSG1 and no SIC in MSG2.
- Intra-SIC in MSG1 and no SIC in MSG2.
- Intra/inter-SIC in MSG1 and no SIC in MSG2.

Remember that in the execution of the intra-SIC process there are two options: one where the packets are always subtracted even if their CRC does not check, and the other where the subtraction is only done if their CRC checks. Here it is considered the option that obtained the best performance for each

one of the architectures in study.

Also, remember that when using MMSE-MRC in the inter-SIC process there is no need for a pilot activity detection block in this process.

Hence, the total complexity of the three systems are:

- $O_{sys1} = O_{no\ SIC1} + O_{no\ SIC2}$ (5.1)

$$O_{no\ SIC1} = p_1 \cdot K_{pd} + n_1 \cdot K_{ch} + n_1 \cdot K_{det} + n_1 \cdot K_{desc} + n_1 \cdot K_{derm} + n_1 \cdot K_{dec} + n_1 \cdot K_{CRCcheck} \quad (5.2)$$

$$O_{no\ SIC2} = w_1 \cdot K_{pd} + t_1 \cdot K_{ch} + t_1 \cdot K_{det} + t_1 \cdot K_{desc} + t_1 \cdot K_{derm} + t_1 \cdot K_{dec} + t_1 \cdot K_{CRCcheck} \quad (5.3)$$

- $O_{sys2} = O_{Intra-SIC1} + O_{no\ SIC2}$ (5.4)

$$O_{Intra-SIC1} = p_2 \cdot K_{pd} + n_2 \cdot K_{ch} + n_2 \cdot K_{det} + n_2 \cdot K_{desc} + n_2 \cdot K_{derm} + n_2 \cdot K_{dec} + n_2 \cdot K_{CRCcheck} + q_2 \cdot K_{enc} + q_2 \cdot K_{rm} + q_2 \cdot K_{sc} + q_2 \cdot K_{sm} + q_2 \cdot K_{mux} \quad (5.5)$$

$$O_{no\ SIC2} = w_2 \cdot K_{pd} + t_2 \cdot K_{ch} + t_2 \cdot K_{det} + t_2 \cdot K_{desc} + t_2 \cdot K_{derm} + t_2 \cdot K_{dec} + t_2 \cdot K_{CRCcheck} \quad (5.6)$$

- $O_{sys3} = O_{Intra/Inter-SIC1} + O_{no\ SIC2}$ (5.7)

$$O_{Intra/Inter-SIC1} = p_3 \cdot K_{pd} + n_3 \cdot K_{ch} + n_3 \cdot K_{det} + n_3 \cdot K_{desc} + n_3 \cdot K_{derm} + n_3 \cdot K_{dec} + n_3 \cdot K_{CRCcheck} + q_3 \cdot K_{enc} + q_3 \cdot K_{rm} + q_3 \cdot K_{sc} + q_3 \cdot K_{sm} + q_3 \cdot K_{mux} + d_3 \cdot K_{pd} + x_3 \cdot K_{CRCAtt} + x_3 \cdot K_{enc} + x_3 \cdot K_{rm} + x_3 \cdot K_{sc} + x_3 \cdot K_{mod} + x_3 \cdot K_{ch} + x_3 \cdot K_{mux} \quad (5.8)$$

$$O_{no\ SIC2} = w_3 \cdot K_{pd} + t_3 \cdot K_{ch} + t_3 \cdot K_{det} + t_3 \cdot K_{desc} + t_3 \cdot K_{derm} + t_3 \cdot K_{dec} + t_3 \cdot K_{CRCcheck} \quad (5.9)$$

where, $K_{pd}, K_{ch}, K_{det}, K_{desc}, K_{derm}, K_{dec}, K_{CRCcheck}, K_{enc}, K_{rm}, K_{sc}, K_{sm}, K_{mux}, K_{CRCAtt}, K_{mod}$ represent the complexity of pilot detection, channel estimation, detection, descrambling, de-rate-matching, decoder, CRC check and de-segmentation, encoder, rate-matching, scrambling, soft modulation, MUX, CRC attachment and segmentation and modulation blocks respectively and p, n, w, t, q, d, x represent the number of times that the system goes through these blocks in a simulation.

Due to time restrictions, it was done an upper bound of the complexity. To be possible to distinguish between the MMSE-MRC and MMSE-IRC block complexity, it was considered 100 for every K except for K_{ch} in the case where MMSE-IRC is used, because its complexity depends on the number of interferers. Meaning that, for example, when doing the channel estimation of a signal of interest with interfering signals present in the received signal of a slot, because this channel estimation also has to estimate the channel of all interfering signals, it is considered that

$$K_{ch-IRC} = (1 + N_{interferes}) \cdot K_{ch-MRC} \tag{5.10}$$

where $N_{interferes}$ is the number of interferers in the received signal of a slot. To know how many interferers were in a received signal of a slot, and considering the calculation of an upper bound complexity, some assumptions were done:

- For the reception of MSG1, it was counted on average how many transmissions of MSG1 happened per slot, and assuming that there is perfect pilot activity detection, this amount was considered in all channel estimation blocks that use MMSE-IRC in the MSG1 reception process.

- For the reception of MSG2, the process was the same as for MSG1, the number of transmissions of MSG2 per slot were counted and taking into account in the channel estimation blocks that use MMSE-IRC in the MSG2 reception process. So, it was considered that all MSG2 were transmitted in a common subcarrier, which is the worst case in terms of usage of resources for MSG2.

In Figure 5.18, it is depicted the average complexity of the systems for different arrivals rates. The parameters used in this simulation are the same as the ones used in the SLS and LLS in the performance results.

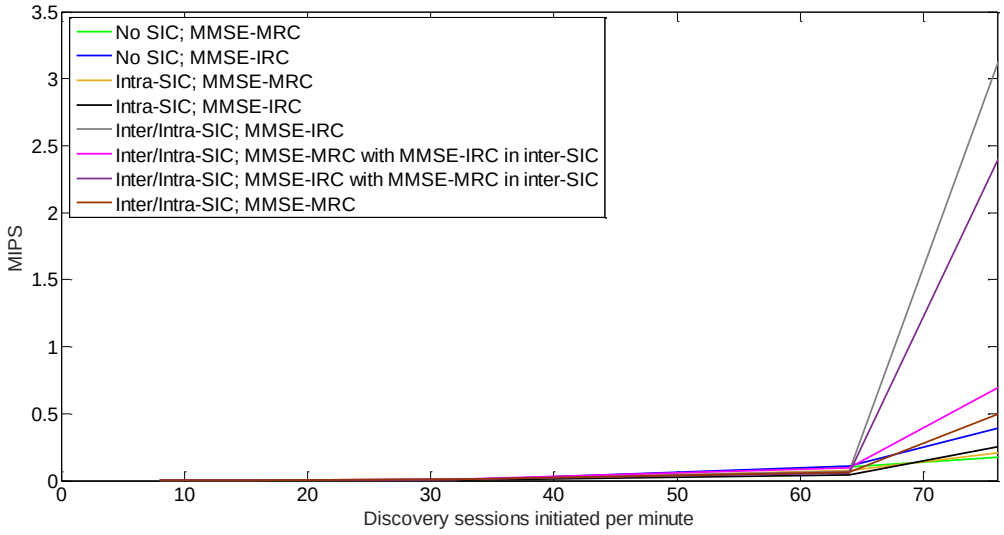

Figure 5.18: Comparison of complexity between all systems for the two types of channel estimation in consideration (in MIPS – Millions of Instructions Per Second).

For lower rates the complexity is very similar and lower for all architectures. However, around 64 discovery sessions initiated per minute, which is the time where the system starts to have more than one transmission per slot, the complexity increases rapidly. It is possible to see that in general as expected the use of two types of SIC is more complex that the use of only intra-SIC which is already more complex that the no use of SIC at all. However, there is one result that seems out of place – “No SIC; MMSE-IRC”. The reason why the complexity of this architecture appears higher than the architectures that use intra-SIC is because with the increase of the number of transmissions per slot, this architecture cannot handle the number of collisions that starts to appear and so these MSGs start to accumulate in the system. At the same time, because it is using MMSE-IRC, with the number of transmissions accumulating, the complexity of the channel estimation block will also increase its complexity due to all interferers channels that it has to estimate. Also, for each architecture, it is possible to see that the use of MMSE-IRC requires higher system complexity.

6. Conclusion

Finally, this last chapter presents the conclusions that can be drawn from this project development and future work that can be done for further research.

6.1. Summary

The purpose of this master thesis was to study and develop a solution that could deal with the interference problem, in an advanced and innovative manner, during the discovery phase of D2D communications in an uncoordinated and un-scheduled network.

In chapter 1, in order to have a better understanding of the problem in question, the reason why D2D systems appeared and why interference tend to be a problem in D2D communications without cellular infrastructure support is explained. Also, it was clarified why the current existing systems do not fulfil the established requirements of the work in study and which are the solutions found in the literature for the problem in consideration.

After having a well-defined purpose for this work, in chapter 2, fundamental concepts needed to understand the solution proposed in this thesis were described. It started with the explanation of the SIC process following with the clarification of some concepts related to the PHY and MAC layers which were essential in the development of the proposed solution not only in theory, but also experimentally in the construction of the LLS and SLS.

In chapter 3, the proposed solution was described, employing the two sides of a communication:

- In the transmitter side, it is created a set of transmissions patterns that are randomly chosen by the transmitter to send its packets and a set of multiple orthogonal pilot sequences from where a user can randomly choose to put in its payload.

- In the receiver side, it is developed an adaptive architecture that employs two different types of SIC, intra and inter.

In this chapter, all details related with the transmitter and receiver side of the solution were depicted. Here the core of the work and the actual matter that gave rise to the three inventions disclosure reports, and consequently the Intel patent, was exposed.

To evaluate the proposed solution, two simulators (LLS and SLS) were designed. In chapter 4, the way the implementation of these simulators was done was described. With these simulators, a D2D network was created and with it, different techniques were tested in terms of performance and complexity. Here, three types of systems were studied: a system where SIC is not applied, where is only applied intra-SIC, and where intra-SIC and inter-SIC are applied (proposed solution). During the testing phase, two different types of channel estimation were considered: MMSE-MRC and MMSE-IRC.

Then, in chapter 5, comparisons of the different systems were performed. From these results, certain conclusions, that will be exposed next, can be drawn.

A first conclusion that was taken even during the development of this project was that the use of orthogonal pilot sequences by the devices increases the performance of the system. This is due to the fact that with the pilot activity detection block, the receiver can detect which orthogonal pilot sequences is active and from that detect the signal that is associated with it.

Another conclusion taken from this project development is that the application of MMSE-IRC increases the performance in respect to MMSE-MRC no matter what receiver architecture is applied. This was expected because MMSE-IRC takes into consideration the interfering signals. Also, for that reason, if the number of interferers increases, the number of instructions executed in the MMSE-IRC block also increases, raising its complexity.

Finally, it was proven that the use of SIC although it increases the complexity of the system, it also boosts its performance. In higher channel loads, for example with 75 discovery sessions initiated per minute, as expected, not using any kind of SIC implies a low system performance. However, with the increase of complexity, applying only intra-SIC, the performance of the system can increase up to 50%. It was also conclude that a receiver architecture that uses inter and intra-SIC, also increasing the complexity of the system, can increase the performance up to 70%.

6.2. Future Work

The topic explored in this master thesis is very broad and continues to be intensively discussed by researchers and telecommunication companies. Hence, although this project already made so many technical contributions, here are some aspects that can be further explored and researched:

- In the proposed solution, there are some parameters such as, for example, the size of the VF that depend on the load of the network. In here it is assumed that this load is known, however in a real system that does not happen. Hence, a good research path would be to explore ways to detect what is the current load of a D2D network without infrastructure network support. For example, for the case of the VF size, it can be created a dedicated signal between devices which will carry the information of the experienced interference. This information can be directly exchanged between all devices if no central node is elected or between the central node and the other devices, when this type of device organization is present. Based on interference level (high, medium, low) experienced, the device decides on the size of the virtual frame accordingly, as shown in an example in Table 6.1.

Table 6.1: Size of the VF based on level of interference experienced.

Level of Interference	Size of VF
Low	< 4
Medium	4 - 10
High	> 10

- Also, as seen before, the implementation of intra and inter-SIC implies the increasing of system complexity. One important path to follow in terms of research would be discover similar techniques, with the same purpose but requiring less complexity.

- Another possibility of research could be extend the proposed solution to work in other types of systems, e.g. cellular networks, or crossing different types of interference.

Bibliography

[1] “Population Pyramid,” 2018. [Online]. Available: https://www.populationpyramid.net/world/2025/. [Accessed 12 June 2018].

[2] “Artificial Intelligence,” 2018. [Online]. Available: https://en.wikipedia.org/wiki/Artificial_intelligence. [Accessed 15 June 2018].

[3] “Statista,” 2018. [Online]. Available: https://www.statista.com/statistics/471264/iot-number-of-connected-devices-worldwide/. [Accessed 10 May 2018].

[4] “Getting to 5G: Comparing 4G and 5G system requirements,” 2017. [Online]. Available: http://www.qorvo.com/design-hub/blog/getting-to-5g-comparing-4g-and-5g-system-requirements. [Accessed 15 November 2017].

[5] A. Asadi, Q. Wang and V. Mancuso, “A Survey on Device-to-Device Communication in Cellular Networks,” *IEEE Communication Surveys & Tutorials,* vol. 16, no. 4, pp. 1801-1819, 2014.

[6] M. N. Tehrani, M. Uysal and H. Yanikomeroglu, “Device-to-Device Communication in 5G Cellullar Networks: Challenges, Solutions, and Future Directions,” *IEEE Communications Magazine,* pp. 86-92, 2014.

[7] 3GPP, “Technical Specification Group Radio Access Network; Study on LTE Device to Device Proximity Services; Radio Aspects. 3GPP TR 36.843 V12.0.1,” 2014.

[8] E. Ferro and F. Potorti, “Bluetooth and Wi-Fi Wireless Protocols: A Survey and a Comparison,” *IEEE Wireless Communications,* pp. 12-26, 2005.

[9] “GSM EDGE: 2G EDGE cellphone evolution,” [Online]. Available: https://www.electronics-notes.com/articles/connectivity/2g-gsm-edge/what-is-gsm-edge-evolution.php. [Accessed 20 June 2018].

[10] M. Haus, M. Waqas, A. Y. Ding, Y. Li, S. Tarkoma and J. Ott, “Security and Privacy in Device-to-Device (D2D) Communication: A Review,” *IEEE Communications Surveys & Tutorials,* vol. 19, no. 2, pp. 1054-1079, 2017.

[11] M. Chen, Y. Miao, Y. Hao and K. Hwang, “Narrow Band Internet of Things,” *IEEE Access,* vol. 5, pp. 20557-20577, 2017.

[12] B. Ismaiel, M. Albolhasan, D. Smith, W. Ni and D. Franklin, “A Survey and Comparison Of Device-To-Device Architecture Using LTE Unlicensed,” in *2017 IEEE 85th Vehicular Technology Conference (VTC Spring)*, Australia, 2017.

[13] G. A. Safdar, M. Ur-Rehman, M. Muhammad, M. A. Imran and R. Tafazolli, “Interference Mitigation in D2D Communication Underlaying LTE-A Network,” *IEEE Access,* vol. 4, pp. 7967-7987, 2016.

[14] M. Noura and R. Nordin, “A survey on interference management for Device-to-Device (D2D) communication and its challenges in 5G networks,” *Journal of Network and Computer Applications,* pp. 130-150, 2016.

[15] “Iterative Interference Cancellation Receivers,” [Online]. Available: http://shodhganga.inflibnet.ac.in/bitstream/10603/1224/10/10_chapter%202.pdf. [Accessed 20 November 2017].

[16] A. Memmi, Z. Rezki and M.-S. Alouini, “Power Control for D2D Underlay Cellular Networks With Channel Uncertainty,” *IEEE Transactions on Wireless Communications,* vol. 16, no. 2, pp. 1330-1343, 2017.

[17] A. Goldsmith, “Multiuser Systems,” in *Wireless Communications*, Cambridge University Press, 2005, pp. 422-460.

[18] N. Pratas and P. Popovski, “Zero-Outage Cellular Downlink With Fixed-Rate D2D Underlay,” *IEEE Transactions on Wireless Communications,* vol. 14, no. 7, pp. 3533-3543, 2015.

[19] “Troubleshooting a Network Issue With the OSI Model,” 17 March 2016. [Online]. Available: https://www.pei.com/2016/03/troubleshooting-a-network-issue-with-the-osi-model/. [Accessed 20 November 2017].

[20] S. Ahmadi, “Downlink Physical Layer Functions,” in *LTE-Advanced: A Practical Systems Approach to Understanding the 3GPP LTE Releases 10 and 11 Radio Access Technologies*, Elsevier, 2014, pp. 399-712.

[21] 3GPP, “Technical Specification Group Radio Access Network; Evolved Universal Terrestrial Radio Access (E-UTRA); Physical channels and modulation. 3GPP TS 36.211 V15.0.0,” 2017.

[22] G. Berardinelli, L. R. d. Temino, S. Frattasi, M. I. Rahman and P. Mogensen, “OFDMA vs SC-FDMA: Performance Comparison in Local Area IMT-A Scenarios,” *IEEE Wireless Communications,* vol. 15, no. 5, pp. 64-72, 2008.

[23] S. Ahmadi, “Coordinated Multipoint Transmission and Reception (CoMP),” in *LTE-Advanced: A Practical Systems Approach to Understanding the 3GPP LTE Releases 10 and 11 Radio Access Technologies*, Elsevier, 2014, pp. 951-981.

[24] E. Paolini, S. Cedomir, G. Liva and P. Popovski, “Coded Random Access: Applying Codes on Graphs to Design Random Access Protocols,” *IEEE Communications Magazine,* pp. 144-150, June 2015.

[25] M. Ivanov, F. Brannstrom, A. G. Amat and P. Popovski, “All-to-all Broadcast for Vehicular Networks Based on Coded Slotted ALOHA,” in *IEEE International Conference on Communication Workshop (ICCW)*, 2015.

[26] M. Ivanov, F. Brannstrom, A. G. Amat and P. Popovski, “Broadcast Coded Slotted ALOHA: A Finite Frame Length Analysis.,” *IEEE Transactions on Communications,* vol. 65, no. 2, pp. 651-662, 2017.

[27] 3GPP, “Technical Specification Group Radio Access Network; Evolved Universal Terrestrial Radio Access (E-UTRA); Multiplexing and channel coding. 3GPP TS 36.212 V15.0.0,” 2017.

[28] J. Meinilä, P. Kyösti, L. Hentilä, T. Jämsä, E. Suikkanen, E. Kunnari and M. Narandžić, “D5.3: WINNER + Final Channel Models V1.0,” 2010.

[29] P. Kyösti, J. Meinilä, L. Hentilä, X. Zhao, T. Jämsä, C. Schneider, M. Narandzić, M. Milojević, A. Hong, J. Ylitalo, V.-M. Holappa, M. Alatossava, R. Bultitude, Y. Jong and . T. Rautiainen, “WINNER II Channel Models D1.1.2 V1.2,” 2008.

Appendix A

In this appendix it is described how the deployment of the devices was computed, including the creation of their coordinates and the calculation of the distance and path loss and shadowing between them and their associated UE.

To get a distribution of DIs and DRs in space, it was done a random deployment of device pairs (DI, DR) in a given area. From here it was possible to obtain the Cartesian coordinates of the devices as depicted, as example, in Figure A.1.

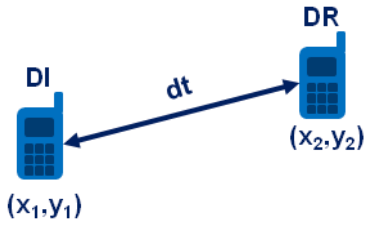

Figure A.1: Example of a communication between a DI and a DR.

With the Cartesian coordinates of both devices, the distance between them was calculated as following,

$$dt = \sqrt{(x_1 - x_2)^2 + (y_1 - y_2)^2} \quad \text{(A.1)}$$

where dt is the distance between associated devices and (x_1, y_1) and (x_2, y_2) are the Cartesian coordinates of the two devices in consideration.

In respect to the channel model used for the calculation of the path loss, it was used the one from LTE D2D ProSe standardized in 3GPP TR 36.843 [7] for outdoor to outdoor and channel type “B1”. Hence, the total path loss is calculated as following

$$PL_{B1_{total}} = \max\left(PL_{FreeSpace}, PL_{B1}\right) \quad \text{(A.2)}$$

where $PL_{FreeSpace}$ is the free space path loss and PL_{B1} is the Winner + B1 channel model for hexagonal layout from D5.3 [28] with the following offsets:

- Line of sight (LoS) offset = 0 dB.
- Non line of sight (NLoS) offset = -5 dB.

Also, concerning the variables in this channel model, according to [7], in the D2D mode, it is considered that the antenna heights at the BS (h_{BS}) and at mobile station (MS) (h_{MS}) are 1.5 m and that the effective antenna heights at the BS (h'_{BS}) and MS (h'_{MS}) are 0.8 m.

To obtain the total path loss, first the free space path loss is computed according to WinnerII D1.1.2 [29] as following,

$$PL_{FreeSpace} = 20 \cdot \log_{10}(dt) + 46.4 + 20 \cdot \log_{10}\left(\frac{f_c}{5}\right) \quad \text{(A.3)}$$

where f_c is the system frequency.

Then, to calculate PL_{B1}, it is necessary to determine the existence of NLoS/LoS propagation. Hence, according to Table 4-7 from WinnerII D1.1.2 [29], the line of sight probability can be computed as following,

$$\Pr_{LoS} = \min\left(\frac{18}{dt}, 1\right) \cdot \left(1 - e^{-\frac{dt}{36}}\right) + e^{-\frac{dt}{36}}. \quad \text{(A.4)}$$

This probability will allow the choice between the two types of propagation – LoS and NLoS – during the simulation.

Finally, using the Winner + B1 channel model from D5.3 [28] and having into account the respective offsets, it is possible to calculate the path loss in LoS and NLoS.

For LoS the path loss is the following,

$$\mathrm{PL}_{B1} = \begin{cases} 0, dt < 10m \\ 22.7 \cdot \log_{10}(dt) + 27 + 20 \cdot \log_{10}(f_c), 10m < dt < d'_{BP} \\ 40 \cdot \log_{10}(dt) + 7.56 - 17.3 \cdot \log_{10}(h'_{BS}) - 17.3 \cdot \log_{10}(h'_{MS}) + 2.7 \cdot \log_{10}(f_c), d'_{BP} < dt < 5km \end{cases} \quad \text{(A.5)}$$

with

$$d'_{BP} = 4 \cdot h'_{BS} \cdot h'_{MS} \cdot \frac{f_c}{c} \quad \text{(A.6)}$$

where c is the propagation velocity in free space.

While for NLoS the path loss is defined as

$$PL_{B1} = (44.9 - 6.55 \cdot \log_{10}(h_{BS})) \cdot \log_{10}(dt) + 5.83 \cdot \log_{10}(h_{BS}) + 16.33 + 26.16 \cdot \log_{10}(f_c) - 5. \quad \text{(A.7)}$$

Finally, after obtaining the total path loss between the associated UEs, a random number of shadowing is added, creating the total amount of path loss and shadowing.

$$Pathloss\&Shadowing = PL_{B1_{total}} + ShadowingRV. \quad \text{(A.8)}$$

Note that the random number of shadowing is generated from the normal distribution with mean 0 and standard deviation 7 dB, as defined in the standard 3GPP TR 36.843 [7].